

**Beiträge
zur
Vibro- und Psychoakustik**

Herausgeber: Helmut Fleischer und Hugo Fastl

Helmut Fleischer

**DEAD SPOTS OF ELECTRIC BASSES
I. Structural Vibrations**

DEAD SPOTS OF ELECTRIC BASSES

I. Structural Vibrations

2nd Edition

by

Helmut Fleischer

Institut für Mechanik
Fakultät für Luft- und Raumfahrttechnik
Universität der Bundeswehr München
D-85577 Neubiberg

Heft 2/99 der Reihe

Beiträge zur Vibro- und Psychoakustik

Herausgeber: Helmut Fleischer und Hugo Fastl

ISSN 1430-936X

Herausgeber:

Prof. Dr.-Ing. habil. Helmut Fleischer
Institut für Mechanik
Fakultät für Luft- und Raumfahrttechnik
Universität der Bundeswehr München

Prof. Dr.-Ing. habil. Hugo Fastl
Lehrstuhl für Mensch-Maschine-Kommunikation
Fakultät für Elektrotechnik und Informationstechnik
Technische Universität München

Postanschrift:

LRT 4 UniBwM
D-85577 Neubiberg

Fleischer, Helmut:
Dead spots of electric basses. I. Structural vibrations; 2nd Edition
Beiträge zur Vibro- und Psychoakustik 2/99
Neubiberg 1999
ISSN 1430-936X

Postanschrift des Verfassers:

Prof. Dr.-Ing. Helmut Fleischer
LRT 4 UniBwM
85577 Neubiberg
Helmut.Fleischer@UniBw.de

Dieses Werk ist urheberrechtlich geschützt. Jede Verwertung außerhalb der Grenzen des Urheberrechtsgesetzes ist unzulässig und strafbar. Insbesondere gilt dies für die Übersetzung, den Nachdruck sowie die Speicherung auf Mikrofilm, mit vergleichbaren Verfahren oder in Datenverarbeitungsanlagen.

CONTENT

FOREWORD

1.	INTRODUCTION	1
2.	INSTRUMENTS UNDER CONSIDERATION	3
2.1.	Overview	3
2.2.	Action Bass	4
2.3.	Music Man Bass	5
2.4.	Dyna Bass	6
2.5.	Carvin Bass	7
2.6.	Riverhead Bass	7
2.7.	Concluding Remarks	8
3.	THEORY OF BEAM VIBRATIONS	9
3.1.	Theoretical Foundations	9
3.2.	Boundary Condition Clamped-Free	10
3.3.	Boundary Condition Free-Free	11
3.4.	Boundary Condition Simply Supported-Free	12
3.5.	Comparing Different Boundary Conditions	13
3.6.	Concluding Remarks	14
4.	EXPERIMENTAL MODAL ANALYSIS	15
4.1.	Method and Set-up	15
4.2.	Modes of the Action Bass	16
4.3.	Modes of the Dyna Bass	17
4.4.	Comparison to Beam Modes	18
4.4.1.	Modes of a Beam of Constant Stiffness	18
4.4.2.	Modes of the Action Bass	18
4.4.3.	Modes of the Dyna Bass	19
4.5.	Concluding Remarks	21
5.	OPERATING DEFLECTION SHAPES	22
5.1.	Measuring Set up and Procedure	22
5.2.	Experimental Results for the Action Bass	23
5.3.	Experimental Results for the Music Man Bass	28
5.4.	Experimental Results for the Dyna Bass	32
5.5.	Experimental Results for the Carvin Bass	36
5.6.	Experimental Results for the Riverhead Bass	41
5.7.	Concluding Remarks	45
6.	COMPARISON OF THE PRINCIPAL ODSs	46
6.1.	ODSs of the Action Bass	46
6.2.	ODSs of the Music Man Bass	47
6.3.	ODSs of the Dyna Bass	48
6.4.	ODSs of the Carvin Bass	49
6.5.	ODSs of the Riverhead Bass	50

6.6.	Eigenmodes of the Simply Supported-Free Beam.....	51
6.7	Comparison of the Bass ODSs to Beam Eigenmodes.....	52
6.7.1.	Survey	52
6.7.2.	Rigid Body Motion	52
6.7.3.	First Bending Vibration	53
6.7.4.	Second Bending Vibration.....	53
6.7.5.	Third Bending Vibration.....	53
6.7.6.	Fourth Bending Vibration.....	54
6.8.	Concluding Remarks.....	54
7.	MECHANICAL ADMITTANCE.....	55
7.1.	Measuring Parameters and Set-up.....	55
7.2.	Comparing In-plane and Out-of-plane Admittance on the Neck.....	56
7.3.	Lateral Dependence of the Neck Admittance	57
7.4.	Admittance, Conductance and Susceptance.....	61
7.5.	Neck and Bridge Conductance.....	62
7.6.	Concluding Remarks.....	63
8.	NECK CONDUCTANCES OF THE BASSES.....	64
8.1.	Experimental Results for the Action Bass	64
8.2.	Experimental Results for the Music Man Bass.....	64
8.3.	Experimental Results for the Dyna Bass.....	65
8.4.	Experimental Results for the Carvin Bass	66
8.5.	Experimental Results for the Riverhead Bass.....	66
8.6.	Concluding Remarks.....	67
9.	FINAL DISCUSSION	68
	LITERATURE.....	71

FOREWORD

This is the first volume of our anthology on vibroacoustics and psychoacoustics written in English. Perhaps the fact that there is no adequate German term for "dead spot" prompted Helmut Fleischer to continue his report from the very first word of the title in English language.

In the present volume, Fleischer's series of measurements on electric guitars is extended to electric basses with the goal to uncover the mysteries of and to understand the causes for "dead spots" of stringed instruments. Comprehensive experimental investigations of the vibration behaviour of five different electric basses are described, including Modal Analysis and the determination of Operating Deflection Shapes (ODSs) using laser vibrometry.

The experimental results are compared to theoretical considerations on the bending beam with the aim to derive a simple model capable to describe the basic relations. Since the vibrations of a structure depend crucially on the boundary conditions, Fleischer takes special care to provide comparable and - even more important - "natural" conditions in the experiments. Measurements "*in situ*", where the bass is held in normal playing position during the experiments, lead to realistic results directly applicable in musical practice.

The mechanical conductance, *i.e.* the real part of the complex point admittance, is measured in order to characterise the transfer of vibration energy from the string to the structure of the instrument. As a key parameter for the diagnosis of dead spots, the conductance of the instrument's neck is elaborated.

Therefore, in a second part of the investigation, dead spots of instruments have been diagnosed on the basis of their neck conductance. The corresponding results will be reported in a subsequent volume of our anthology.

Munich, in June 1999

Hugo Fastl

SUMMARY

The "sustain", i.e. the long decay, of the string signal of the solid-body electric bass is commonly considered as a quality attribute. In musical practice, particular locations on the fingerboard are observed where, for a particular string, the sustain is significantly shorter than at adjacent frets. This phenomenon is well-known among bass players; the corresponding location is called a "dead spot". Its origin is the fact that the string may cause the mechanical structure of the instrument to vibrate with the consequence that energy flows from the string to the instrument body which results in a faster decay of the string signal.

Five structurally different electric basses (with and without head, made from wood and carbon fibre, neck screwed and glued to the body, four through six strings) served as measuring objects. At first, the structural vibrations of two instruments positioned in an experimental set-up were determined by conventional Modal Analysis. In the next step, Operating Deflection Shapes (ODSs) of all basses were ascertained *in situ*, i.e. in normal playing position held by a subject sitting on a chair, by means of a Laser Scanning Vibrometer. Finally, the mechanical point admittance at the neck-end supports of the strings (nut and frets, respectively) was ascertained *in situ* using a straightforward experimental procedure. The real part of the complex admittance, denoted conductance, is a measure of the energy transfer via the end support under consideration. All experiments confirm that the instruments are not at all rigid but tend to vibrate. The main vibration patterns compare to the bending modes of a simply supported-free beam with the support at the body and the free end at the head of the bass. As a rule - for a well-made instrument - the body at the bridge proves as generally less mobile than the neck, *i.e.* the nut and frets. That means that energy will most probably flow from the string to the instrument structure at the neck termination of a string. Thus, the conductance measured at the neck of an electric solid-body bass promises to be a key parameter for the diagnosis of dead spot. This will be investigated and validated in the second part of our study.

ZUSAMMENFASSUNG

Dead Spots elektrischer Bässe. I. Strukturschwingungen

Das "Sustain", d.h. das lange Anhalten des Saitensignals des elektrischen Basses mit massivem Korpus wird gemeinhin als Qualitätsmerkmal betrachtet. In der musikalischen Praxis beobachtet man Stellen auf dem Griffbrett, an denen für eine bestimmte Saite das "Sustain" deutlich kürzer als an benachbarten Bündeln ist. Diese Erscheinung ist unter Baßspielern wohlbekannt; der betreffende Ort wird als "Dead Spot" bezeichnet. Ihre Ursache ist die Tatsache, daß die Saite die mechanische Struktur des Instruments zum Mitschwingen bringen kann mit der Folge, daß Energie von der Saite in den Instrumentenkörper fließt, was zu einem schnelleren Abklingen des Saitensignals führt.

Fünf elektrische Bässe unterschiedlicher Bauweise (mit oder ohne Wirbelbrett, aus Holz oder kohlefaserverstärktem Kunststoff gefertigt, Hals an den Korpus geschraubt oder geleimt, vier bis sechs Saiten) dienten als Meßobjekte. Zuerst wurden die Strukturschwingungen zweier in einer Versuchseinrichtung gelagerter Instrumente mittels herkömmlicher Modalanalyse bestimmt. Im nächsten Schritt wurden die "Operating Deflection Shapes" (ODSs; aktuelle Schwingungsmuster) aller Bässe *in situ*, d.h. in normaler Spielhaltung gehalten von einer auf einem Stuhl sitzenden Person, mittels eines Scanning Vibrometers bestimmt. Abschließend wurde die mechanische Punktadmittanz an den halsseitigen Auflagern der Saiten (Sattel bzw. Bündel) *in situ* mit einer einfachen und direkten Meßmethode ermittelt. Der Realteil der komplexen Admittanz, die Konduktanz, ist ein Maß für das Abfließen von Energie am betrachteten Auflager. Die Experimente bestätigen, daß die Instrumente keineswegs starr, sondern schwingungsfähig sind. Die Haupt-Schwingungsmuster entsprechen den Biegemoden eines Balkens der Lagerungsart gelenkig gelagert-frei mit dem Auflager am Korpus und dem freien Ende am Wirbelbrett des Basses. In aller Regel erweist sich - bei einem gut gefertigten Instrument - der Korpus am Steg als weniger beweglich als der Hals, d.h. der Sattel und Bündel. Das bedeutet, daß Schwingungsenergie von der Saite zur Instrumentenstruktur mit größter Wahrscheinlichkeit über das Halsende der Saite fließen wird. Somit verspricht die Konduktanz, gemessen auf dem Hals eines Elektrobasses, ein zentraler Kennwert für die Diagnose von Dead Spots zu sein. Dies wird im zweiten Teil der Studie untersucht und bestätigt werden.

1. INTRODUCTION

In modern popular music, the electric bass is the most important instrument of its class. Electric basses are constructed in a similar way as electric guitars. Four to six strings are used. As a rule, the body is made from solid material. In spite of the importance of the electric guitar and bass, relatively little scientific work has been published on this subject. In some books on electric guitars (*e.g.* Meinel (1987), Lemme (1994)) electric basses are mentioned. A doctoral thesis (May (1984)) refers to electric stringed instruments in general and their role in popular music. Textbooks dealing with musical instruments (*e.g.* Fletcher and Rossing (1998)) emphasise classic, *i.e.* acoustic, instruments rather than electric ones. Only recently interest has been beginning to focus on electric plucked string instruments (*e.g.* Heise (1993), Wogram (1994), Fleischer (1998 and 1999), Fleischer and Zwicker (1996, 1997, 1998 and 1999)).

Mechano-electric (in general: electromagnetic) transducers are used to pick up the musical signal. From this point of view, electric basses belong to two instrument families. On one hand, they are plucked chordophones (stringed instruments) because the signal is generated by string vibrations in the same way as in a traditional acoustic bass guitar or plucked double bass. On the other hand, they are electrophones in the sense that the vibration of the strings is picked up as an electric signal and manipulated and amplified by electronic means. Thus, the tasks of generating and radiating the musical signal are separated.

This is the fact from which the fundamental difference between electric and traditional basses results: The bridge does not have to be mobile in order to transfer energy from the string to the body. On the contrary, the body of an electric bass is commonly equipped with a solid body and constructed in such a way that the bridge is as immobile as possible. In consequence, much less energy flows from the string to the body and the string signal does not decay as rapidly for a solid-body bass as for an acoustic one. Thus, as a rule, the "sustain" of an electric bass is "better" than that of a conventional one.

The sustain, *i.e.* the long decay of the string signal, depends on several factors, for example on the quality, age and state of the strings. Investigations on guitar strings are reported by deDayans and Behar (1979), Chaigne (1986 and 1991) as well as Valenzuela (1999). That is why the decay data of different strings are hard to compare. For one and the same given string a uniform decrease of the sustain with increasing frequency is expected. (A more detailed study of damping mechanisms is scheduled for the second part of this work.) However, exceptions to this rule are observed. On the fingerboard of practically every bass there are particular locations where the sustain proves to be worse than for adjacent frets. Players call this a "dead spot".

Theoretical considerations suggest pronounced interactions between the vibrations of the non-ideal string and a non-rigid instrument body; cf. Fletcher (1964), Zimmermann (1967), Müller (1967/68), Wolf and Müller (1968), Gough (1981) and Jansson (1990). Consequently, when studying the generation and decay of the musical signal, the end supports of the strings have to be analysed. In particular the damping of the string vibration by mobile end supports, which was investigated *e.g.* by Fletcher (1977), has to be taken into account. First attempts have been made to use Finite Element Analysis to compute the vibrations of the bodies of electric guitars; cf. Carlson (1998). Heise (1993), Wogram (1994), Garrelfs and Schneiders (1995) used experimental Modal Analysis in order to ascertain the vibrational behaviour of electric basses. The shortcoming of these studies results from the fact that the boundary conditions during the experiment differ from those in normal use of the instrument. This can be overcome by *in-situ* measurements of the vibrations under "human" boundary conditions as described for electric guitars by Fleischer and Zwicker (1998) which promise to yield more realistic results. They are obtained in normal playing position and thus make sure that the boundary conditions of measurement and playing practice coincide.

From the "view" of the string the mechanical admittance (or its reciprocal, the mechanical impedance) at the terminations is a more direct measuring parameter. Admittance measurements at the bridges of acoustic instruments are reported by several authors. Moral and Jansson (1982), Pfaffelhuber (1993), Jansson and Niewczyk (1997) investigated violins, while Eggers (1987 and 1991) dealt with the violoncello and Fleischer (1997a and 1998b) with bells. Acoustic guitars were the measuring objects of *e.g.* Jansson (1993b) and Fleischer (1997b and 1998b). Ziegenhals (1997) treated the admittance of the bridge of electric semi-resonance guitars. In contrast, Fleischer and Zwicker (1996 and 1997) investigated not only the admittance at the bridge of electric solid-body guitars, but also at the necks. In the course of this work, it proved as promising to ascertain the real part of the admittance, the conductance.

Conductance measurements on electric guitars were performed by Fleischer and Zwicker (1998 and 1999) and Fleischer (1999). The scope of the present report is to apply this technique to electric basses. A number of basses are investigated regarding structural vibration, admittance and conductance. A simple model is given in order to ease the understanding of the underlying principles. In a subsequent report, dead spots will be quantified by measuring the decay times of the string signals of two basses. From the correlation found between the decay time of the fundamental tone and the conductance at the corresponding string-fret combination, a method will be derived to predict dead spots from neck conductance diagrams.

2. INSTRUMENTS UNDER CONSIDERATION

2.1. Overview

Tab. I gives a survey on the instruments which are considered in the following. The basses carry 20 to 24 frets and four to six strings with a speaking length between 85 cm and 90 cm. They all have a solid body and are equipped with electromagnetic pick-ups (which are not subject to investigation but should be regarded in more detail in the future). The neck is reinforced with an adjustable steel rod. The price range covers one order of magnitude between about 200 Euro and 2000 Euro.

No.	Name	Number of strings	Number of frets	String length	Remarks
1	Action Bass	4	20	86 cm	Neck screwed; copy of a Fender Precision Bass
2	Music Man Sting Ray 5	5	22	87 cm	Neck screwed; Ernie Ball
3	Dyna Bass	4	21	90 cm	Neck glued to the body; made by Peavey
4	Carvin	6	24	87 cm	Neck glued; LB 76
5	Riverhead	4	24	85 cm	Headless; body and neck from carbon fibre; Headway

Tab. I. Main parameters of the instruments under consideration.

2.2. Action Bass

The four-string Action Bass (cf. Fig. 1 and No. 1 in Tab. I) is manufactured by an unidentified East German manufacturer (most probably Musima from Markneukirchen) and can be regarded as a lower-priced copy of a Fender Bass. The neck is attached to the body by four screws. Experimental results of this instrument have already been published by Fleischer and Zwicker (1996 and 1997).



Fig. 1. Action Bass (Instrument No. 1).

2.3. Music Man Bass

The instrument No. 2 is Music Man Sting Ray 5 by Ernie Ball, a higher-priced bass equipped with five strings. The neck is screwed to the body. The wood under the transparent lacquer is visible. Fig. 2 shows a photograph.



Fig. 2. Ernie Ball Music Man Sting Ray 5 (Instrument No. 2).

2.4. Dyna Bass

The Dyna Bass (cf. Fig. 3 and No. 3 in Tab. I) carries four strings and is manufactured by Peavey. The neck and body are covered by coloured paint and appear as one piece; presumably the neck is glued to the body. Experimental results of this instrument have already been published by Fleischer and Zwicker (1996).

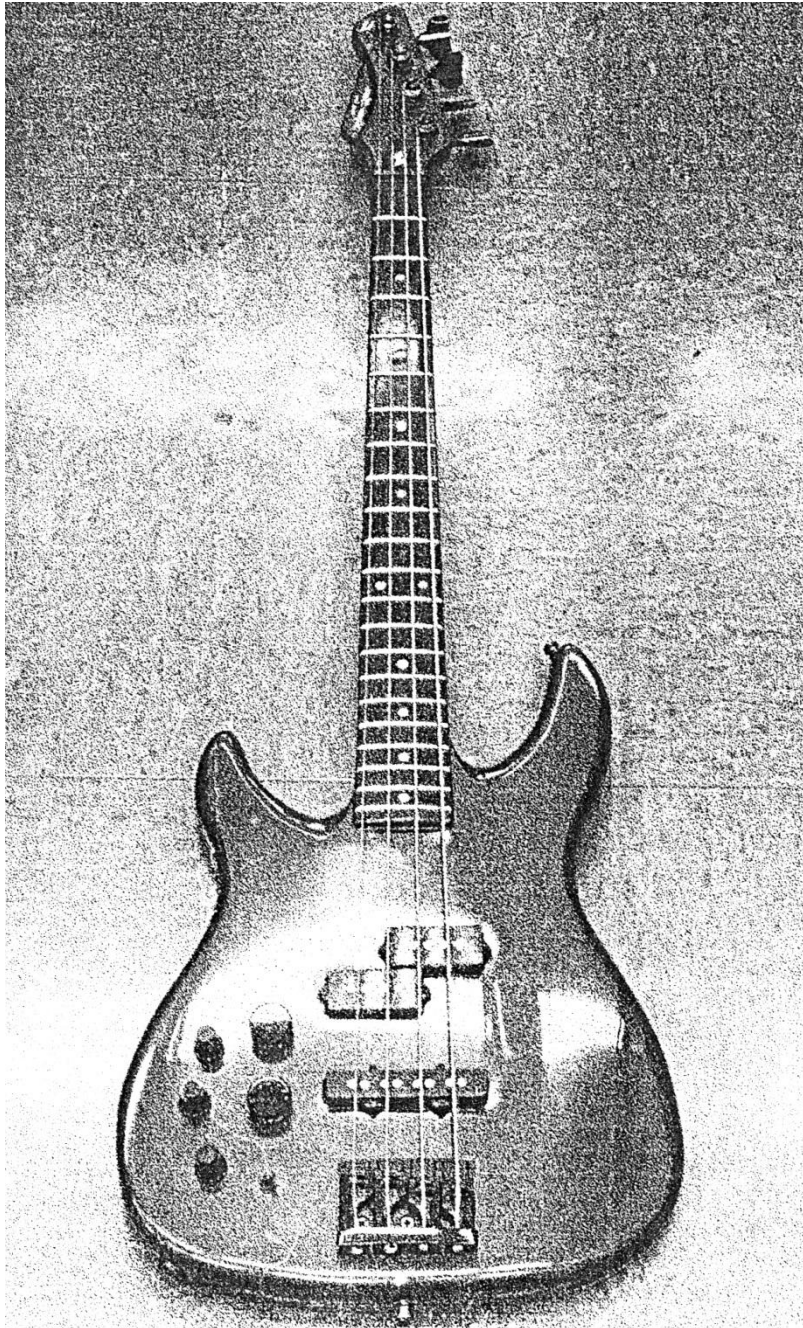


Fig. 3. Dyna Bass (Instrument No. 3).

2.5. Carvin Bass

The Carvin LB 76 Bass (cf. Fig. 4 and No. 4 in Tab. I) is six-stringed. The neck and body are painted with the appearance of one single piece. Most probably the body parts are glued from both sides to the extension of the neck. This instrument is high in reputation and price.



Fig. 4. Carvin Bass (Instrument No. 4).

2.6. Riverhead Bass

The Riverhead Bass (No. 5 in Tab. I), shown in Fig. 5, is conventionally equipped with four strings. The rest of the instrument, however, appears relatively unconventional. The instrument is headless, *i.e.* the mechanism for the adjustment of the string tension is located at the body-end. The neck and body are one common symmetric structure which is manufactured from plastic-carbon fibre compound material. Of all five basses considered in this report, this one is the most adequate for an Aerospace Faculty because of its material and design.

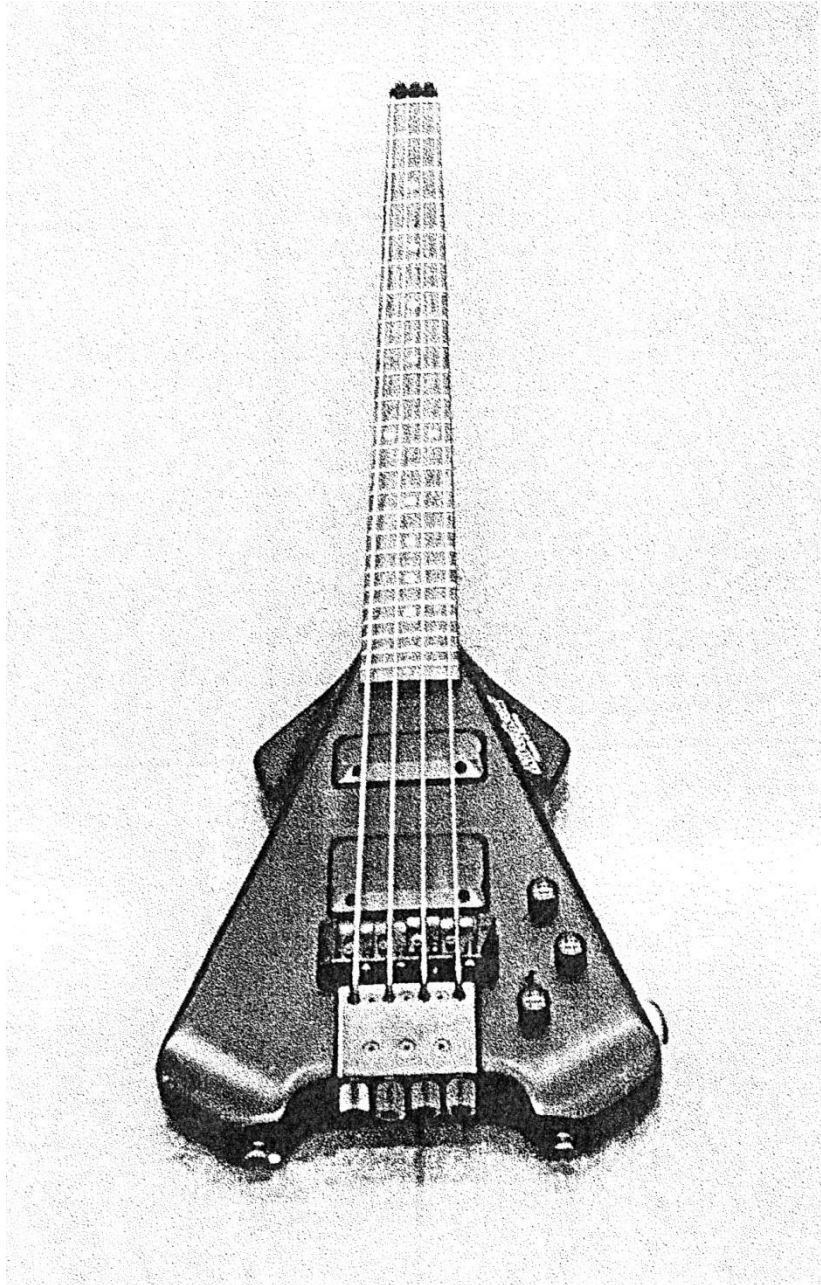


Fig. 5. Riverhead Bass (Instrument No. 5).

2.7. Concluding Remarks

The ensemble of the basses under consideration comprises different types of instruments. They differ in

- material (wood: No. 1 - No. 4 and carbon fibre: No. 5, respectively),
- fixation of the neck to the body (screwed: No. 1 and No. 2, glued or integrated: No. 3 - No. 5, respectively),
- number of strings (four: No. 1, No. 3 and No. 5, five: No. 2 and six: No. 4, respectively).

Thus, a certain variety of test objects is provided in order to test the applicability of the methods suggested in the following and to yield a certain impression of the behaviour of commercially available instruments.

3. THEORY OF BEAM VIBRATIONS

3.1. Theoretical Foundations

Theoretical considerations yield the general differential equation of the bending deflection w of a beam

$$-(EI_y w'')'' + (\rho I_y w''')' + (Nw')' + q_z = \rho A w'' \quad (1)$$

Neglecting the rotatory inertia (considered by the term $(\rho I_y w''')'$) and the influence of the normal force N leads to the simplified differential equation of beam vibrations

$$-(EI_y w'')'' + q_z = \rho A w'' \quad (2)$$

which is of second order with respect to the time t and fourth order with respect to the coordinate x . For free vibrations $q_z = 0$ and under the assumption of $EI_y = \text{const}$ Eq. (2) simplifies to

$$EI_y w'''' + \rho A w'' = 0 \quad (3)$$

with E Young's modulus,

I_y geometrical moment of inertia,

w deflection of the centre line of the beam in z direction,

ρ density,

A area of the cross section of the beam,

'''' fourth derivative with respect to the coordinate x and

'' second derivative with respect to the time t .

The further treatment using standard methods yields the eigenfunctions and eigenfrequencies of the vibrating beam. The latter are

$$f_j = \frac{\lambda_j^2}{2\pi l^2} \sqrt{\frac{EI_y}{\rho A}} \quad (4)$$

For a rectangular cross section of width b and height h with

$$I_y = \frac{b h^3}{12} \quad \text{and} \quad A = b h$$

Eq. (4) becomes

$$f_j = \frac{\lambda_j^2}{4\sqrt{3}\pi} \frac{h}{l^2} \sqrt{\frac{E}{\rho}} \quad (5)$$

From Eq. (5) the influence of the parameters of the beam becomes obvious:

The eigenfrequencies of a beam are proportional to

- * the square of the eigenvalues λ_j (which depend on the boundary conditions),
- * the height h of the beam,
- * the inverse of the square of the length l of the beam,
- * the speed $c = \sqrt{E/\rho}$ of longitudinal waves, *i.e.* on the fraction E/ρ .

For beams of equal geometry and material, the eigenfrequencies depend exclusively on the eigenvalues. These, in turn, are characteristic for the way in which the beam is supported at its terminations. Three particular cases, characterised by boundary conditions closely related to the supports of the bass during the experiments, are considered in the following.

3.2. Boundary Condition Clamped-Free

For the vibrating cantilever beam the characteristic equation is

$$\cos\lambda_j \cosh\lambda_j + 1 = 0 \quad (6)$$

which yields the eigenvalues

$$\begin{aligned} \lambda_1 &= 1.875 \quad , \\ \lambda_2 &= 4.694 \quad , \\ \lambda_3 &= 7.855 \quad , \\ \lambda_4 &= 10.996 \quad , \\ \lambda_5 &= 14.137 \quad , \\ &\vdots \\ \lambda_j &= (2j - 1)\pi/2 \quad , \\ \lambda_{j+1} &= \lambda_j + \pi \quad . \end{aligned} \quad (7)$$

Thus, the lower eigenfrequencies (Eq. (4 or 5)) are related by the squares of the eigenvalues, *i.e.*

$$f_1 : f_2 : f_3 : f_4 : f_5 : \dots = 1 : 6.267 : 17.547 : 34.386 : 56.843 : \dots \quad (8)$$

and the eigenfunctions are

$$\hat{w}(x) = \cos\lambda_j \frac{x}{l} - \frac{\cos\lambda_j + \cosh\lambda_j}{\sin\lambda_j + \sinh\lambda_j} \sin\lambda_j \frac{x}{l} - \cosh\lambda_j \frac{x}{l} + \frac{\cos\lambda_j + \cosh\lambda_j}{\sin\lambda_j + \sinh\lambda_j} \sinh\lambda_j \frac{x}{l} . \quad (9)$$

Sketches of the first three vibrational patterns are given in Fig. 6 including the eigenfrequencies, normalised to the first eigenfrequency according to Eq. (8).

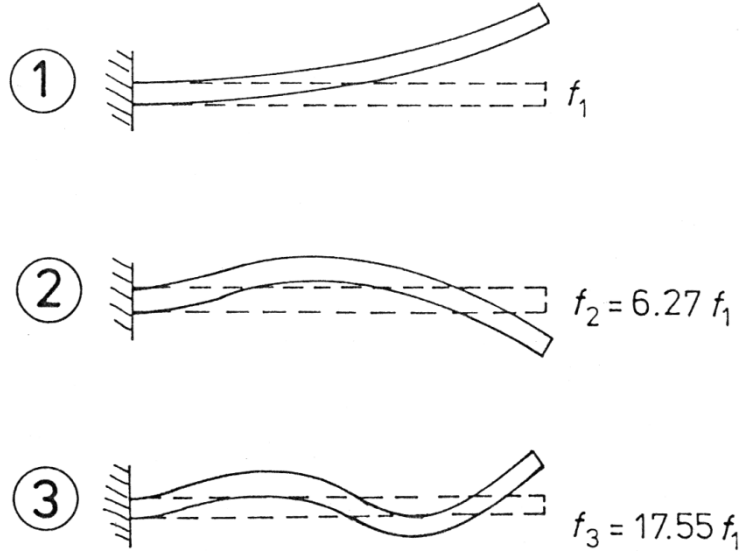


Fig. 6. Bending eigenmodes of a clamped-free beam and normalised eigenfrequencies.

3.3. Boundary Condition Free-Free

The characteristic equation of a beam which is free at both ends is

$$\cos\lambda_j \cosh\lambda_j - 1 = 0 \quad (10)$$

yielding the eigenvalues

$$\begin{aligned} \lambda_1 &= 4.730 \quad , \\ \lambda_2 &= 7.853 \quad , \\ \lambda_3 &= 10.996 \quad , \\ \lambda_4 &= 14.137 \quad , \\ \lambda_5 &= 17.279 \quad , \\ &\vdots \\ \lambda_j &= (2j + 1)\pi/2 \quad . \end{aligned} \quad (11)$$

Thus, the first eigenfrequencies (Eq. (4 or 5)) are related by

$$f_1 : f_2 : f_3 : f_4 : f_5 : \dots = 1 : 2.757 : 5.404 : 8.933 : 13.344 : \dots \quad ; \quad (12)$$

the corresponding eigenfunctions are

$$\hat{w}(x) = \cos\lambda_j \frac{x}{l} - \frac{\cos\lambda_j - \cosh\lambda_j}{\sin\lambda_j - \sinh\lambda_j} \sin\lambda_j \frac{x}{l} + \cosh\lambda_j \frac{x}{l} - \frac{\cos\lambda_j - \cosh\lambda_j}{\sin\lambda_j - \sinh\lambda_j} \sinh\lambda_j \frac{x}{l} \quad . \quad (13)$$

The first three vibrational patterns are sketched in Fig. 7 together with the eigenfrequencies, normalised to the first eigenfrequency according to Eq. (11).

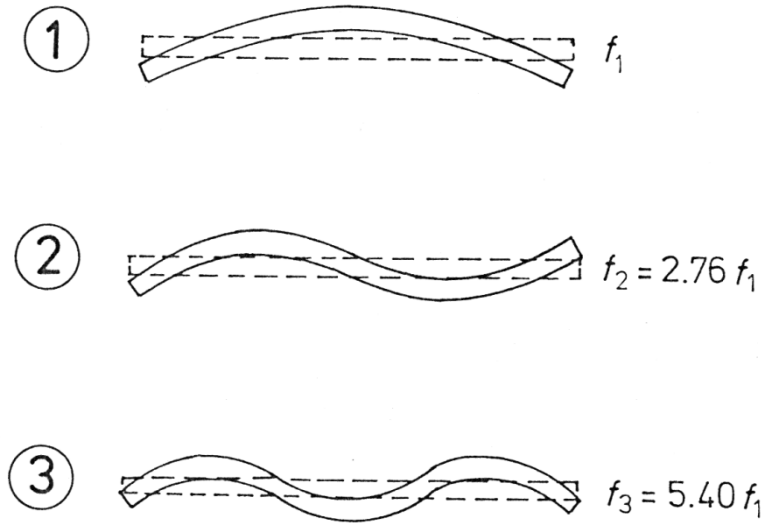


Fig. 7. Bending eigenmodes of a free-free beam and normalised eigenfrequencies.

3.4. Boundary Condition Simply Supported-Free

The characteristic equation for the boundary conditions simply supported (also denoted hinged) and free is

$$\tanh\lambda_j - \tan\lambda_j = 0 \quad (14)$$

with the eigenvalues

$$\lambda_1 = 3.927 \quad ,$$

$$\lambda_2 = 7.069 \quad ,$$

$$\lambda_3 = 10.210 \quad ,$$

$$\begin{aligned}
\lambda_4 &= 13.352 \quad , \\
\lambda_5 &= 16.493 \quad , \\
&\vdots \\
\lambda_j &= (j + 1/4)\pi \quad , \\
\lambda_{j+1} &= \lambda_j + \pi \quad .
\end{aligned} \tag{15}$$

Consequently, the eigenfrequencies (Eq. (4 or 5)) are related by

$$f_1 : f_2 : f_3 : f_4 : f_5 : \dots = 1 : 3.241 : 6.761 : 11.562 : 17.643 : \dots \tag{16}$$

and the eigenfunctions are

$$\hat{w}(x) = \sin \lambda_j \frac{x}{l} + \frac{\cos \lambda_j}{\cosh \lambda_j} \sinh \lambda_j \frac{x}{l} \quad . \tag{17}$$

Fig. 8 gives an impression of the first three vibrational patterns. The eigenfrequencies, normalised to the first eigenfrequency according to Eq. (16), are added.

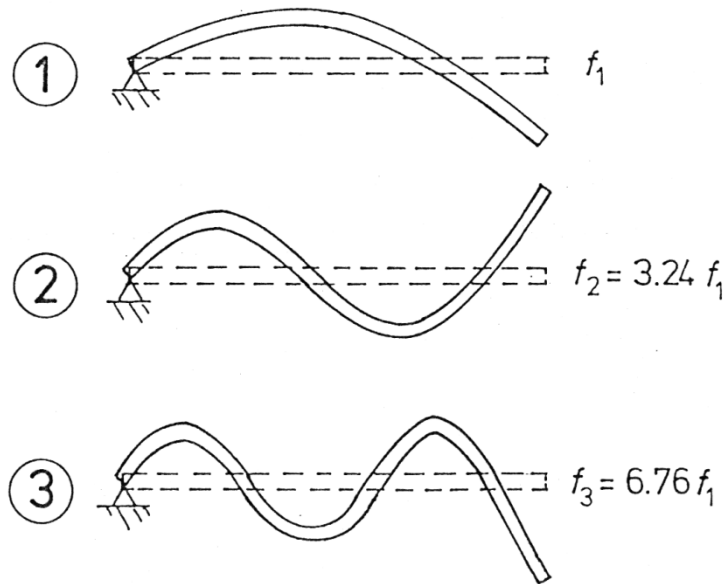


Fig. 8. Bending eigenmodes of a simply supported-free beam and normalised eigenfrequencies.

3.5. Comparing Different Boundary Conditions

According to Eq. (5) the eigenfrequency of the eigenmode of number j is

$$f_j = \frac{\lambda_j^2}{4\sqrt{3}\pi} \frac{h}{l^2} \sqrt{\frac{E}{\rho}} \quad .$$

Provided that the geometry (h, l) and the material (E, ρ) of the beam remain unchanged, the eigenfrequencies f_j depend on the eigenvalues λ_j according to

$$f_j = \text{const } \lambda_j^2 \quad (18)$$

In Tab. II the squares of the eigenvalues (Eqs. (7, 11 and 15)) are compiled.

Boundary condition	c - f	f - f	ss - f
1 st mode: λ_1^2	3.516	22.373	15.418
2 nd mode: λ_2^2	22.034	61.673	49.965
3 rd mode: λ_3^2	61.697	120.903	104.248
4 th mode: λ_4^2	120.902	199.859	178.270
5 th mode: λ_5^2	199.860	298.556	272.031

Tab. II. Squared eigenvalues for beams with different boundary conditions.

If, at one and the same beam, the clamping is removed, and thus a clamped-free (c-f) boundary condition turns into free-free (f-f), on the first mode two major effects are observed:

1. The mode shape changes; instead of one node at the clamped support two nodes appear; cf. the upper (No. 1) patterns in Figs. 6 and 7.
2. The frequency of the first mode is lifted by a factor of $22.373/3.516 = 6.363$.

This example shows that the first eigenfrequency may be more than six times higher in the f-f case compared to the c-f case. This immense increase gives an impression of what an important role the boundary conditions play for the shape and frequency of a structural vibration.

3.6. Concluding Remarks

It is obvious that a bass differs from a beam the geometry and material of which is not dependent on the length coordinate. Nevertheless, the beam suits as a simplified model in order to study the basic relations between the eigenfunctions and eigenfrequencies on one hand, and the boundary conditions, the dimensions and the material properties on the other hand. The experimental results on basses, which will be given in the following chapters, can be compared to this model which will be done in Paragraphs 4.4, 6.6 and 6.7. This way, the beam serves as a standard of a vibrating structure by means of which the results of the vibration measurements on basses can be interpreted and organised.

4. EXPERIMENTAL MODAL ANALYSIS

A common way for investigating the vibrational behaviour is Modal Analysis. Results of experiments on basses are reported by Heise (1993) and Wogram (1994). Investigations executed at the Institute of Mechanics are described in detail by Garrelfs and Schneiders (1995). Results are documented and discussed by Fleischer and Zwicker (1996, 1997).

4.1. Method and Set-up

The instruments No. 1 (Action Bass) and No. 3 (Dyna Bass), both made from wood and carrying four strings, served as measuring objects. The body of the instrument lied with its back on a foam layer on a positioning device; cf. Fig. 9. The neck and head were free. The positioning in the direction of two coordinates was provided by stepping motor drives and controlled by a computer via GP interface bus. An electrodynamic mini-shaker was used for excitation of the bass structure close to the bridge. It was pressed from the rear side against the back. As an excitation signal, pseudo random noise within the frequency range up to 500 Hz was applied. The force perpendicular to the body plane was picked up by a piezoelectric force gauge and used as a reference.



Fig. 9. Action Bass on the positioning plate ready for Modal Analysis.

For the non-contact measurement of the structural vibration a Laser Doppler Vibrometer (Polytec OFV 3000 with OFV 302) was applied which detects the velocity in the direction of the laser beam. The component perpendicular to the body-neck-plane, *i.e.* in the same direction as the exciting

force, was ascertained. The transfer function velocity/force was determined for each measuring point by means of a dual-channel FFT analyser (Ono Sokki CF 6400) and transferred via GPIB to a computer. Modal Analysis was performed by the program system SMS StarModal. Typical results are given in the following paragraphs.

4.2. Modes of the Action Bass

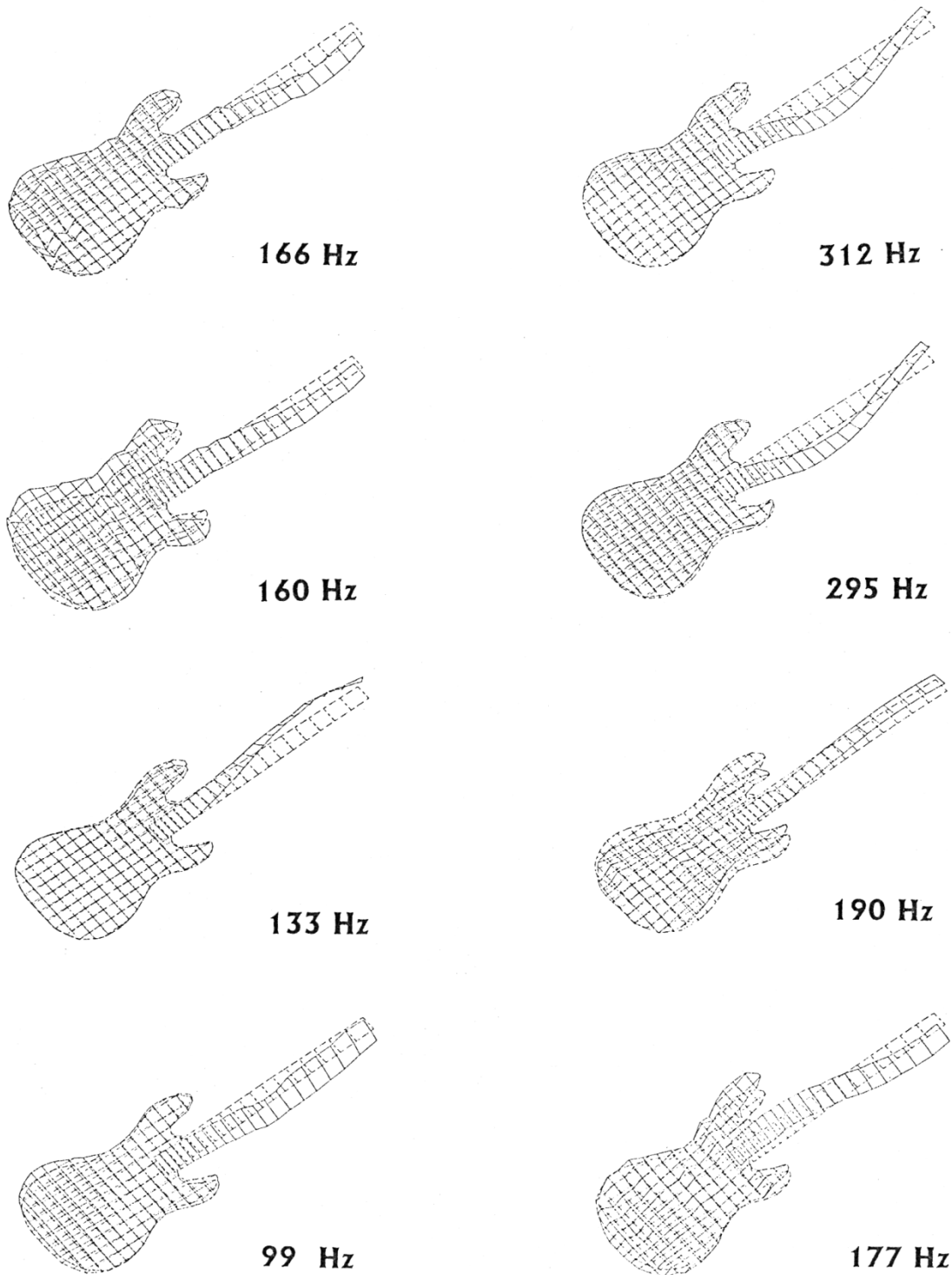


Fig. 10. Some eigenmodes and eigenfrequencies obtained by Modal Analysis for the Action Bass 1.

Selected vibration eigenmodes as obtained by the above mentioned procedure are compiled in Fig. 10 for frequencies between 99 Hz and 312 Hz. Broken lines represent the undeformed instrument (the head is dropped). The vibration patterns for eight eigenfrequencies are indicated by solid lines.

On the whole, the body exhibits less motion than the neck. Only the appendices of the body ("horns"), which are created by the two cutaways, prove as relatively mobile (cf. 190 Hz in Fig. 10). The rest of the body responds almost rigid to the excitation and sometimes tends to a twisting motion (cf. 160 Hz and 190 Hz). As expected, the neck is much more flexible than the body. For 133 Hz torsion predominates. An expressed bending motion ("beam behaviour") of the neck is observed for 160 Hz, 166 Hz and 177 Hz. Only minor differences occur which are mainly restricted to the appendices of the body, which becomes obvious when regarding the animated vibration. A different bending pattern with an additional node on the neck is observed for 295 Hz and 312 Hz.

4.3. Modes of the Dyna Bass

Six selected modes as obtained by the experiments are given in Fig. 11 for frequencies from 60 Hz up to 298 Hz. Like in Fig. 10, broken lines indicate the undeformed structure (excluding the head), while the solid lines mark the vibration patterns as obtained by Modal Analysis.

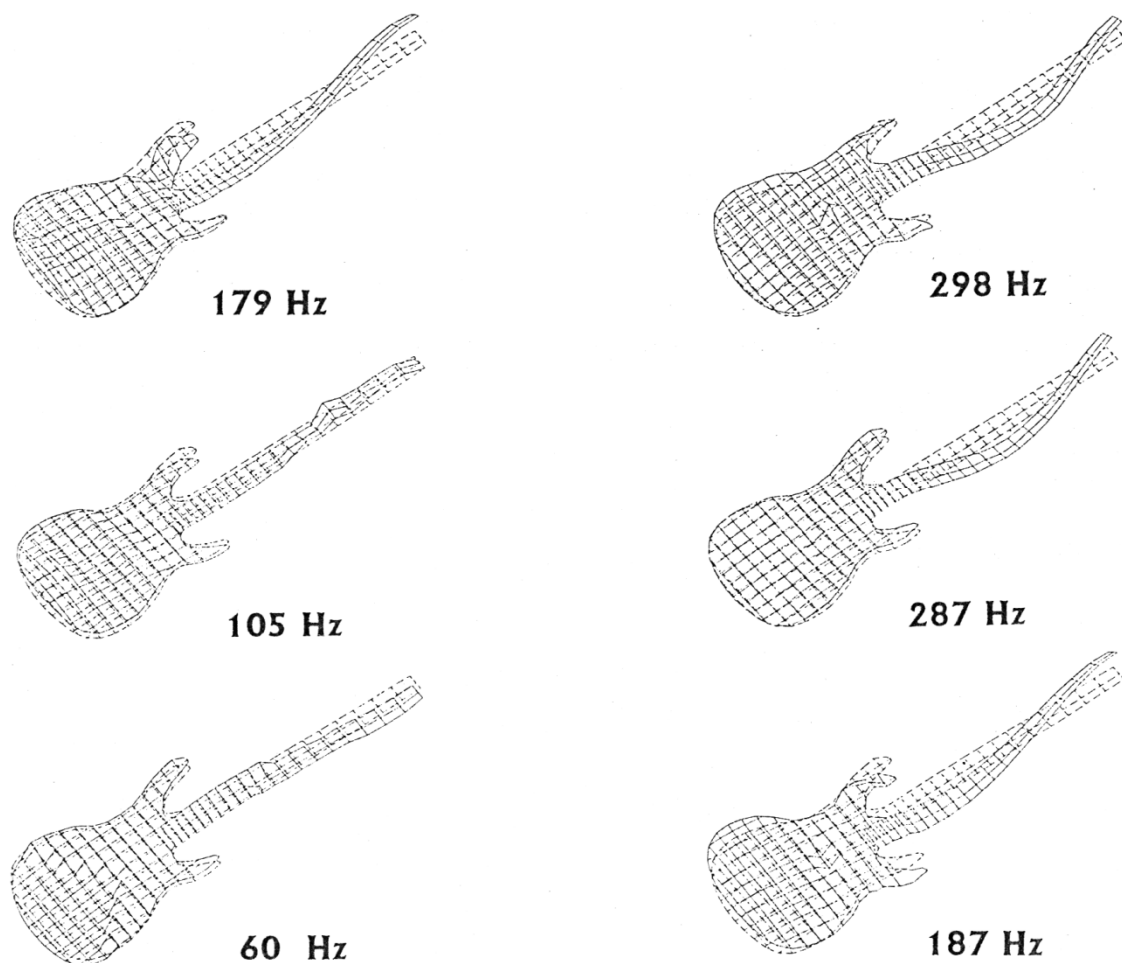


Fig. 11. Some eigenmodes and eigenfrequencies obtained by Modal Analysis for the Dyna Bass 3.

The experimental data for this instrument confirm what has already become obvious for the Action Bass: The body proves as less mobile than the neck with the exception of the two horns (cf. 179 Hz in Fig. 11). A twisting motion of the body is observed *e.g.* for 187 Hz. The neck, which is much more flexible than the body, shows an expressed bending motion for 179 Hz and 187 Hz with one node. An eigenpattern with two nodes on the neck occurs for 287 Hz and 298 Hz. Again, only small differences between adjacent modes become visible which are mainly restricted to the horns or an in-phase or anti-phase motion with respect to the neck.

4.4. Comparison to Beam Modes

In the following paragraph the modes and frequency ratios found by Modal Analysis are compared to beam modes for standard boundary conditions as dealt with in the Paragraphs 3.2 through 3.4.

4.4.1. Modes of a Beam of Constant Bending Stiffness

The relations of the eigenfrequencies of an ideal beam are given by Eqs. (8, 12, 16). In Tab. III the ratios of the second through forth eigenfrequency, normalised to the first eigenfrequency, are gathered.

Boundary condition	c - f	f - f	ss - f
1 st eigenfrequency	f_1	f_1	f_1
2 nd eigenfrequency f_2/f_1	6.267	2.757	3.241
3 rd eigenfrequency f_3/f_1	17.547	5.404	6.761
4 th eigenfrequency f_4/f_1	34.386	8.933	11.562

Tab. III. Ratios f_j/f_1 of the eigenfrequencies for beams with different boundary conditions.

In conjunction with the mode shapes (Figs. 6 through 8) the frequency ratios compiled in Tab. III can serve to identify the boundary conditions which suit best for modelling the bass as a beam.

4.4.1. Modes of the Action Bass

On the top of Fig. 12 the undeformed structure is shown. Three modes in which the bending motion of the neck dominates the torsion are compiled with the frequencies 69 Hz, 166 Hz and 295 Hz. Assuming that $f_1 = 69$ Hz, the frequency ratios are

$$\begin{aligned} f_2/f_1 &= 2.41 \quad \text{and} \\ f_3/f_1 &= 4.28 \quad . \end{aligned}$$

Obviously, this estimation is very sensitive to the normalising value, *i.e.* the frequency of the first mode. Comparing the mode shapes and the frequency ratios to the standard cases (cf. Tab. III) ex-

cludes the boundary condition clamped-free. To a certain approximation, a relationship to the boundary conditions free-free (or simply supported-free) can be seen with the bass body free (or

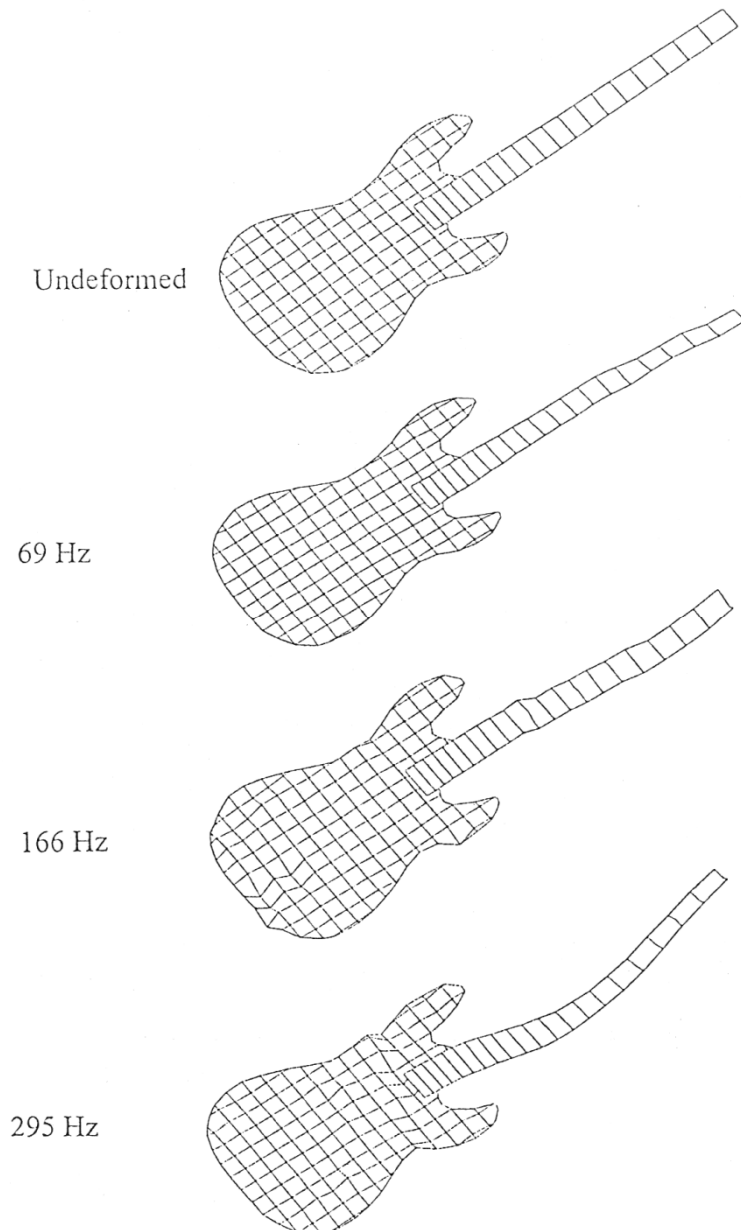


Fig. 12. Some bending modes of the Action Bass including the undeformed structure.

supported) and the head free. However, in both cases the experimental frequency ratios are smaller than the ratios for the beam.

4.4.2. Modes of the Dyna Bass

Figs. 13 and 14 show results for the Dyna Bass. In Fig. 13 two modes with the frequencies 50 Hz and 179 Hz are displayed. They could be identified as the first and second bending modes and are similar to the simply supported-free patterns 1 and 2 of the beam in Fig. 8. The frequency ratio is

$$f_2/f_1 = 3.58$$

which is higher than the corresponding ratios for the free-free or simply supported-free beam (cf. Tab. III).

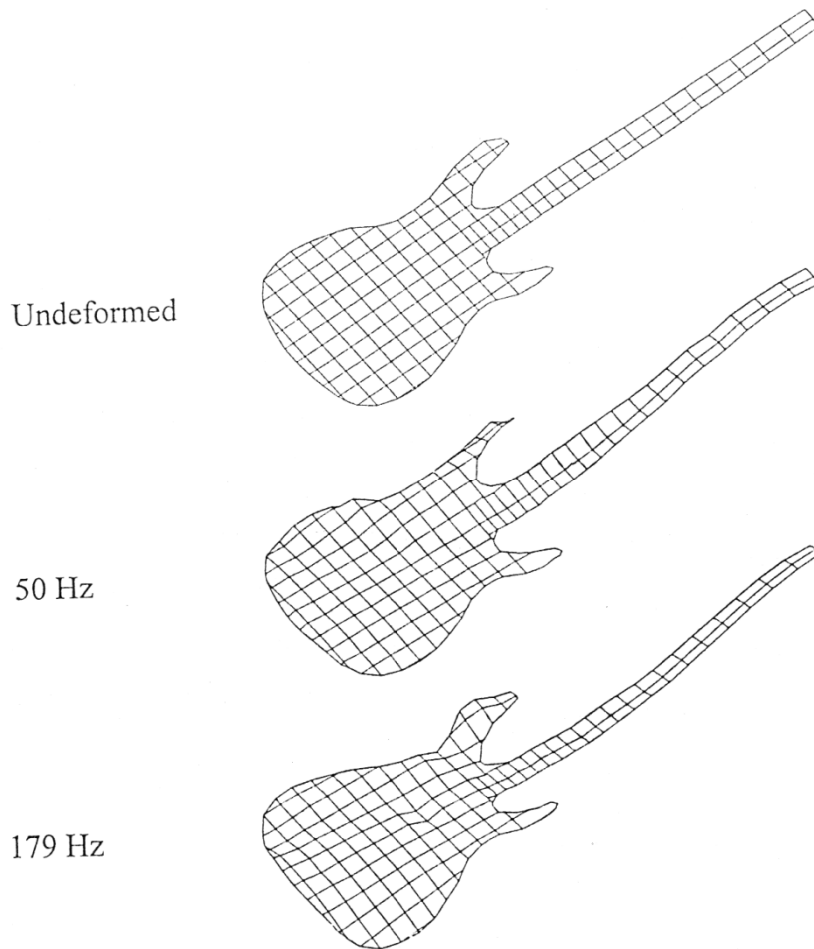


Fig. 13. Two different bending modes of the Dyna Bass including the undeformed structure.

If two further modes (see Fig. 14) are chosen from the series of experimental results, the ratio is

$$f_2/f_1 = 5.95 \quad .$$

In this case, the boundary condition clamped-free (Tab. III) seems to be most closely related to the vibrating bass. Obviously, the base of the collected experimental data is not yet sufficient to allow for a definite vote of an apt beam model.

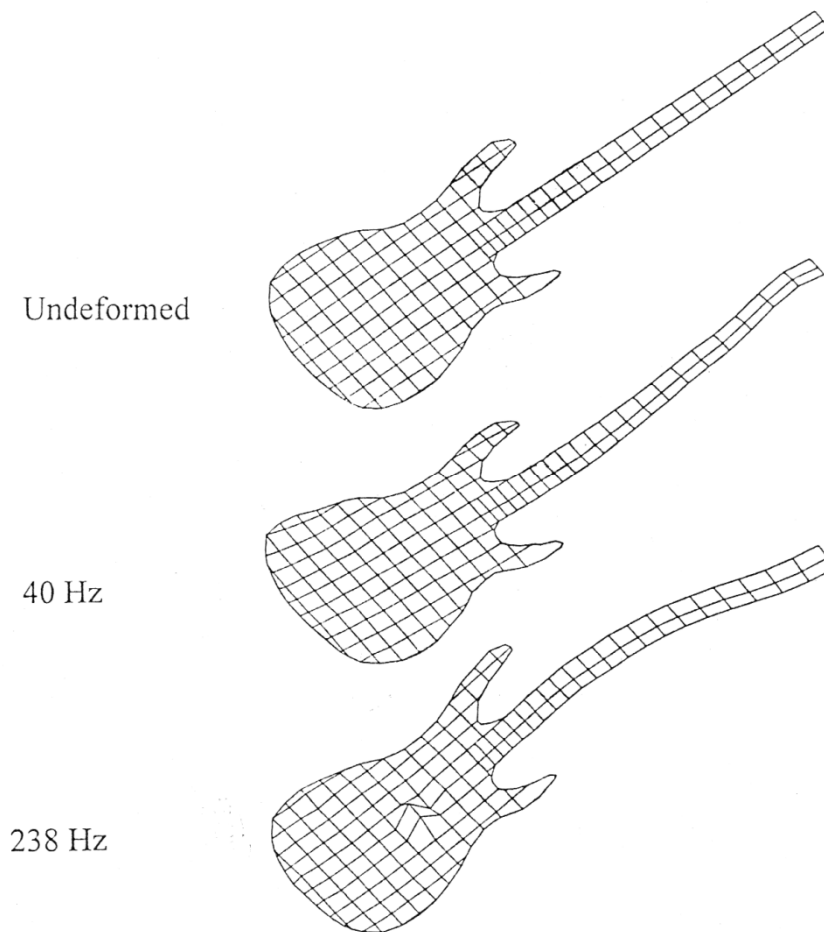


Fig. 14. Two further bending modes of the Dyna Bass including the undeformed structure.

4.5. Concluding Remarks

The Modal Analysis yields a great amount of modes, for the Action Bass *e.g.* 32 modal patterns and frequencies in the frequency range up to 300 Hz. In some cases, the differences between these modes are only minor. Since the amplitudes are normalised, there is no objective control to which extent a particular vibration pattern develops in practical playing use. It should be mentioned that therefore the selection of the modes which are actually relevant for the function of the bass as a musical instrument is very delicate and subject to some ambiguousness.

Above all, there is strong evidence that the boundary conditions are quite different during the measurement and in playing practice. In this sense, the measuring set-up as used for Modal Analysis with a foam-coated plate as a support for the body, and the neck as well as the head freely vibrating, is not optimal. It should be tried to better simulate the conditions of the bass during normal playing, *i.e.* there is need for a more "natural" support and excitation in the experiments. That is the motivation for laying less stress on a highly sophisticated processing of the vibration data, but more stress on realistic boundary conditions.

5. OPERATING DEFLECTION SHAPES

For the measurements described in the following chapter a Polytec Scanning Vibrometer was used. It consists in a Laser Vibrometer which determines the velocity of a vibrating surface by means of the Doppler effect. The laser beam is deflected by small galvo mirrors which offers the possibility of fast area scans. In our example a typical scan lasts only some minutes. This way, measurements *in situ* are feasible with a subject holding the instrument in normal playing position and the boundary conditions during the experiment being very close to the "natural" conditions.

5.1. Measuring Set-up and Procedure

The vibrometer ascertains the component of the surface velocity in the direction of the laser beam; cf. Twork (1997). Since an electric bass is an almost plane structure it suits well to this measuring method. The velocity is derived from the shift of the frequency of the reflected compared to the frequency of the original laser light. As a rule, the reflection from the bass surfaces proved as strong enough to yield a sufficient amount of reflected beam in order to allow for the comparison and to yield a satisfactory signal-to-noise ratio.

In the vibration measurement, the velocity at a particular measuring point represents the output signal, while the force which excites the bass serves as the input. It is generated by a B&K mini-shaker which is pressed against the rear of the neck close to the seventh fret. The force is measured by a B&K piezoelectric force gauge and a B&K charge amplifier. In the data processing system of the Scanning Vibrometer a dual-channel FFT is performed and the frequency response function computed, which gives the complex ratio of the velocity and the exciting force. The result is a transfer admittance for each measuring point.

All transfer functions are stored and processed in the computer of the measuring system or transferred to other computers for further calculations. They can be averaged to serve as a basis for selecting the frequencies at which the vibrational patterns are to be displayed. In the following, this averaged frequency response function (FRF) is given for each bass including the frequency bands which were selected for the visualisation of the vibrations. The advanced data processing necessary for Modal Analysis (such as *e.g.* curve fitting) could be performed on the basis of these data using an additional software package such as StarModal, but was not executed in the present investigation. This implies that the direct results of the vibrometer measurements, which will be presented in the following, are not modes in the closer sense, but operating deflection shapes (ODSs; cf. Richardson (1997)). They reflect the state in which the instrument vibrates at the selected frequency at the underlying boundary conditions and excitation. Neither the modal frequency (eigenfrequency) nor the modal damping, as calculated by Modal Analysis, are available. The FRF represents a superposition of the contributions of all modes. Nevertheless, the higher a maximum in the FRF is, the more dominates one mode and the less contribute the remaining modes. That means, if the frequency is thoroughly chosen from a peak in the FRF, it may serve as a good estimate for the eigenfrequency, and the displayed ODS may serve as a good estimate for the mode shape.

This procedure is practised for the following considerations. The standard software of the Scanning Vibrometer is used for selecting and displaying the most essential ODSs. The results are scaled in m/s per N or s/kg and refer to an excitation of the neck close to the seventh fret by a force perpendicular to the fingerboard plane. Each measurement was four times averaged. 200 frequency lines in

the range from 0 Hz to 500 Hz were used which corresponds to a frequency resolution of 2.5 Hz. The velocity was measured on a grid of about 100 (Carvin Bass) and 200 (the other basses) points, respectively. A sitting person held the bass during the whole experiment in playing position on his right thigh with the left hand grasping the neck at the lower frets. Each individual measuring situation can be taken from the video pictures which are presented at the beginnings of the following paragraphs.

5.2. Experimental Results for the Action Bass

The way in which a person held the Action Bass No. 1 for measurement is shown in Fig. 15. The vibration exciter acts on the neck from the rear side in the vicinity of the seventh fret. The bass body is lying with its lower part on the thigh of the person. The right arm of the person is resting on the upper part of the bass body. The left hand is grasping the neck near the lower frets. This configuration was not changed during the measuring procedure.

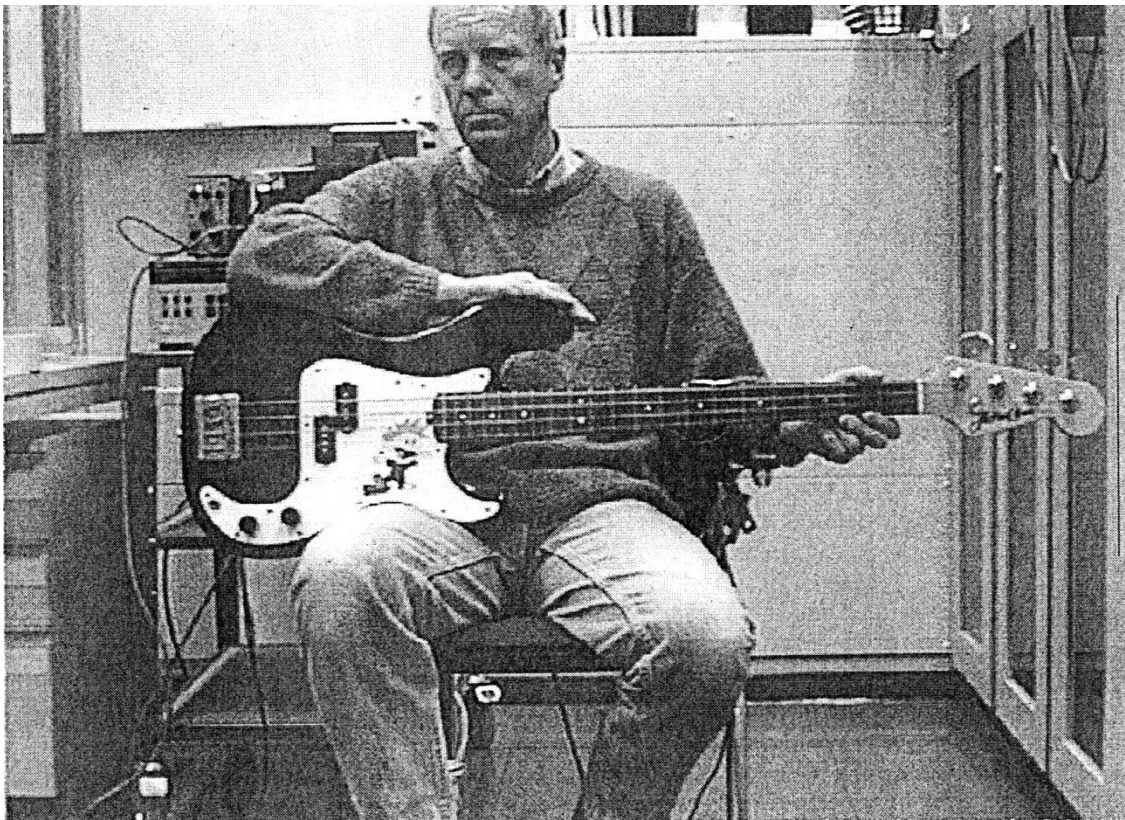


Fig. 15. Action Bass No. 1 during the experimental determination of the operating deflection shapes by means of the Scanning Vibrometer.

The whole of the results is presented in Fig. 16 as the average of all measured frequency response functions. The maxima reach -50 dB to -40 dB with a normalising value of 1 m/s per N or 1 s/kg.

That means that in a maximum the averaged FRF reaches 3 ms/kg to 10 ms/kg. As indicated by the bands in Fig. 16, the peaks serve as indicators for resonances and for the corresponding ODSs. Six frequencies were chosen for presentation. The corresponding vibrational patterns are compiled in Figs. 17 and 18.

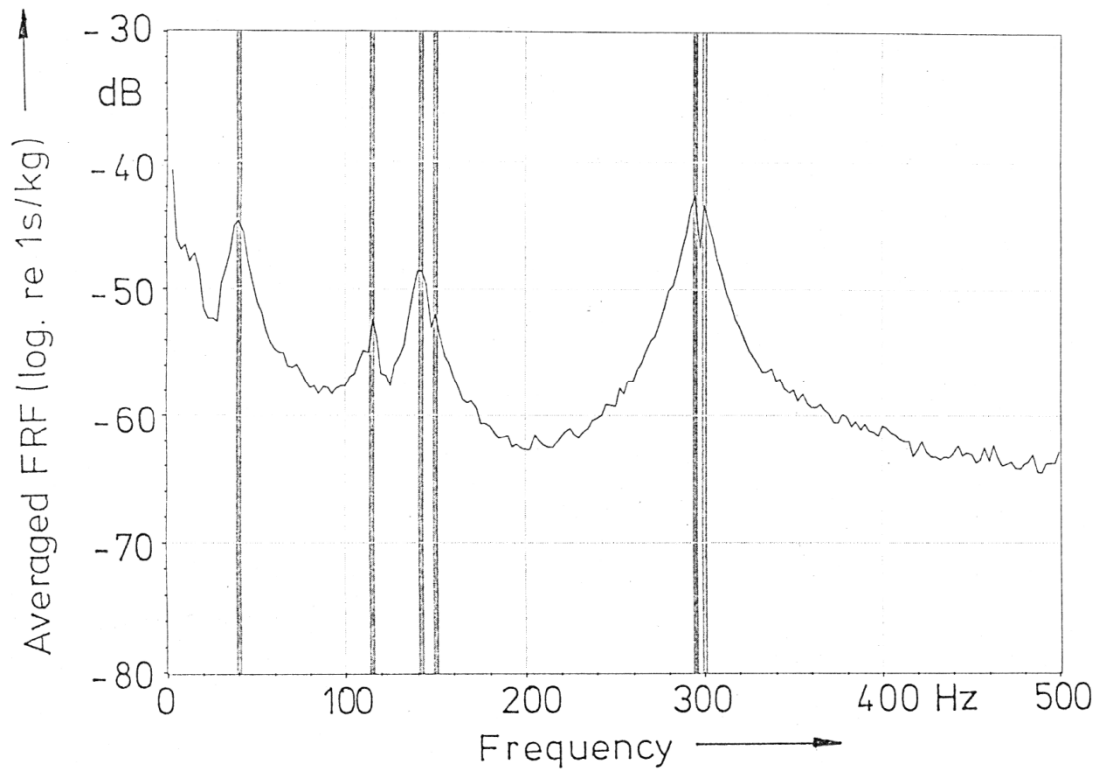


Fig. 16. Averaged frequency response function (measured velocity at all points normalised to the excitation force as a function of frequency) of the Action Bass No. 1. The stripes mark the bands chosen for the visualisation of the main operating deflection shapes.

The magnitude of the velocity, normalised to an excitation force of 1 N, is coded in black and white tones which creates pictures comparable to Chladni figures; cf. Chladni (1787). It is useful to imagine that a white bass is covered with black powder. While the bass is vibrating, the powder grains move to locations where the bass is not in motion. This way, the nodes become visible as black portions and the antinodes as white portions. From the example in Fig. 17 can be taken that for the Action Bass vibrating at a frequency of 300 Hz the body, in particular the bridge, is practically immobile. In contrast, the neck vibrates with two antinodes and a nodal region in the vicinity of the person's left hand. The gauge at the left side indicates a dynamic range from 0 mm/s (absolute black) to 10 mm/s (absolute white) for 1 N excitation force. For the sake of simplicity, the gauges are dropped in the following images.

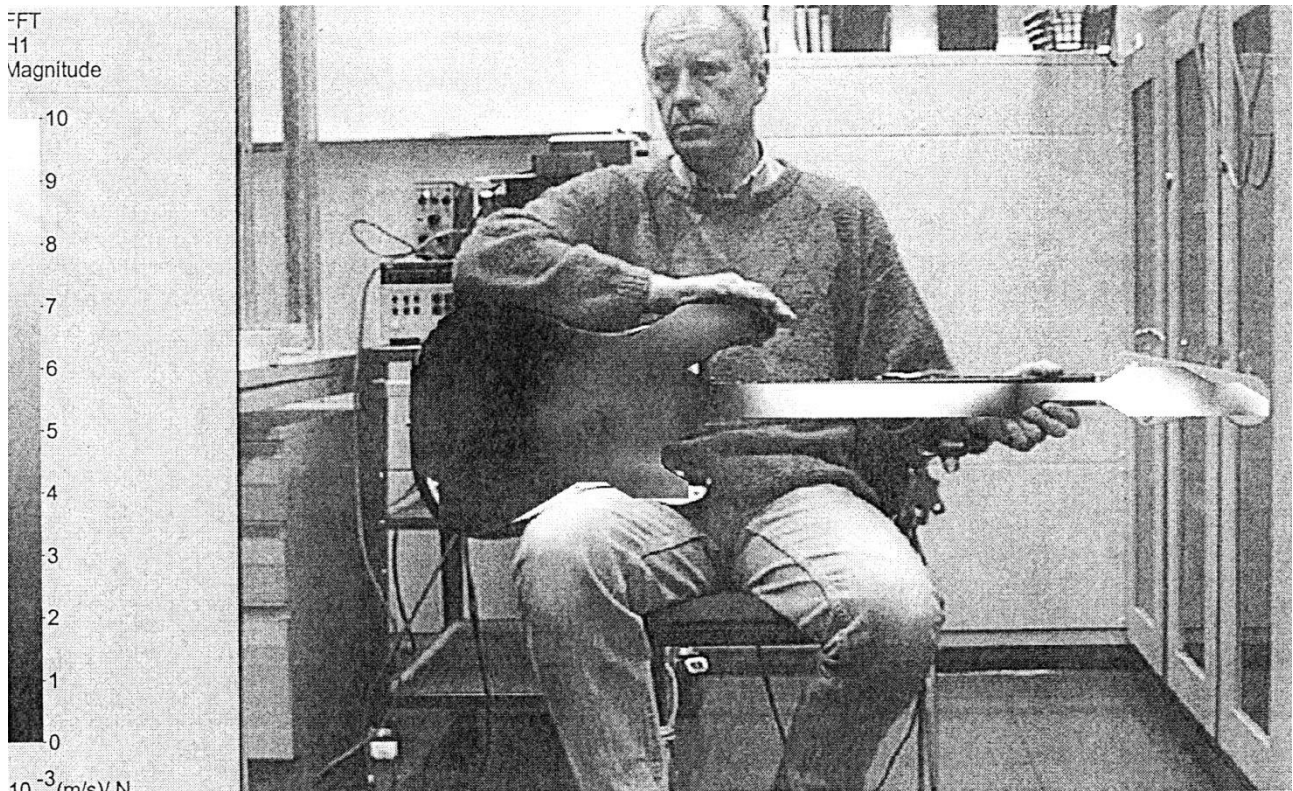
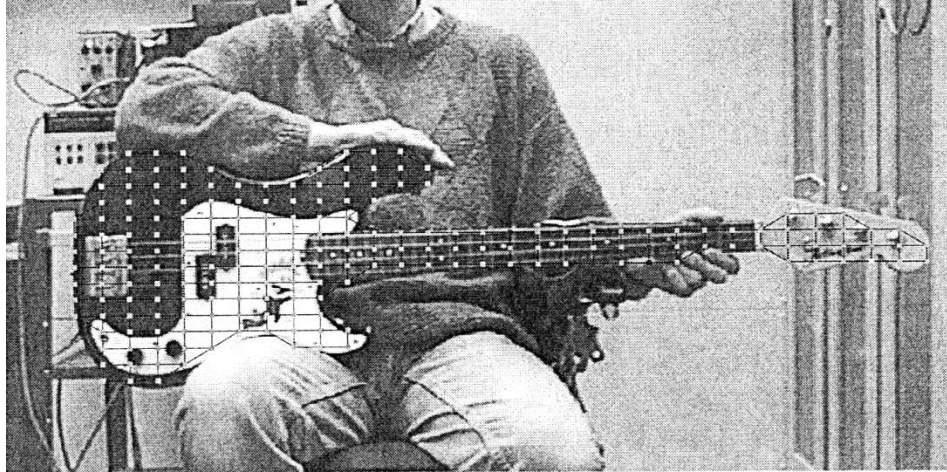


Fig. 17. Operating deflection shape of the Action Bass No. 1 for 300 Hz. The gauge in the left part indicates the correspondence of grey tones to the magnitude of the velocity for 1 N excitation force: Black means no vibration while white marks a velocity magnitude of 10 mm/s.

In Figs. 18b - g six ODSs are displayed. In addition, Fig. 18a shows the measuring grid in order to give an impression of the spatial resolution. The frequency of the ODS in Fig. 18b is 40 Hz, *i.e.* close to the fundamental of the open E_1 string (41 Hz). The frequencies of the other five ODSs range from 115 Hz (G_2 string 3rd fret) to 300 Hz (G_2 string 19th fret). Three fundamental vibrational patterns are observed with a node (Fig. 18b), an antinode (Figs. 18c - e) and a node again (Figs. 18f - g) in the vicinity of the grasping left hand. The differences between the ODSs which belong to the same main type are minor. For instance, they consist in an in-phase and anti-phase, respectively, motion of the body horns or in an additional torsion of the neck which superimposes the fundamental bending motion.

*Fig. 18a.
Measuring
grid.*



*Fig. 18. In-situ operating deflection shapes of the Action Bass No. 1:
Measuring grid and vibrational patterns for the announced frequencies.
Black areas indicate a low vibration magnitude, white areas a high magnitude
in the order of 10 mm/s for 1 N excitation force.*

*Fig. 18b.
40 Hz.*



*Fig. 18c.
115 Hz.*



Fig. 18d.
142 Hz.

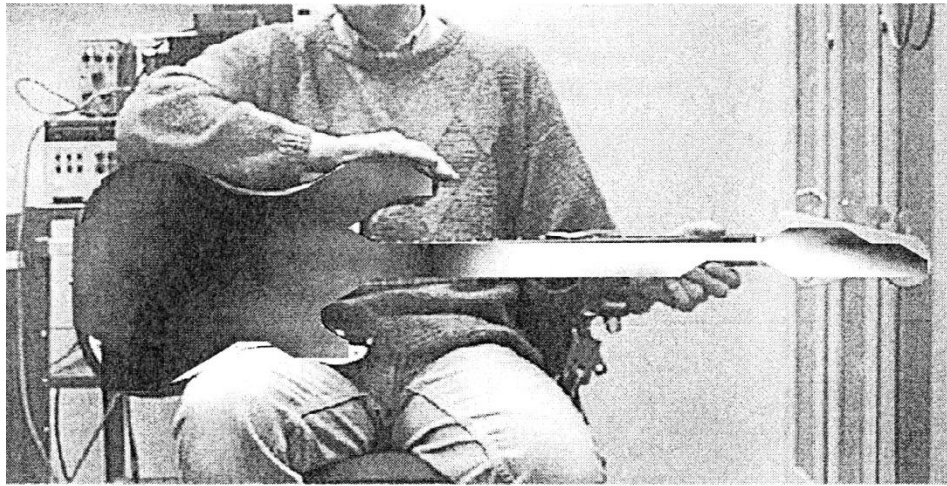


Fig. 18e.
150 Hz.



Fig. 18f.
295 Hz.

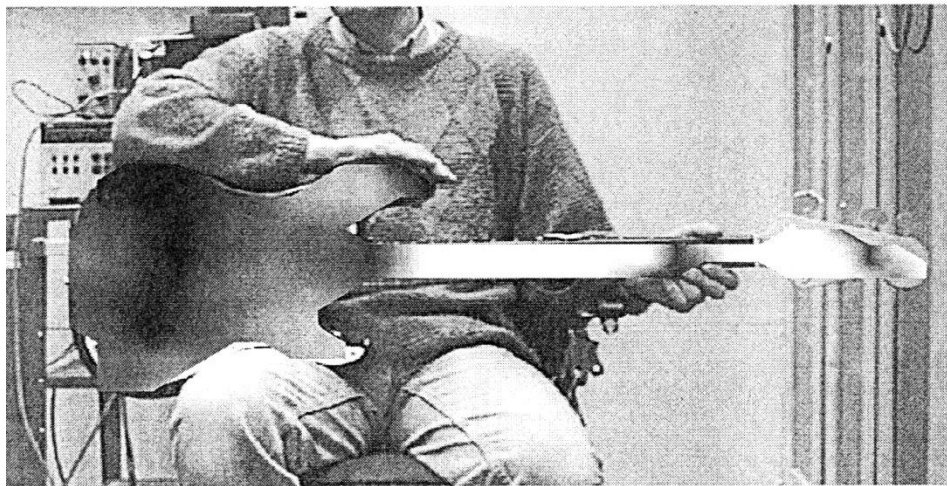
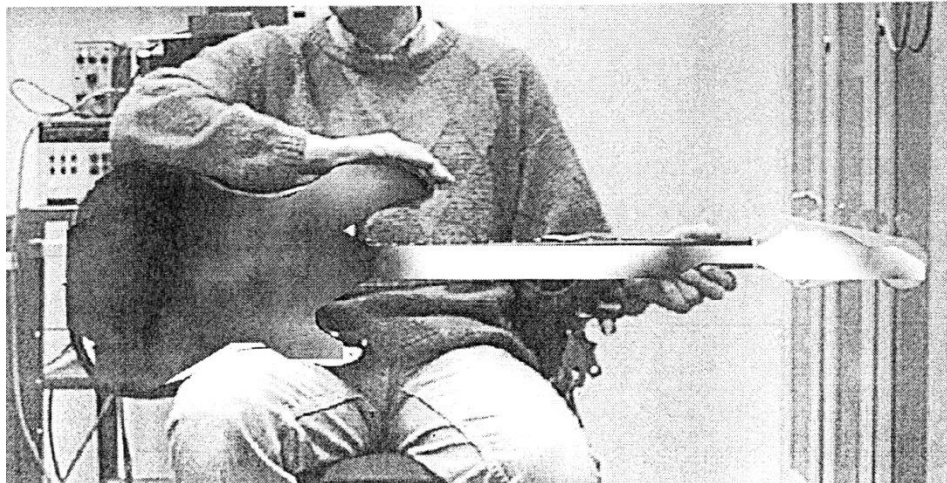


Fig. 18g.
300 Hz.



5.3. Experimental Results for the Music Man Bass



Fig. 19. Music Man Bass No. 2 during the experimental determination of the operating deflection shapes by means of the Scanning Vibrometer.

Experimental results for the Music Man Bass No. 2 (Fig. 19) are given in the present paragraph. The averaged FRF in Fig. 20 shows three main peaks at about 40 Hz, 140 Hz and 280 Hz with seven local maxima. The corresponding ODSs are compiled in Fig. 21. Besides the measuring grid (displayed in Fig. 21a) seven ODSs are selected with frequencies between 42 Hz (B_0 string 5th fret or open E_1 string) and 295 Hz (G_2 string 19th fret).

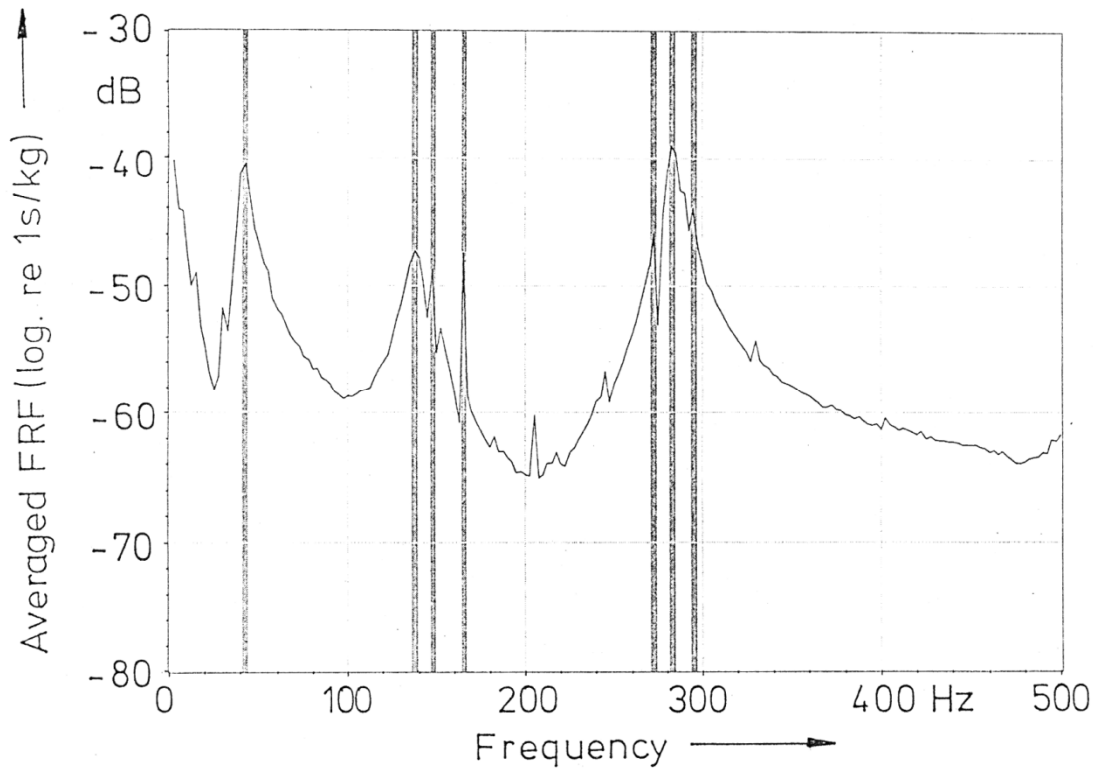


Fig. 20. Averaged frequency response function (measured velocity at all points normalised to the excitation force as a function of frequency) of the Music Man Bass No. 2. The stripes mark the bands chosen for the visualisation of the main operating deflection shapes.

Comparable to the Action Bass (Fig. 16) the averaged FRF of the Music Man Bass exhibits three main peaks. The upper two peaks show several local maxima. In Fig. 21 seven ODSs are displayed. According to the main peaks in the FRF of Fig. 20 three fundamental vibrational patterns are separable. The first one (Fig. 21b) has a node close to the left hand that grasps the neck at the low frets. The second type (Figs. 21c - e) is characterised by an antinode in the vicinity of the hand. The third type (Figs. 21f - h), again, shows a node at the grasping left hand.

Fig. 21a.
Measuring
grid.

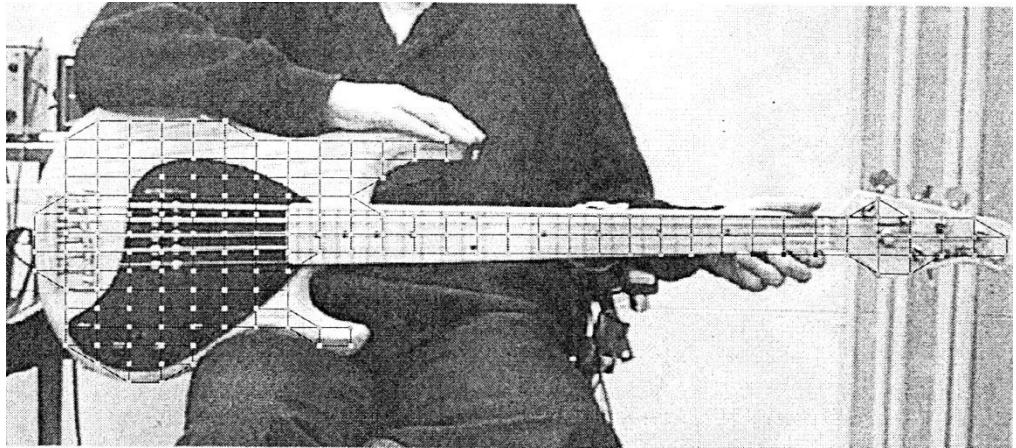


Fig. 21. In-situ operating deflection shapes of the Music Man Bass No. 2: Measuring grid and vibrational patterns for the announced frequencies. Black areas indicate a low vibration magnitude, white areas a high magnitude in the order of 10 to 20 mm/s for 1 N excitation force.

Fig. 21b.
42 Hz.

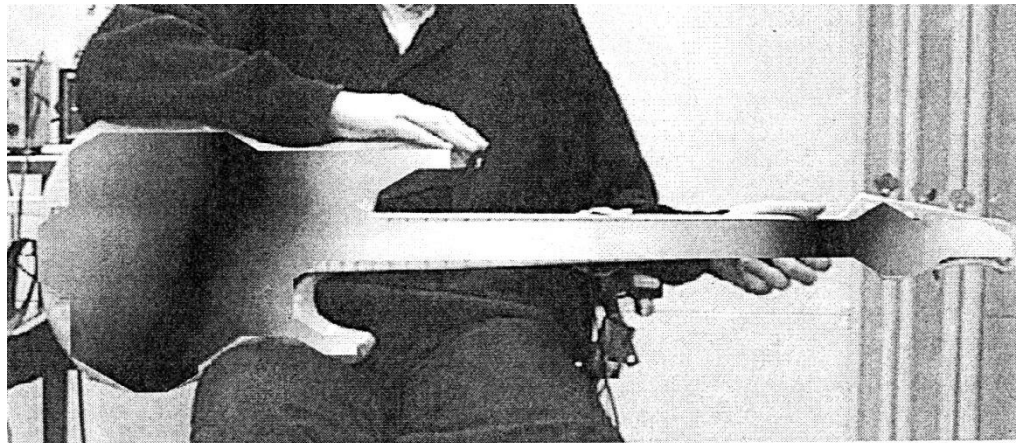


Fig. 21c.
137 Hz.

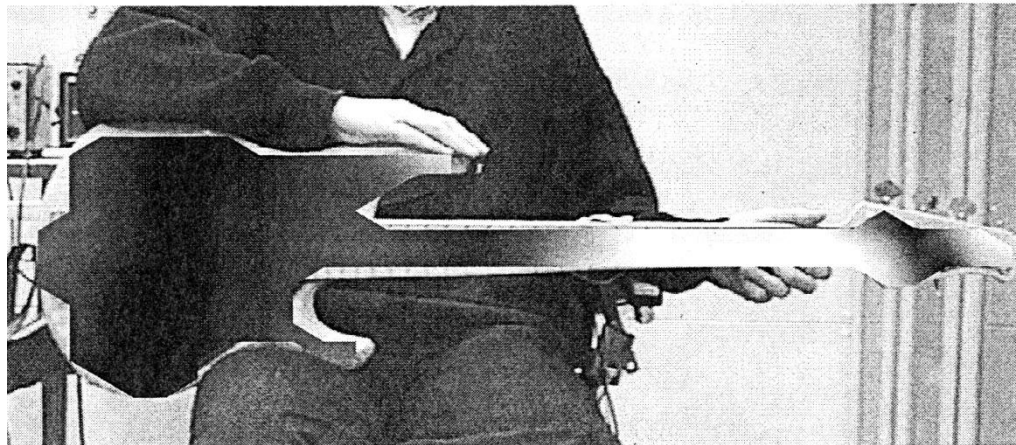


Fig. 21d.
147 Hz.

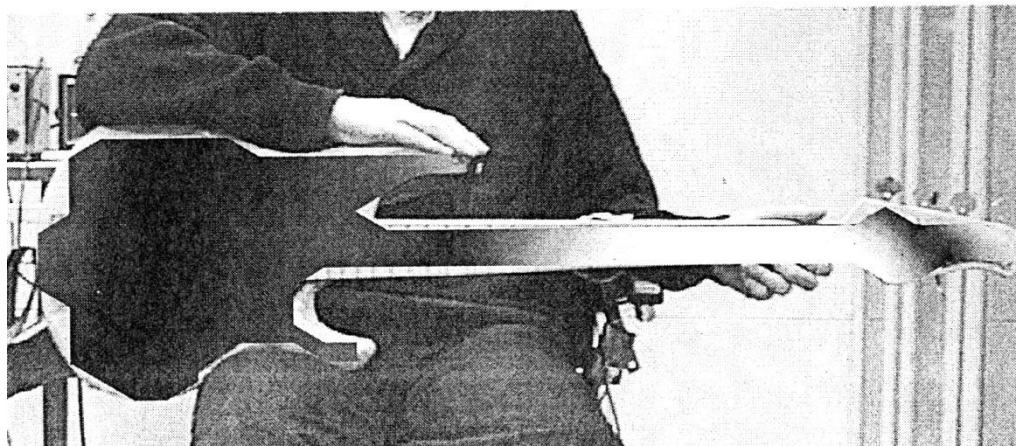


Fig. 21e.
165 Hz.

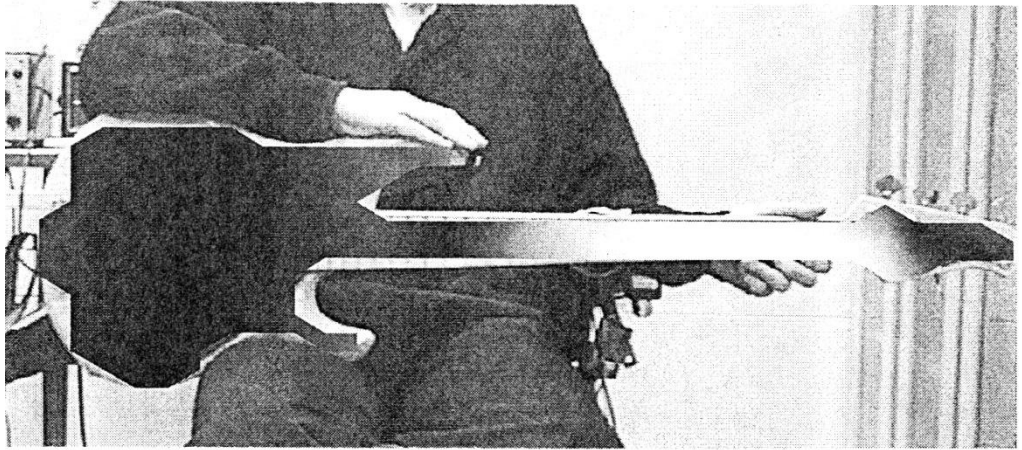


Fig. 21f.
272 Hz.

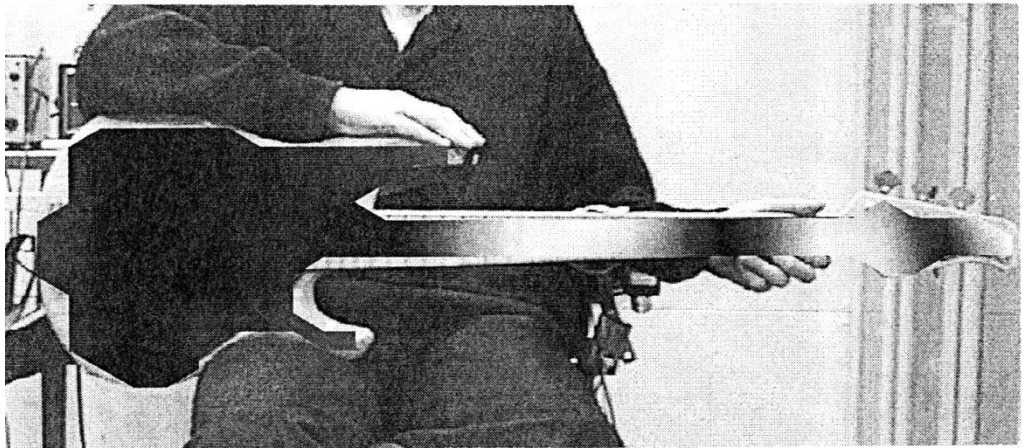


Fig. 21g.
283 Hz.

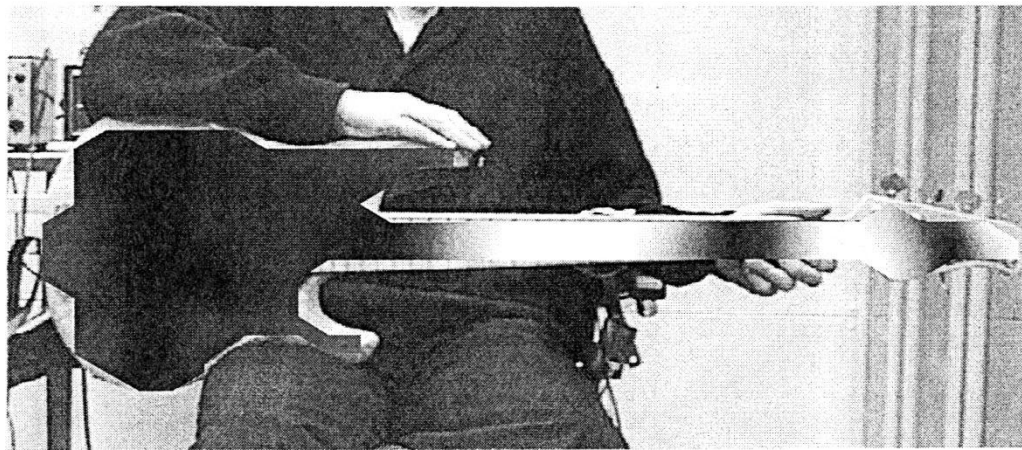
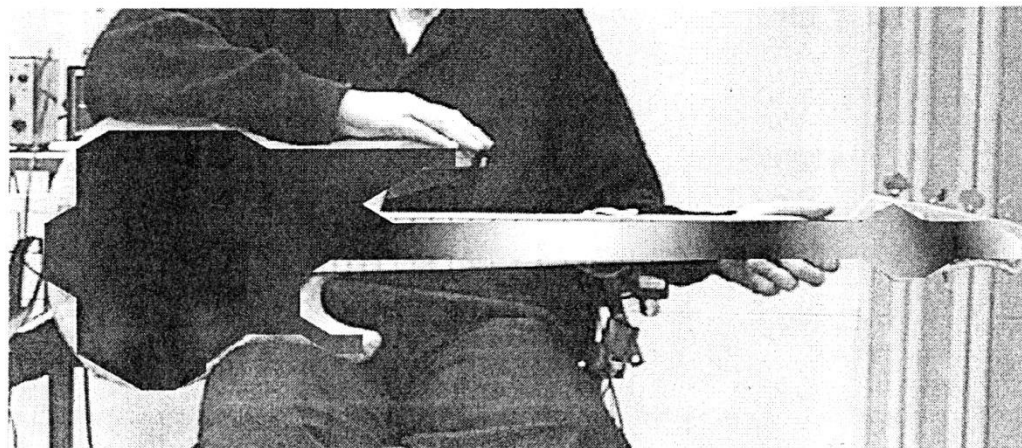


Fig. 21h.
295 Hz.



5.4. Experimental Results for the Dyna Bass



Fig. 22. Dyna Bass No. 3 during the experimental determination of the operating deflection shapes by means of the Scanning Vibrometer.

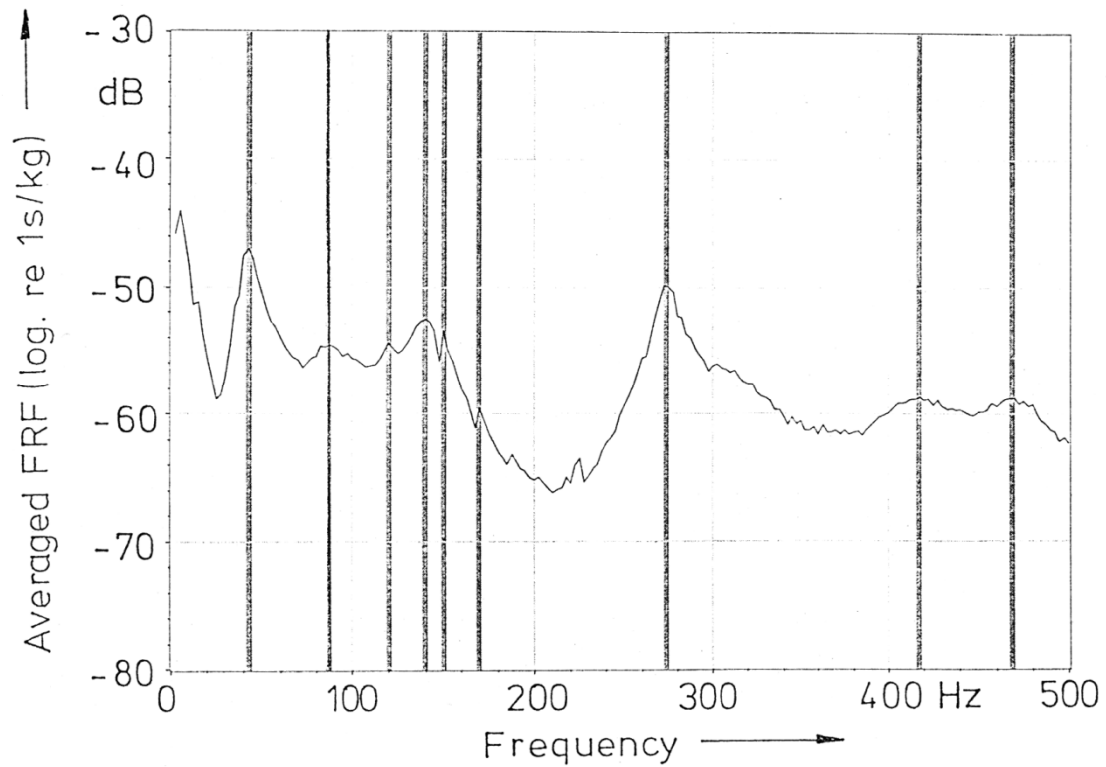


Fig. 23. Averaged frequency response function (measured velocity at all points normalised to the excitation force as a function of frequency) of the Dyna Bass No. 3. The stripes mark the bands chosen for the visualisation of the main operating deflection shapes.

The Dyna Bass No. 3 is shown in Fig. 22 and the average of its FRFs in Fig. 23. Compared to the Action and Music Man Basses more peaks, but less pronounced in height, appear. Nine ODSs were chosen for presentation. As can be taken from Fig. 24, they range from 42 Hz (open E_1 string) up to 468 Hz (second harmonic of 234 Hz corresponding to the G_2 string 15th fret). Several vibrational patterns with different numbers of nodes on the neck are observed. The lower part of the body, which carries the bridge, proves as relatively mobile.

Fig. 24a.
Measuring
grid.

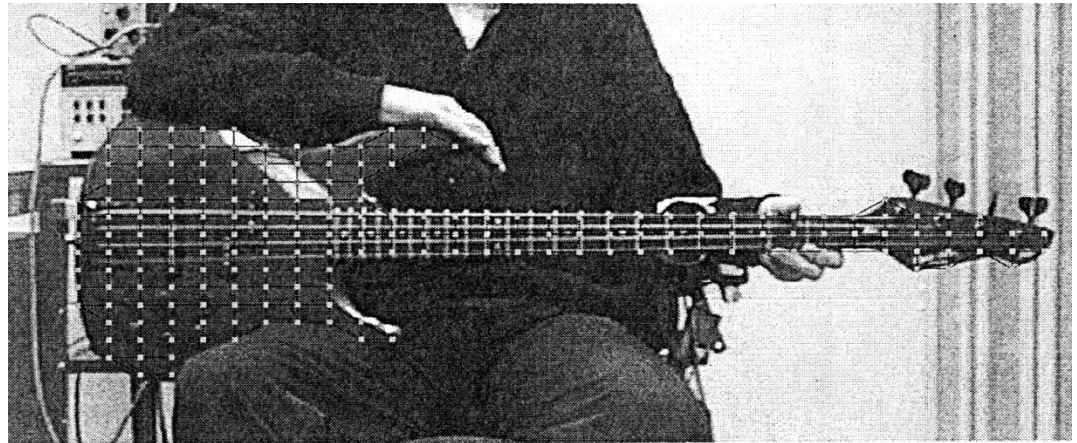


Fig. 24. In-situ operating deflection shapes of the Dyna Bass No. 3:
Measuring grid and vibrational patterns for the announced frequencies.
Black areas indicate a low vibration magnitude, white areas a high
magnitude in the order of 3 to 12 mm/s for 1 N excitation force.

Fig. 24b.
42 Hz.

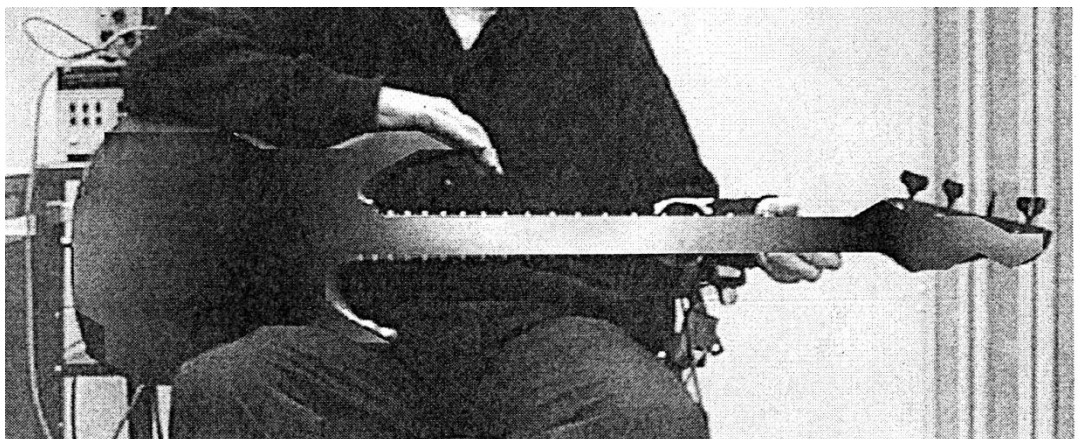


Fig. 24 c.
88 Hz.

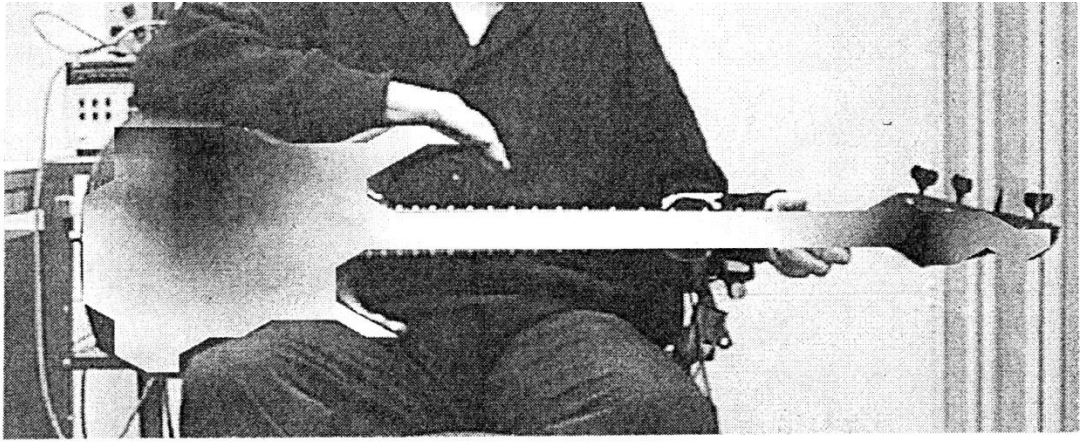


Fig. 24d.
120 Hz.

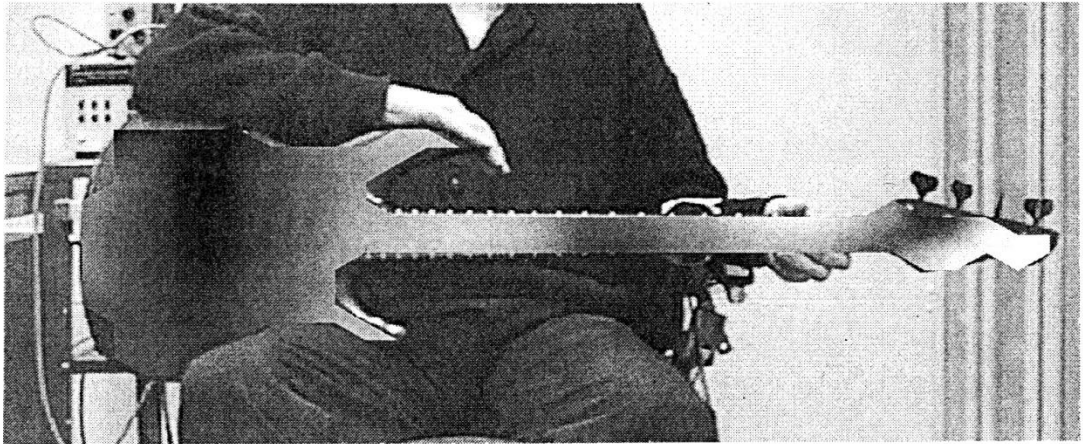


Fig. 24e.
140 Hz.

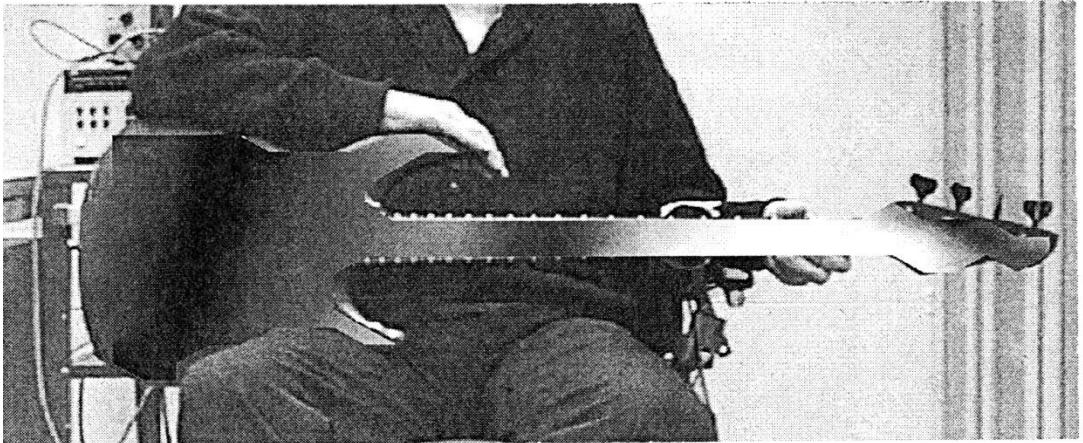


Fig. 24f.
150 Hz.

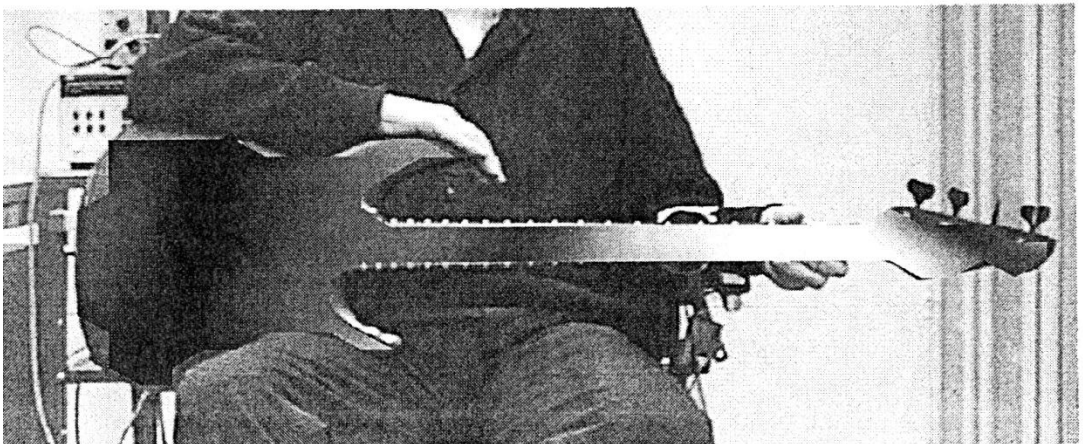


Fig. 24 g.
169 Hz.

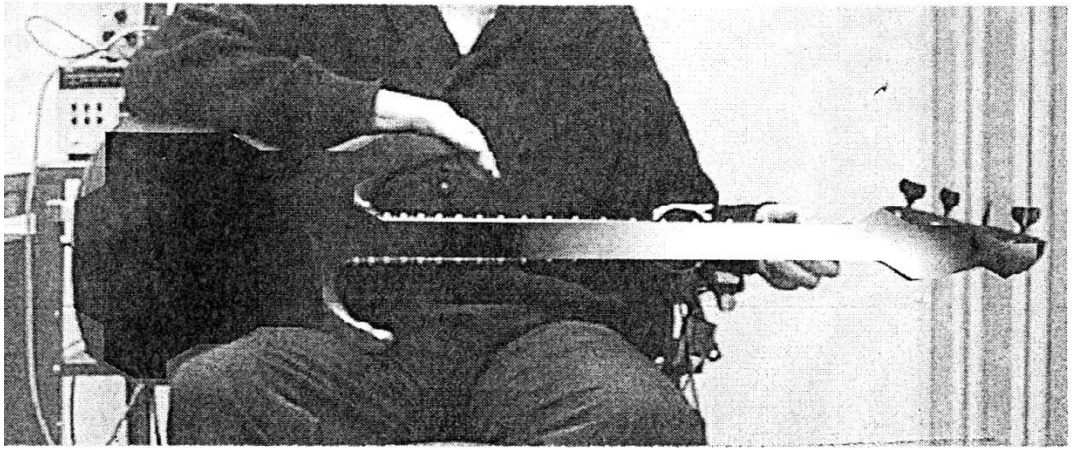


Fig. 24 h.
274 Hz.

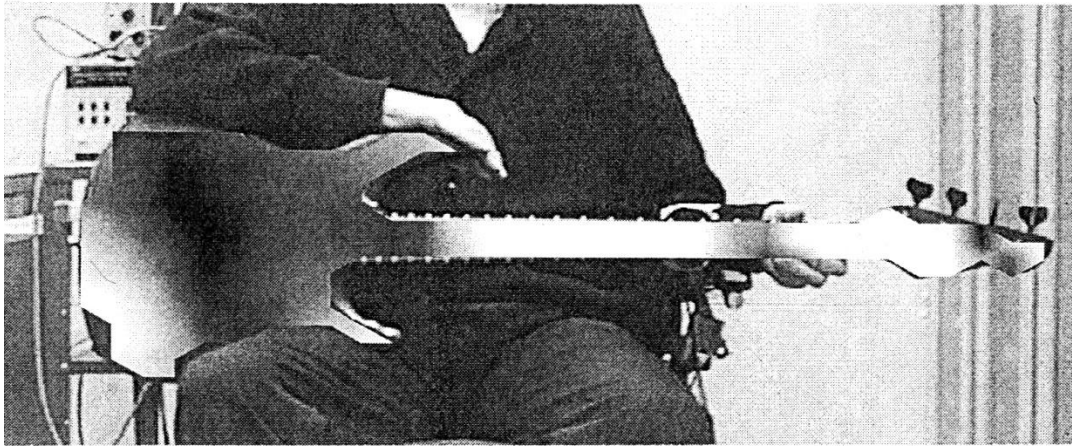


Fig. 24 i.
417 Hz.



Fig. 24 j.
468 Hz.



5.5. Experimental Results for the Carvin Bass



Fig. 25. Carvin Bass No. 4 during the experimental determination of the operating deflection shapes by means of the Scanning Vibrometer.

The Carvin Bass No. 4 (Fig. 25) is equipped with six strings. The additional strings are tuned a fourth lower and a fourth higher, respectively, compared to a normal four-string bass. Thus, the fundamental frequencies of the open strings range from 31 Hz (B_0 string) to 131 Hz (C_3 string). From the average FRF of Fig. 26 can be taken that there are at least four clusters of local maxima in the frequency range between 30 Hz and 500 Hz. As much as eleven ODSs were chosen which - with an additional presentation of the measuring grid - are compiled in Fig. 27.

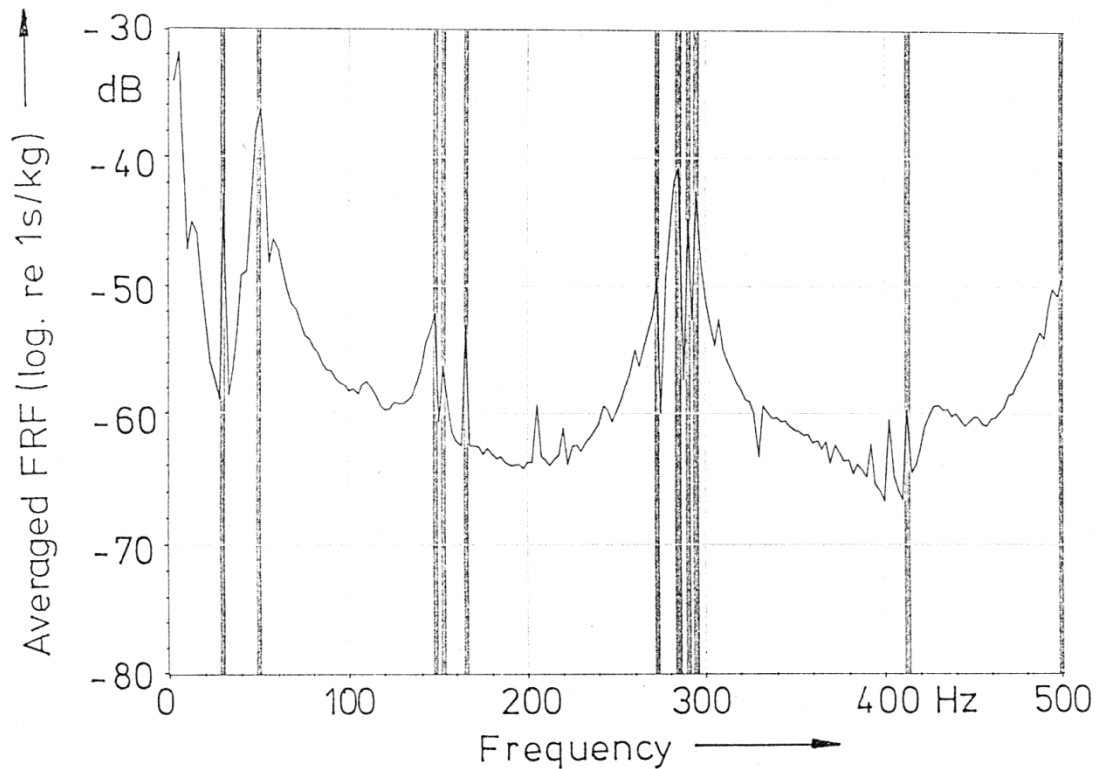


Fig. 26. Averaged frequency response function (measured velocity at all points normalised to the excitation force as a function of frequency) of the Carvin Bass No. 4. The stripes mark the bands chosen for the visualisation of the main operating deflection shapes.

The first ODS (Fig. 27b) occurs at 29 Hz which is close to the fundamental of the open B_0 string. No node is visible on the neck. The next ODS (Fig. 27 c; 49 Hz $\cong E_1$ string 3rd fret) exhibits a node close to the nut. The three ODSs between 147 Hz and 165 Hz (e.g. D_2 string 7th to 9th fret; Figs. 27d - f) are all of the same type with a node at the high frets and an antinode in the vicinity of the grasping hand. A different type of vibrational pattern with a node at the hand shows up at frequencies between 272 Hz and 294 Hz (Figs. 27g - j) with minor differences in the vibration of the rest of the instrument. The frequencies correspond to the 13th to 14th fret of the C_3 string. The two remaining ODSs at 412 Hz (Fig. 27k) and 499 Hz (Fig. 27l) refer to the fundamentals at the very highest frets of the C_3 string. They show two antinodes on the neck, vibrating in antiphase and separated by nodes in the middle as well as at the high and the low frets.

*Fig. 27a.
Measuring grid.*

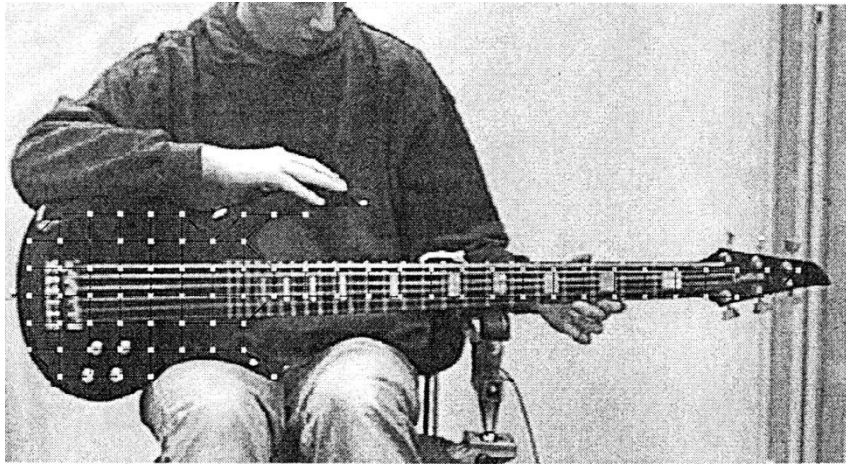


Fig. 27. In-situ operating deflection shapes of the Carvin Bass No. 4: Measuring grid and vibrational patterns for the announced frequencies. Black areas indicate a low vibration magnitude, white areas a high magnitude in the order of 3 to 30 mm/s for 1 N excitation force.

*Fig. 27b.
29 Hz.*



*Fig. 27c.
49 Hz.*



*Fig. 27d.
147 Hz.*



Fig. 27e.
152 Hz.

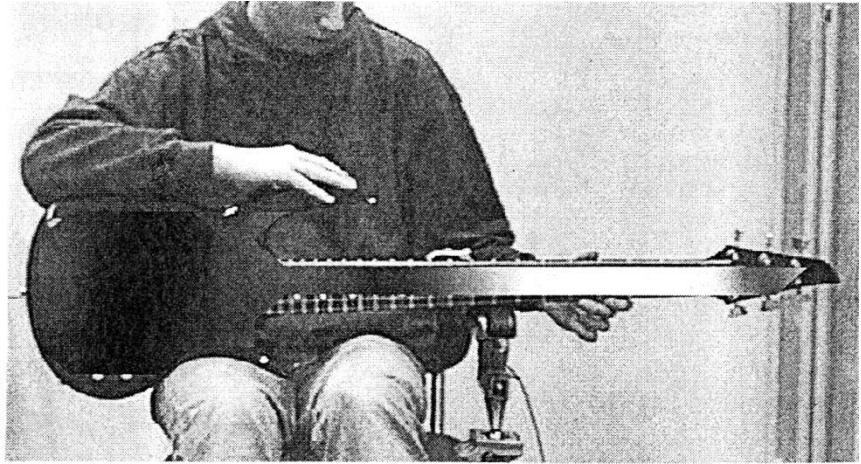


Fig. 27f.
165 Hz.



Fig. 27g.
272 Hz.

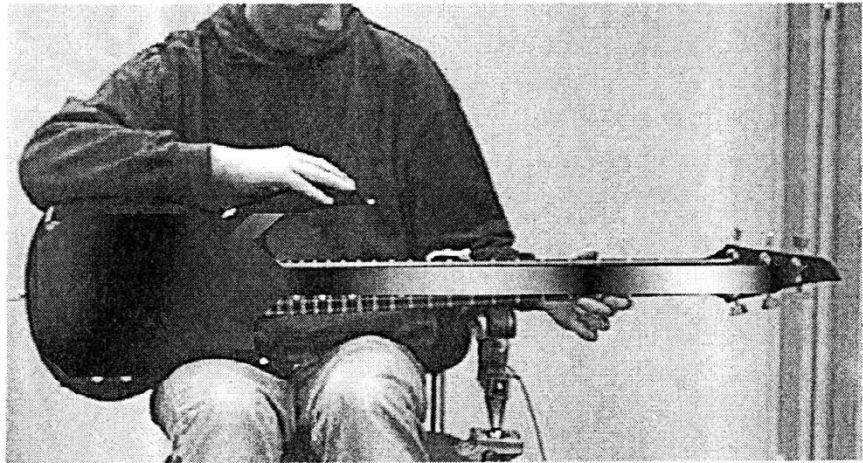


Fig. 27h.
284 Hz.



Fig. 27i.
290 Hz.



Fig. 27j.
294 Hz.

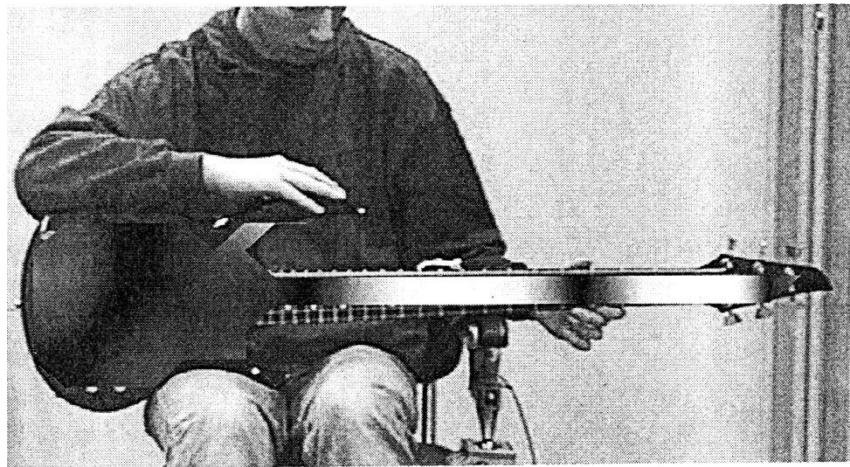


Fig. 27k.
412 Hz.



Fig. 27l.
499 Hz.



5.6. Experimental Results for the Riverhead Bass

The Riverhead Bass No. 5 (Fig. 28) differs totally in design from the four instruments considered in the previous paragraphs. It is made in one piece from carbon fibre. Its shape is very uncommon, as it lacks of a head and is therefore balanced in a different way. From the outer dimensions it looks perfectly symmetric with respect to the neck axis.



Fig. 28. Riverhead Bass No. 5 during the experimental determination of the operating deflection shapes by means of the Scanning Vibrometer.

From the average FRF of Fig. 29, eight ODSs were selected in the frequency range from 40 Hz to 470 Hz. At 40 Hz (Fig. 30b; open E_1 string) the neck vibrates without a node except at the body end. This pattern results from a pendular rigid body motion. At 51 Hz (Fig. 30c; E_1 string 3rd fret) and 67 Hz (Fig. 30d; A_1 string 3rd fret) a node close to the 5th or 6th fret appears. Between 202 Hz (Fig. 30e) and 215 Hz (Fig. 30g) vibrations with two nodes on the neck and very high amplitudes show up. These frequencies correspond to the 13th and 14th fret of the G_2 string. Pronounced torsion is visible for 421 Hz (Fig. 30h) and another bending vibration pattern with two antinodes at 470 Hz (Fig. 30i). These frequencies compare to fundamental tones at the highest frets of the G_2 string.

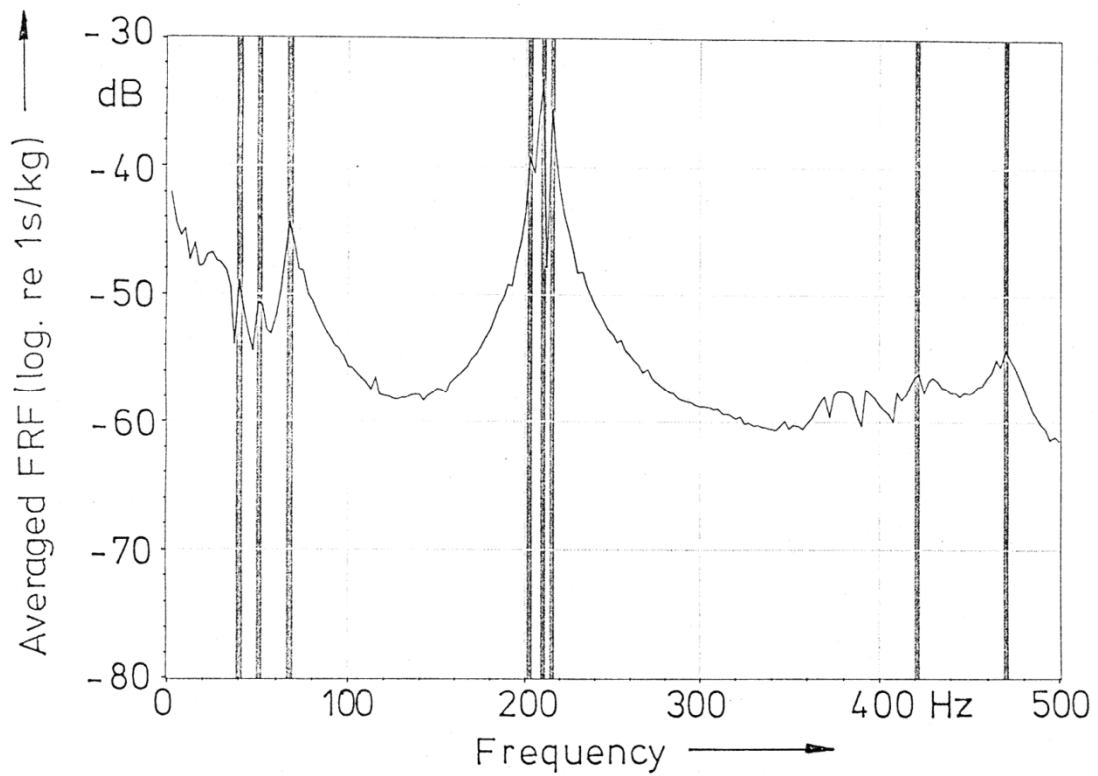


Fig. 29. Averaged frequency response function (measured velocity at all points normalised to the excitation force as a function of frequency) of the Riverhead Bass No. 5. The stripes mark the bands chosen for the visualisation of the main operating deflection shapes.

*Fig. 30a.
Measuring
grid.*

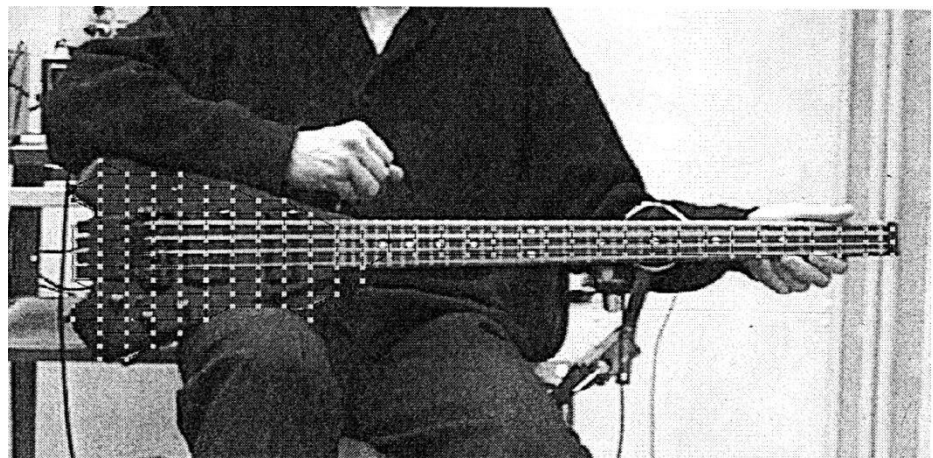


Fig. 30. In-situ operating deflection shapes of the Riverhead Bass No. 5: Measuring grid and vibrational patterns for the announced frequencies. Black areas indicate a low vibration magnitude, white areas a high magnitude in the order of 5 to 40 mm/s for 1 N excitation force.

Fig. 30b.
40 Hz.

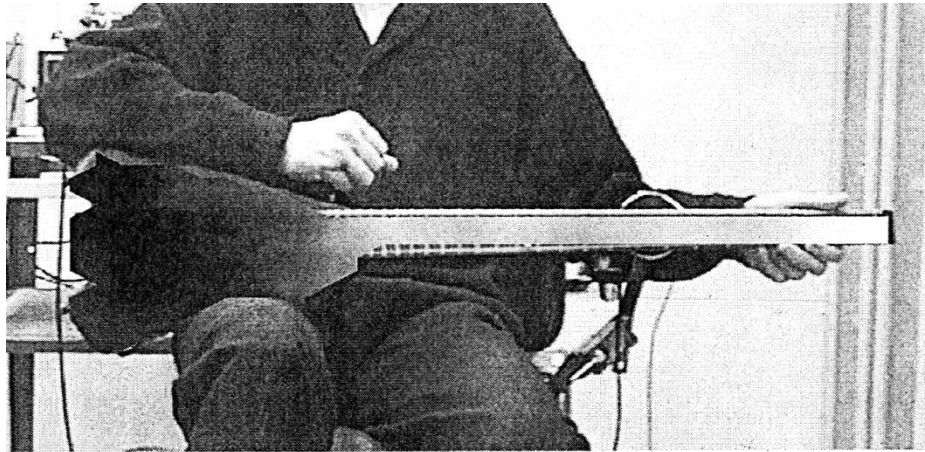


Fig. 30c.
51 Hz.

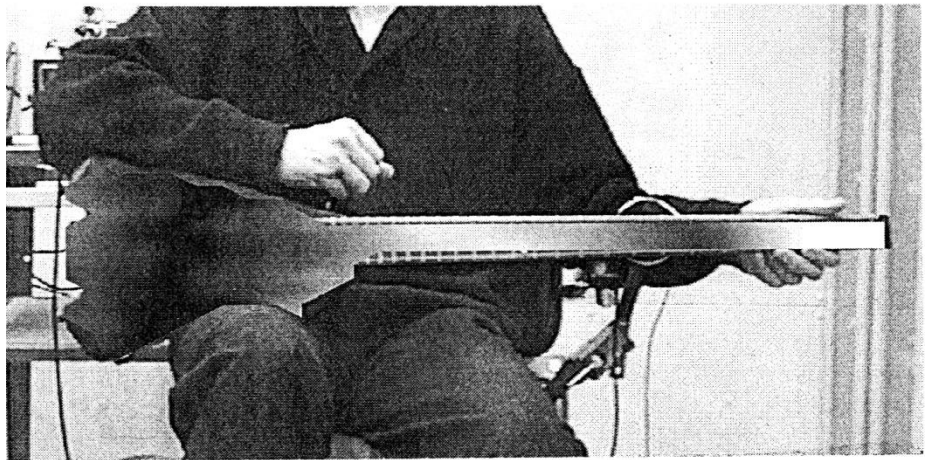


Fig. 30d.
67 Hz.

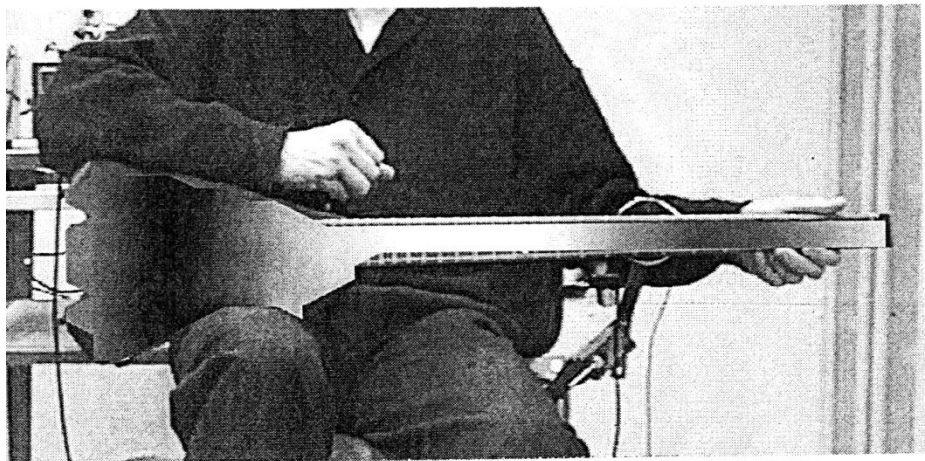


Fig. 30e.
202 Hz.

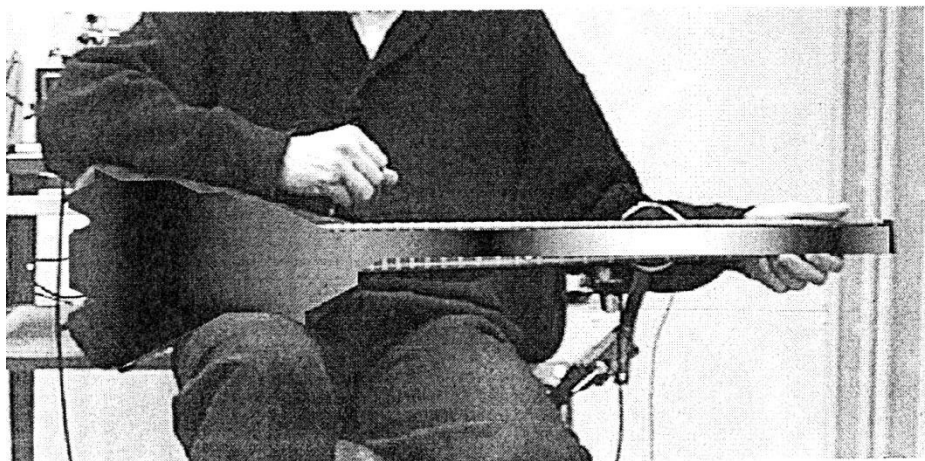


Fig. 30f.
210 Hz.

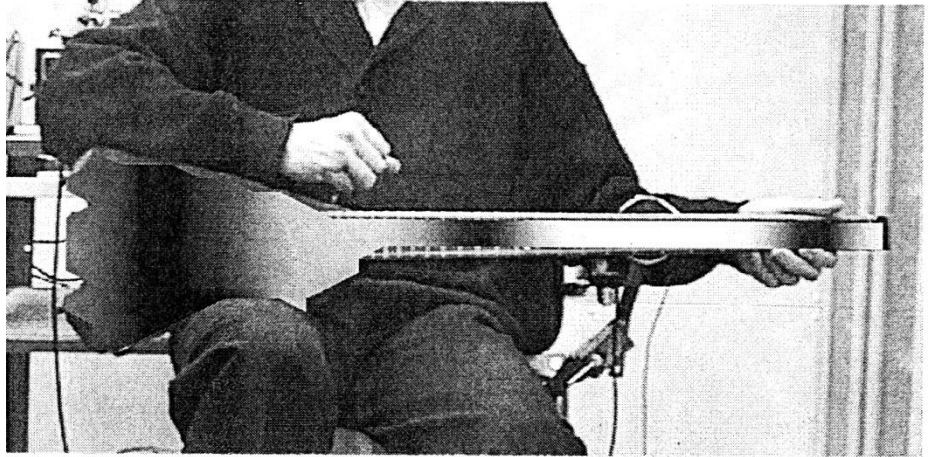


Fig. 30g.
215 Hz.

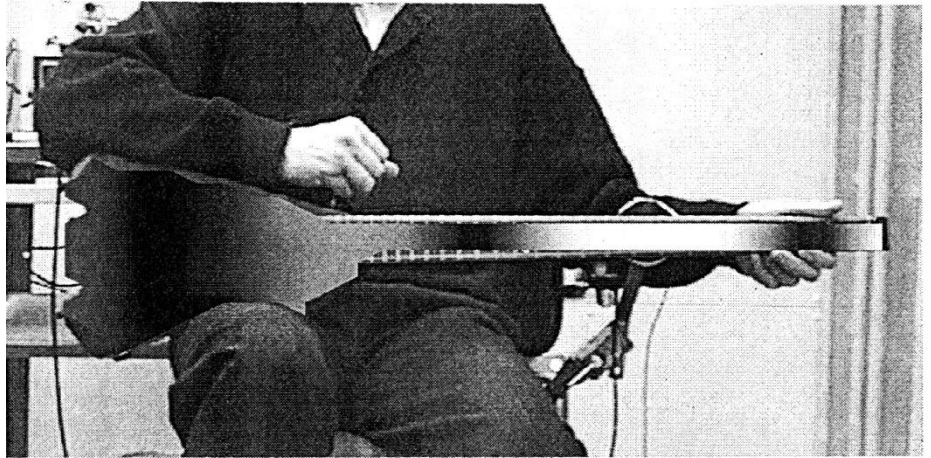


Fig. 30h.
421 Hz.

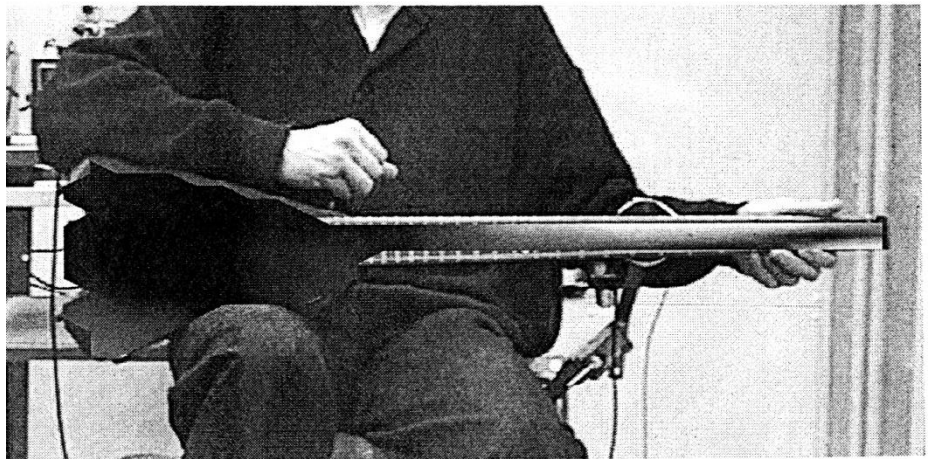
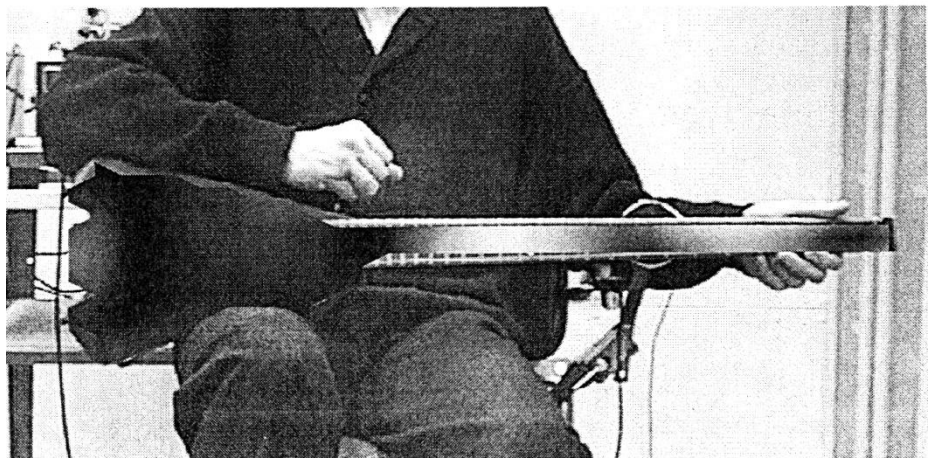


Fig. 30i.
470 Hz.



5.7. Concluding Remarks

Chapter 5 represents a collection of material which was compiled by *in situ* measurements of bass vibrations. For the visualisation of the results the vibration magnitude was coded by grey tones and superimposed to a video image of the measuring object. This way, it is easy to correlate nodes and antinodes to the corresponding locations on the body and neck. The results make clear that for all basses under consideration the structure, especially the neck, does not at all behave rigid but exhibits pronounced continuum vibrations. Under "natural" boundary conditions and for a realistic excitation at the neck the velocity of the fingerboard happens to reach the order of 30 mm/s per 1N excitation force. The phenomenon is obvious, but the experimental material has not yet been structured. This will be the scope of the next chapter.

6. COMPARISON OF THE PRINCIPAL ODSs

6.1. ODSs of the Action Bass

In the present chapter the main types of ODSs are to be extracted, identified and structured. For this purpose, the experimental results of the vibrometer measurement are visualised as 3D meshes similar to the mode shapes obtained by Modal Analysis; cf. chapter 4.

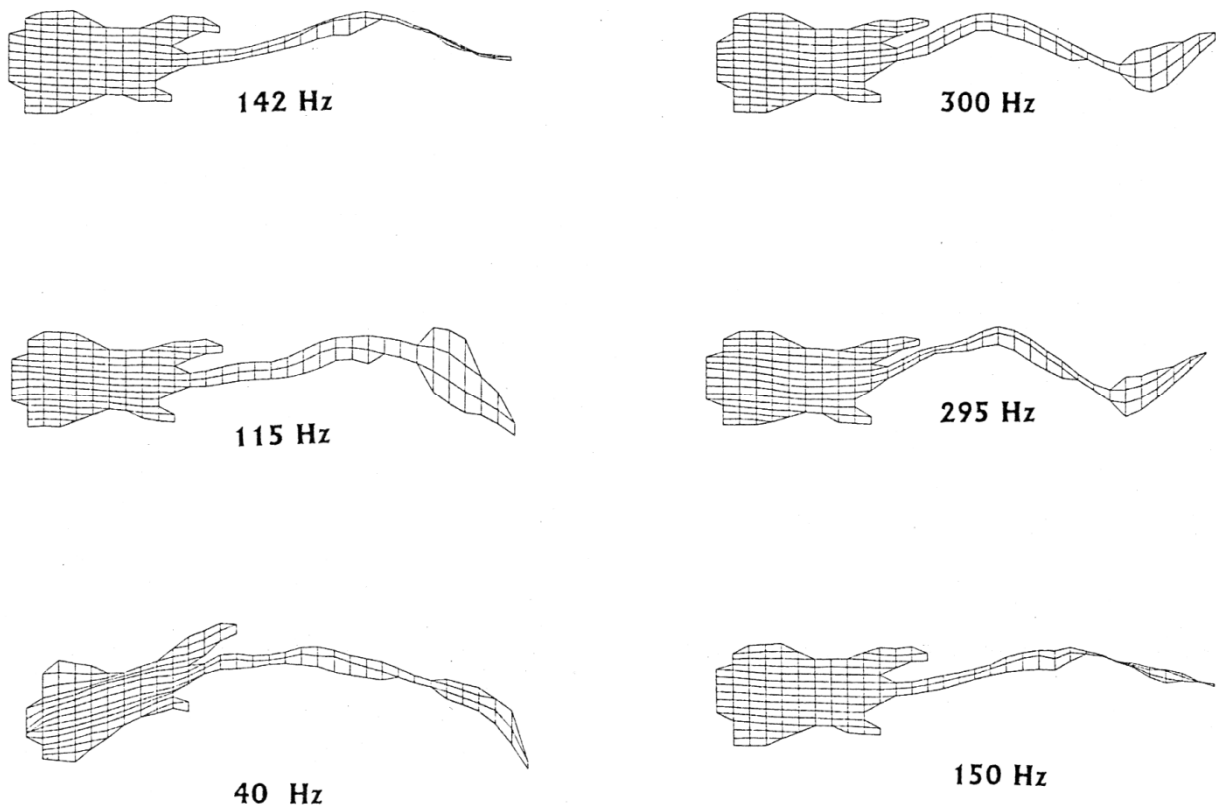


Fig. 31. ODSs of the Action Bass No. 1 in 3D representation.

As an example for this kind of presentation, the six ODSs of the Action Bass No. 1 are compiled in Fig. 31. The measuring grid and, for comparison, the grey tone representation can be taken from Fig. 18. It becomes obvious that within the frequency range up to 500 Hz there are three main types of vibrations:

- * A first type at 40 Hz,
- * a second type at 115 Hz, 142 Hz and 150 Hz and
- * a third type at 295 Hz and 300 Hz.

The different main types are characterised by a fundamental bending motion with a growing number of nodes. The variants differ in a superimposed torsion and/or in out-of-phase or in-phase bending of additional parts of the body, for instance the horns. In the following, the consideration is

restricted to the principal bending motion. If a peak in the average FRF has more than one local maximum, the ODS will be displayed for the frequency for which the highest value is observed.

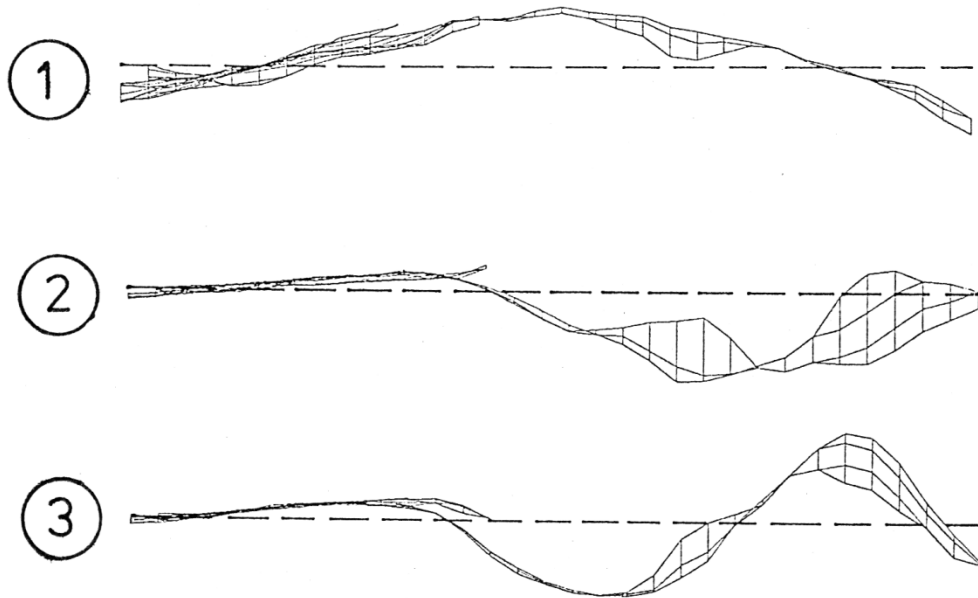


Fig. 32. Principal ODSs of the Action Bass No. 1. The ratios of the corresponding frequencies are $f_1 : f_2 : f_3 = 1 : 3.57 : 7.42$.

According to Fig. 16 the average FRF exhibits three main clusters of maxima. The peak values are reached for the frequencies $f_1 = 39.7$ Hz, $f_2 = 141.7$ Hz and $f_3 = 294.7$ Hz. These frequencies are related by the ratios $1 : 3.57 : 7.42$. The corresponding vibration patterns are gathered in Fig. 32 and denoted by numbers. To a first approximation, the left (body) end of the instrument does not move. On the remaining part there are one (ODS 1), two (ODS 2) and three (ODS 3) nodes, respectively.

6.2. ODSs of the Music Man Bass

Fig. 20 has shown that the average FRF has three main maxima. The frequencies at which the maxima occur are $f_1 = 42.3$ Hz, $f_2 = 137.5$ Hz and $f_3 = 282.8$ Hz. These frequencies are in the ratios $1 : 3.25 : 6.69$. The respective three vibration patterns are compiled in Fig. 33. Comparable to the ODSs of the Action Bass (Fig. 32), the left (body) end of the bass hardly moves. In addition to the left-end node there are one (ODS 1), two (ODS 2) or three (ODS 3) further nodes.

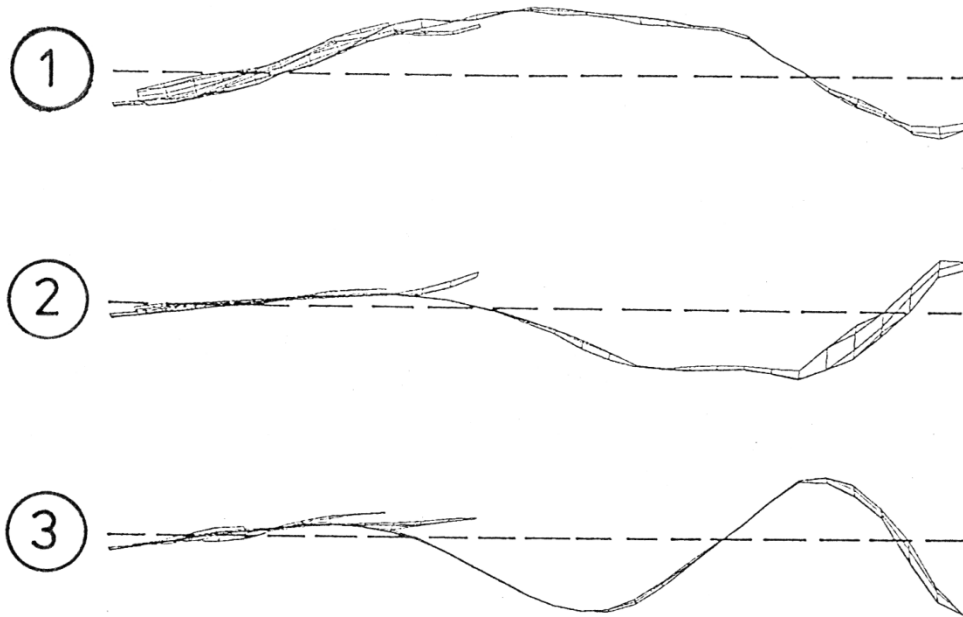


Fig. 33. Principal ODSs of the Music Man Bass No. 2. The ratios of the corresponding frequencies are $f_1 : f_2 : f_3 = 1 : 3.25 : 6.69$.

6.3. ODSs of the Dyna Bass

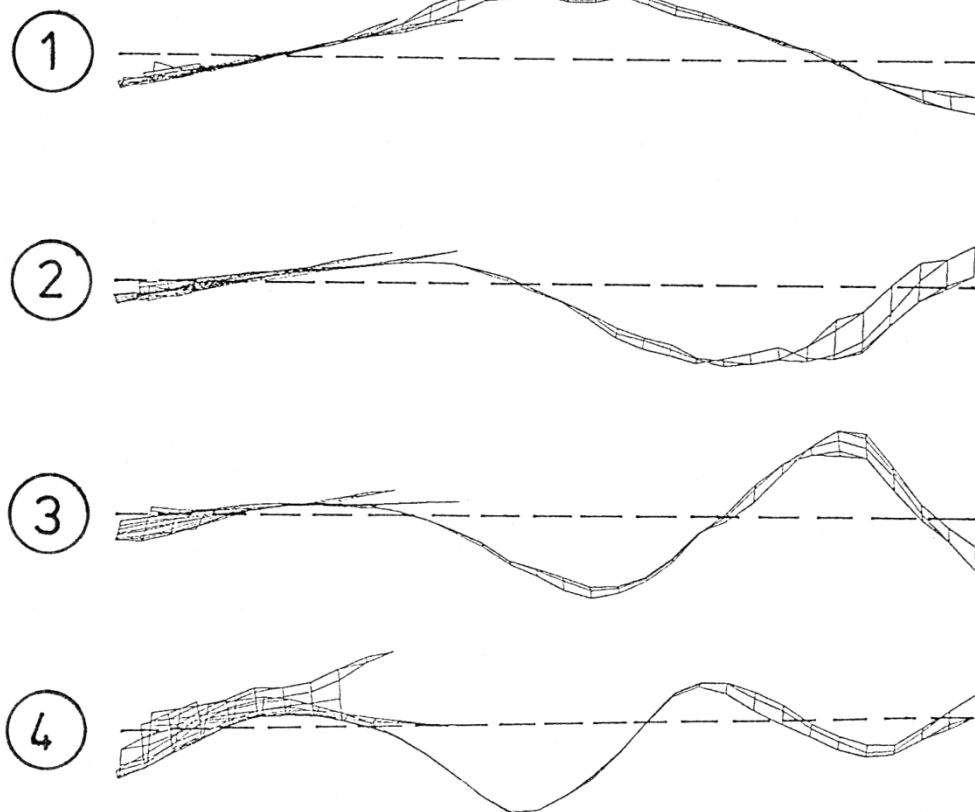


Fig. 34. Principal ODSs of the Dyna Bass No. 3. The ratios of the corresponding frequencies are $f_1 : f_2 : f_3 : f_4 = 1 : 3.28 : 6.44 : 11.02$.

The average FRF in Fig. 23 has shown three pronounced maxima and several additional peaks. In total, four peaks were selected for presentation with the frequencies $f_1 = 42.5$ Hz, $f_2 = 139.5$ Hz, $f_3 = 273.6$ Hz and $f_4 = 468.5$ Hz. This corresponds to the ratios $1 : 3.28 : 6.44 : 11.02$. The four vibration patterns are compiled in Fig. 34. ODS 1, 2 and 3 compare to what was found for the Action Bass (Fig. 32) and Music Man Bass (Fig. 33). A node appears always close to the left end, *i.e.* on the body close to the bridge. In addition, there are one (ODS 1), two (ODS 2) or three (ODS 3) further nodes. This series is continued by ODS 4 which exhibits four further nodes and had not yet been observed during the investigation of the basses No. 1 and 2.

6.4. ODSs of the Carvin Bass

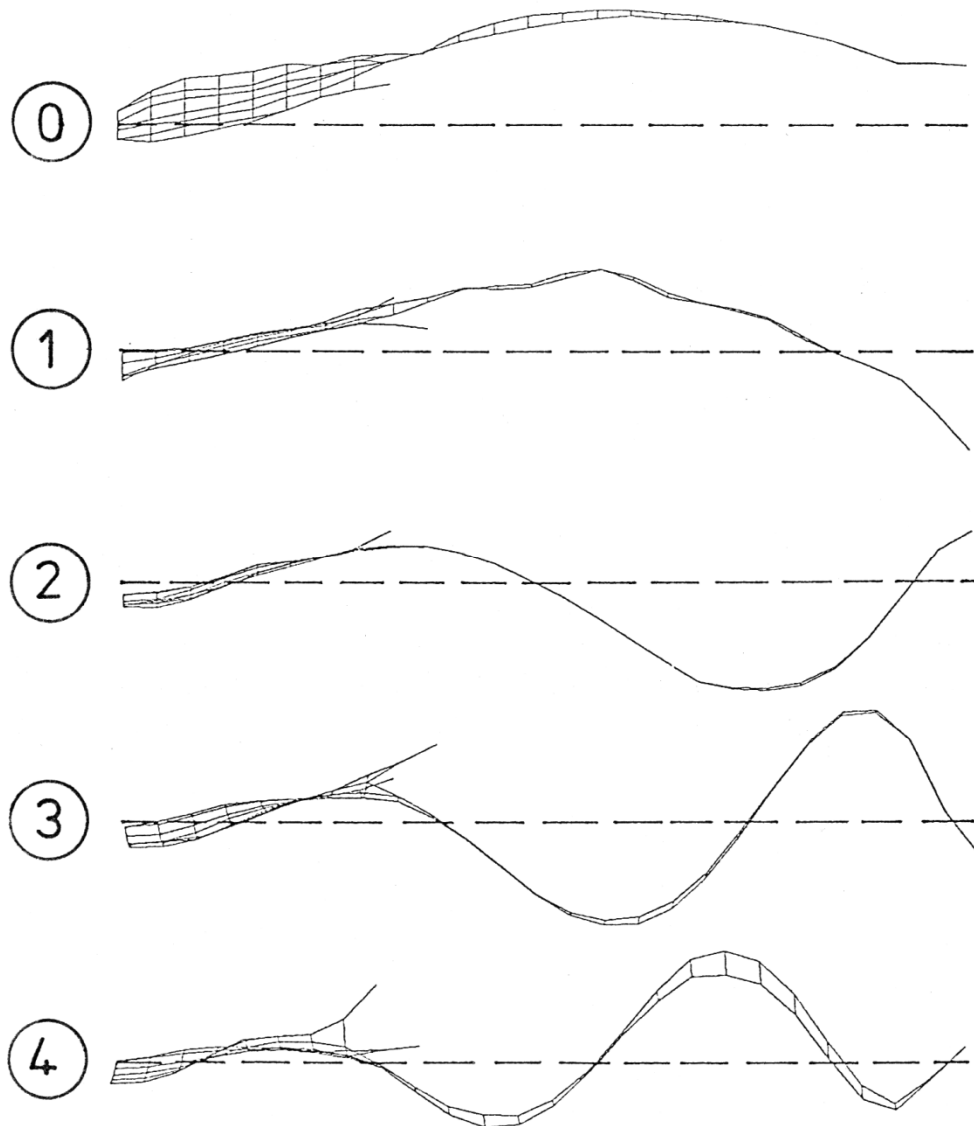


Fig. 35. Principal ODSs of the Carvin Bass No. 4. The ratios of the corresponding frequencies are $f_0 : f_1 : f_2 : f_3 : f_4 = 0.60 : 1 : 3.01 : 5.80 : 10.18$.

From the average FRF in Fig. 26 a large number of maxima can be taken. Five peaks were chosen with the frequencies $f_1 = 49.1$ Hz, $f_2 = 147.5$ Hz, $f_3 = 284.5$ Hz and $f_4 = 499.4$ Hz. An additional maximum at $f_0 = 29.2$ Hz is included and the corresponding ODS displayed because it is close to the

fundamental frequency of the open B_0 string of this particular instrument which carries six strings. The respective ODS 0 in Fig. 35 resembles the first eigenmode of the clamped-free beam; cf. mode 1 in Fig. 7. More probable it consists in a rigid body motion superimposed by the first mode (cf. ODS 1 in Fig. 35). If f_1 is used as a normalising value, the frequencies are in the ratios 0.60 : 1 : 3.01 : 5.80 : 10.18. The five vibration patterns are collected in Fig. 35, the mid three of which were found for all basses. The ODS numbered 0 plays no role for the other basses under consideration. ODS 4, however, was also found for the Peavey Bass (Fig. 33). All patterns exhibit a node close to the left end in the vicinity of the bridge. In addition to this intrinsic node, there are no (ODS 0), one (ODS 1), two (ODS 2), three (ODS 3) or four (ODS 4) further nodes.

6.5. ODSs of the Riverhead Bass

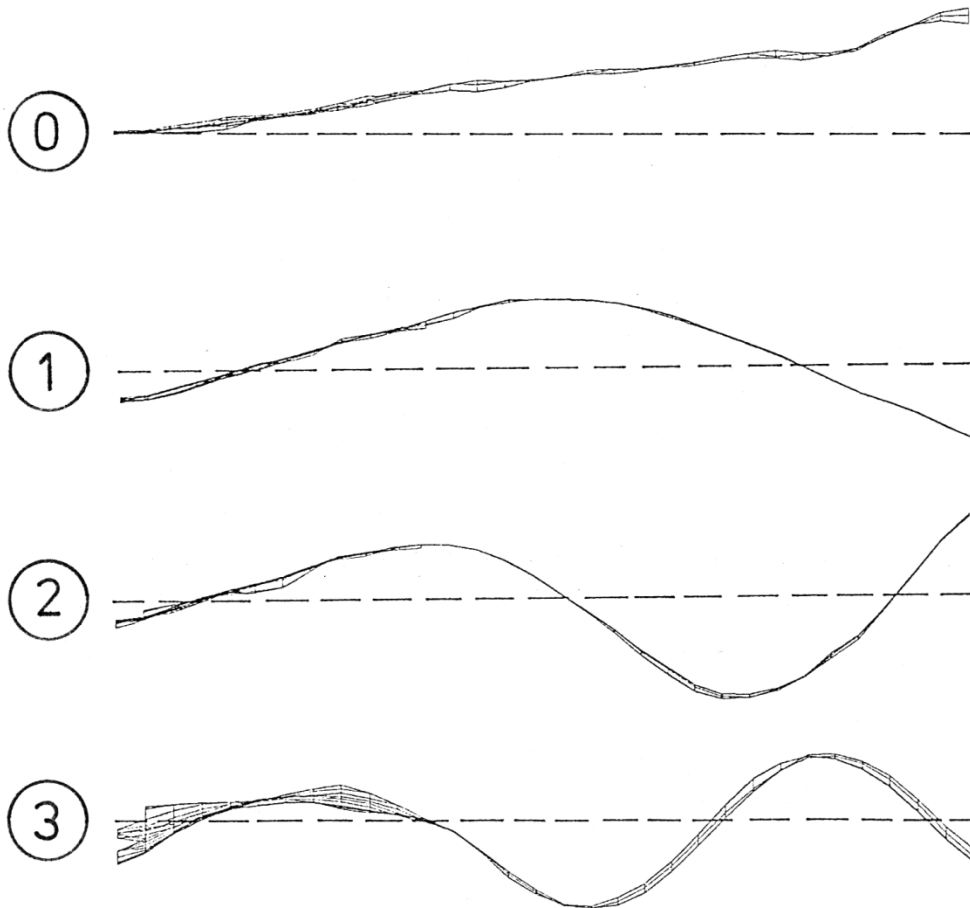


Fig. 36. Principal ODSs of the Riverhead Bass No. 5. The ratios of the corresponding frequencies are $f_0 : f_1 : f_2 : f_3 = 0.59 : 1 : 3.11 : 6.96$.

The average FRF in Fig. 29 is dominated by a cluster of maxima at about 200 Hz. From the range up to 500 Hz four local peaks were chosen with the frequencies $f_1 = 67.5$ Hz, $f_2 = 210.0$ Hz and $f_3 = 470.0$ Hz. In addition, the maximum at $f_0 = 40.0$ Hz was considered. The corresponding ODS 0 in Fig. 36 makes clear that this is a rigid body motion in which the bass as a whole is in pendular motion without flexible bending. Again, f_1 is used as a normalising value which leads to the fre-

quency ratios $0.59 : 1 : 3.11 : 6.96$. Three of the four vibration patterns, which are gathered in Fig. 36, were found for all basses. The ODS numbered 0 plays no role for the other basses (except the six-string Carvin Bass; cf. ODS 0 in Fig. 35). This rigid body motion at the frequency of the open E_1 string seems to be typical for the Riverhead Bass; it could be due the headless design or/and the carbon fibre construction. The further vibration patterns coincide with what had been observed for the other instruments: A node appears always close to the left end in the vicinity of the bridge. In addition to this node which all ODSs have in common, there are no (ODS 0), one (ODS 1), two (ODS 2) or three (ODS 3) extra nodes.

6.6. Eigenmodes of the Simply Supported-Free Beam

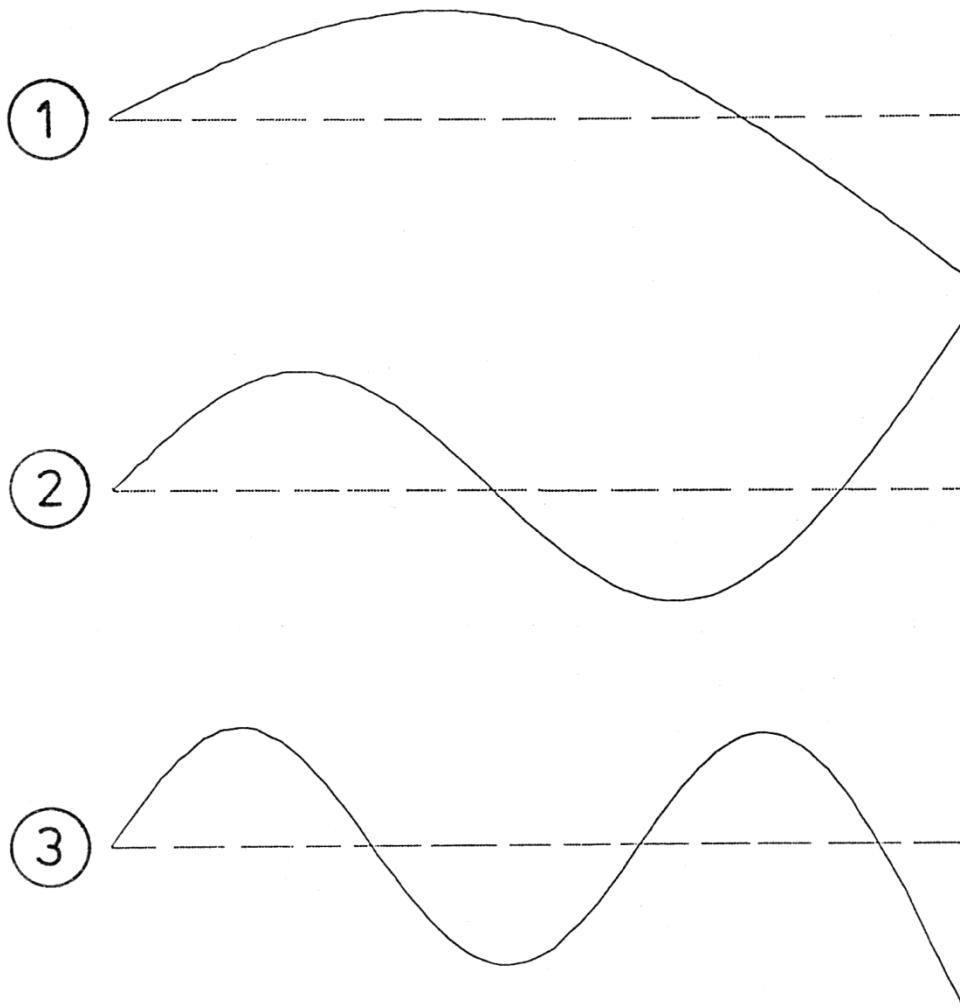


Fig. 37. Eigenmodes of the simply supported-free beam. The ratios of the corresponding eigenfrequencies are $f_1 : f_2 : f_3 = 1 : 3.24 : 6.76$.

From Eq. (16) in Paragraph 3.4 can be taken that the eigenfrequencies of a beam which is simply supported at one end and free at the other end are related by $1 : 3.24 : 6.76 : 11.56$. The first three eigenmodes are plotted in Fig. 37. In contrast to the basses, the left-end node is located exactly at the end of the beam. Apart from the location of the left-end node, which for the basses occurs not directly at, but in a distance of some centimetres away from, the body-end, the modes of the simply supported-free beam prove as very similar to the corresponding vibration modes of the basses.

6.7. Comparison of the Bass ODSs to Beam Eigenmodes

6.7.1. Survey

In Paragraphs 6.1 to 6.5 typical ODSs of the basses as measured *in situ* are compiled. The respective frequency ratios are listed in Tab. IV. The bold numbers refer to the frequencies of the principal ODSs (as characterised by the main maxima). The other ODSs, which are of the same bending type but differ in minor features such as an additionally superimposed torsion, are characterised by normal letters.

	ODS 0	ODS 1	ODS 2	ODS 3	ODS 4
Action Bass No. 1		1	2.89/ 3.57 /3.78	7.42 /7.56	
Music Man Bass No. 2		1	3.25 /3.49/3.90	6.44/ 6.69 /6.98	
Dyna Bass No. 3		1	2.82/ 3.28 / 3.53/3.98	6.44	9.81/ 11.02
Carvin Bass No. 4	0.60	1	3.01 /3.11/3.36	5.55/ 5.80 / 5.91/5.99	8.41/ 10.18
Riverhead Bass No. 5	0.59	1	3.00/ 3.11 /3.19	6.96	
Beam ss - f		1	3.24	6.76	11.56

Tab. IV. Ratios of the frequencies of the ODSs; the frequency of the first bending vibration is used as a reference.

A comparison of the corresponding Figs. 32 through 36 (basses) to Fig. 37 (simply supported-free beam) has shown that the patterns of the beam vibration coincide with the principal ODSs of the basses to a certain extent. Moreover, the data in Tab. IV reveal that the frequency ratios of the corresponding vibrations are relatively close together. This means that the simply supported beam can be taken as a first approximation to describe the bending vibrations of the basses, which will be discussed in detail in the following paragraphs.

6.7.2. Rigid Body Motion

A rigid body motion (ODS 0) was observed for two of the instruments at about 0.6 times the frequency of the first bending vibration. It is most pronounced for the Riverhead Bass No. 5 and oc-

curs at $f_0 = 40$ Hz. The Carvin Bass No. **4** exhibits a vibration at $f_0 = 29$ Hz that can be interpreted as similar to the rigid-body type. For a wooden five- or six-string bass with a head, this motion proves to be within the range of the fundamental frequencies only for one item (Carvin Bass No. **4**). For the four-string Riverhead Bass No. **5**, which is of non-conventional shape and material, it is close to the fundamental of the open E_1 string. It is not clear whether this discrepancy to the wooden basses is due to the carbon fibre, from which the instrument No. **5** is made, or to the design without a head which is suspicious to alter the balance of the whole instrument.

6.7.3. First Bending Vibration

The first principal operating deflection shape, denoted ODS 1, is observed for all basses. It is closely related to the first eigenmode of the simply supported-free beam with a node in addition to the node induced by the support. The frequencies range from 40 Hz to 49 Hz for conventional basses No. **1** to **4** and 67 Hz for the Riverhead Bass No. **5**. Apart from the carbon fibre bass No. **5**, the frequencies appear slightly higher for the wooden one-piece basses (No. **3** and No. **4**) than for the wooden basses with a screwed-on neck (No. **1** and **2**). Because this is the first true continuum vibration and compares to the first eigenmode of the beam, it seems to be justified to use its frequency as a reference. As a rule, it is well pronounced and not superimposed by other vibrations. Therefore, it yields a clear peak in the FRF and one single frequency to characterise it.

6.7.4. Second Bending Vibration

As a rule and in contrast to the first one, the second bending pattern (ODS 2) is split and/or superimposed by torsion. That is why similar vibration patterns with three (support plus two additional) nodes occur at frequencies spread over a certain range. Typically three to six peaks are found in the FRF related to bending patterns which obviously compare all to the second mode of a simply supported-free beam. The corresponding frequencies are

- 115 Hz ... 150 Hz for the Action Bass No. **1**,
- 137 Hz ... 165 Hz for the Music Man Bass No. **2**,
- 120 Hz ... 169 Hz for the Dyna Bass No. **3**,
- 147 Hz ... 165 Hz for the Carvin Bass No. **4** and
- 202 Hz ... 215 Hz for the Riverhead Bass No. **5**.

The frequencies of the second bending pattern seem to be somewhat lower for the screwed basses No. **1** and **2** compared to the glued basses No. **3** and **4**. The highest frequencies are found for the headless carbon bass No. **5**.

6.7.5. Third Bending Vibration

According to theory, the third mode of a simply supported-free beam exhibits one node at the support and additional three nodes which are also found for ODS 3 of the basses. Again, in some cases not only one, but several patterns which have four nodes in common are observed for slightly differing frequencies. The ranges are

- 295 Hz ... 300 Hz for the Action Bass No. **1**,
- 272 Hz ... 295 Hz for the Music Man Bass No. **2**,
- 274 Hz for the Dyna Bass No. **3**,

272 Hz ... 294 Hz for the Carvin Bass No. **4** and
470 Hz for the Riverhead Bass No. **5**.

The observation that the frequency is highest for the bass No. **5** is also confirmed for this ODS.

6.7.6. Fourth Bending Vibration

Within the investigated frequency range up to 500 Hz both one-piece basses No. **3** and **4** show a further vibration pattern (ODS 4) which corresponds to the fourth eigenmode of the simply supported-free beam. The instruments exhibit five nodes and vibrate with the frequencies 417 Hz and 468 Hz (No. **3**) as well as 412 Hz and 494 Hz (No. **4**).

6.8. Concluding Remarks

The comparisons made in this chapter reveal that there are vibration patterns which are common to all basses. They are denoted principal ODSs and identified as bending vibrations of the structure. They compare to particular eigenmodes of a beam. That means that, to a first approximation, the bass can be modelled by a beam of constant bending stiffness which is simply supported at one (the body-)end and free at the other (the neck-)end. If once the frequency of the first bending vibration is known, the frequencies of the other principal ODSs can be estimated by this model to be about 3.2 times, 6.8 times and 11.6 times, respectively, as high as the frequency of the first ODS. In addition, the influence of material (E , ρ) and geometry parameters (l , h , b) can be at least roughly checked. A prominent deviation of reality to model is observed at the body-end. While the node of the beam occurs at the supported end, for the basses it is shifted away from the end. Favourable, the node is located at the bridge in order to ensure that the strings "see" an immobile termination. This deviation in the location of the left-end node may be accounted for by an "effective length" which differs from the geometrical length.

This simplified consideration is restricted to bending. In practice, the principal modes may be superimposed by torsion and/or split by interaction with the in-phase or out-of-phase motion of accessory parts such as the horns of the body. Most probably the head - which is asymmetric as well as the body is for all instruments except the Riverhead Bass - plays an important role for the vibrations of the neck. These are effects which cannot be covered by the beam model. This means that experiments are not made superficial by the basic theory. Therefore, an additional measuring approach is suggested in order to account for the fact that the excitation of the neck takes place at different locations on the fingerboard. The fundamentals will be treated in the next chapter.

7. MECHANICAL ADMITTANCE

An unavoidable shortcoming of the ODS measurement is that there is one fixed excitation point, in our experiments the seventh fret. In playing practice, the neck is excited by the strings which are terminated depending on where they are fingered by the bass player. Until now, no quantitative information is available about the extent to which an ODS of the bass structure is evoked by such a "natural" excitation. In the extreme case, an ODS might be not detected because it exhibits a node at the seventh fret and is consequently not evoked by an excitation at our particular shaker location. Nevertheless, it could be relevant for the playing function of the instrument. The aim of this chapter is to describe a more direct measuring approach apt for the given task.

7.1. Measuring Parameters and Set-up

The main topic of the present work is related to the transfer of energy from the string to the neck or body of the instrument. The response of a particular point of a structure to an excitation can be expressed by the mechanical point impedance (cf. Fletcher and Rossing (1998)) or its reciprocal, the mechanical point admittance. The admittance, which after Jansson (1983b) is sometimes referred to as the "vibration willingness", is used in the following to characterise the mobility of the instrument and its deviation from the fiction of providing immobile terminations to the strings.

The admittance is defined as the ratio of the complex amplitudes of the velocity and the force at the same point in the same direction. A high admittance generally stands for a high mobility of the instrument at this particular location and frequency. According to the German standard DIN 1320 its real part is denoted conductance, and its imaginary part susceptance. The susceptance (velocity and force shifted by $\pm 90^\circ$) is a measure of the spring- or mass-type behaviour of the structure at the driving point. In the problem under consideration it can be relevant for an increase or decrease, respectively, of the frequency of the string compared to ideally rigid supports. The conductance (velocity in phase with the force) characterises the effect that active power generated by the driving system, in the case of a chordophone the string, is transferred to the structure. For an acoustic instrument the transfer of energy from the string to the body, mostly via the bridge, is a necessary prerequisite for the function of the instrument; cf. Fleischer (1997b). For an electric instrument, however, the flow of vibration energy from the string to the body is undesired. It is parasitic in the sense that the vibration of the string decays more rapidly with than without the additional energy loss via the terminations. Thus, a non-zero conductance indicates that the instrument structure is able to accept vibrational energy from the string at this particular location and frequency. This may be the cause for a dead spot.

The following set-up was used to ascertain the complex admittance. A noise generator (B&K 1405) fed pink noise via an amplifier (B&K 2706) to a mini-shaker (B&K 4810). On top of the driving system of the shaker an impedance head (B&K 8001) was mounted for simultaneous acquisition of force and acceleration. The influence of the mass of the transducer "down-stream" the force flow, *i.e.* beyond the force gauge, was minimised by an electric mass compensation unit (B&K 5565). The force and acceleration signals were conditioned in two charge amplifiers (B&K 2626). After having reversed the polarity of the acceleration by a differential amplifier (Tektronix AM 502), FFT and additional calculations were performed in a dual channel analyser (Ono Sokki CF 350) which finally yielded the complex mechanical admittance. Due to a false calibration the experimental values given in the first edition are too large by a factor of about three (according to 10 dB).

The fundamental frequency of the bottom open string on a five- or six-string bass is $B_0 \cong 31$ Hz, on a normal four-string bass $E_1 \cong 41$ Hz. As a rule, 25 Hz was chosen as the lowest frequency in the

admittance measurements. The top string on a four-string bass is $G_2 \cong 98$ Hz and on a six-string bass $C_3 \cong 131$ Hz. If these strings are fingered at the 12th fret, the corresponding fundamental frequencies are 196 Hz and 262 Hz. Since the range of fundamental frequencies up to at least the 12th fret of a six-string bass is covered, a highest frequency of 275 Hz was considered as sufficient.

Great care was taken to ensure "natural" experimental conditions as close as possible to the normal playing situation. That is why the measurements were performed *in situ* in a similar condition as shown in the video images of Chapter 5. The shaker with the impedance head was positioned horizontally in such a way that the bridge, nut or fingerboard of the bass could be slightly pressed against the tip of the impedance head. The pressure was such that the static force was always greater than the alternating force and the impedance head did never lift off. In order to simulate normal fingering conditions, the experimenter's left hand grasped the neck close to the location where the admittance was measured. The output plug of the bass pick-ups was left open-circuited. The strings were under normal tension and left undamped. All experiments were performed by the same person (the author). A comparison of data obtained in repeated measurements revealed that the reproducibility was satisfactory.

7.2. Comparing In-plane and Out-of-plane Admittance on the Neck

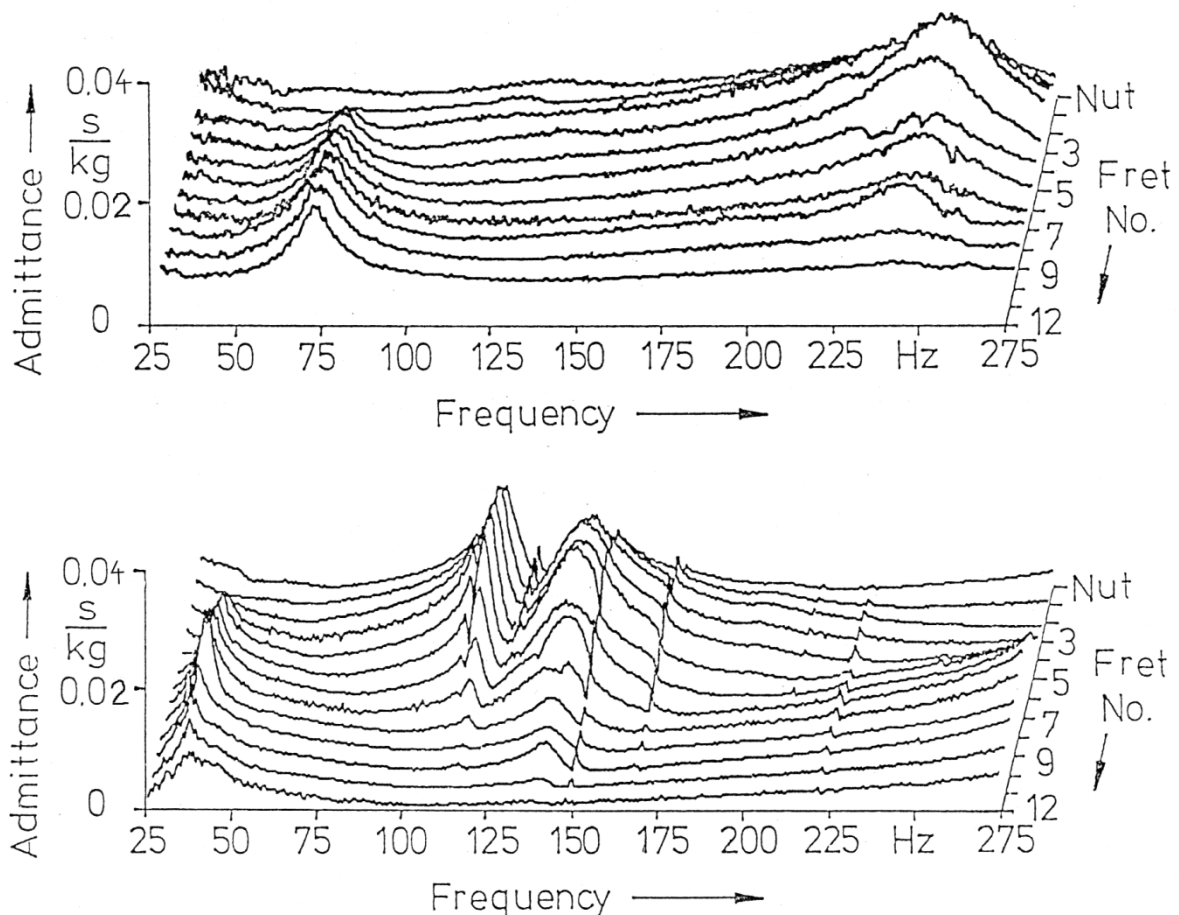


Fig. 38. Admittance on the neck of the Action Bass No. 1 as a function of frequency measured at different locations from the nut to the 10th and 12th fret, respectively. Measuring directions are in the fingerboard plane (top) and perpendicular to the fingerboard (bottom) at the centre line between the A_1 and D_2 strings.

During the playing process, the bass player shortens the string by pressing it against the frets on the fingerboard. In order to study this fingering case, the admittance was measured at the positions of the frets (including the nut to take into account the open-string situation). Fig. 38 shows results as obtained along the neck for the Action Bass No. 1. The impedance head was oriented in two different directions. The upper diagram reflects the measurement along the side of the neck in the fingerboard plane. The lower diagram refers to the measurement along the centre line of the neck perpendicular to the fingerboard.

The reason for measuring in two directions is due to the plucking process. If the player does not make use of the "slapping" technique, he or she plucks the string using his or her thumb, finger or a plectrum. To a certain extent the player is able to choose the angle by which the string is plucked by changing the position and the direction of motion of the finger or plectrum. Consequently, the player can influence the plane in which the string initially vibrates within certain limits. However, there will always be components of vibration parallel (in-plane) and perpendicular (out-of-plane) to the fingerboard. In order to account for both components of the string motion, the measurements of Fig. 38 refer to both directions.

The 3D-representation of the neck admittance creates a mountainous "landscape". The "mountains" indicate increased mobility of the neck for particular measuring positions in certain frequency bands. When measuring in the fingerboard plane (top of Fig. 38), the two mountains are observed which are relatively flat and not very high. In contrast, when measuring out-of-plane along the centre of the fingerboard, three pronounced mountain chains appear which reflect the body-neck ODS 1 (Fig. 32 or Fig. 18b) and ODS 2 (Fig. 32 or Fig. 18c - e).

A comparison reveals that, in principle, the neck is mobile in both directions, but to a different extent. As expected, the neck proves as more mobile perpendicular to the fingerboard than in the fingerboard plane. Obviously, the admittance reaches higher values at lower frequencies out-of-plane than in-plane. In consequence, comparable to the case of an acoustic instrument such as the classic guitars (cf. Jansson (1983b), Fletcher and Rossing (1998)), the out-of-plane admittance will dominate the damping effects. This purely "mechanical" argumentation should be put on an additional basis by an analysis of the direction-dependent sensitivity of the electromagnetic pick-ups. At the moment, it is supposed that the electric output signal depends on the direction of the string motion: If the string moves towards to, and away from, the pick-up, a higher output voltage is produced than if the string moves in parallel to the pick-up front. This tentative assumption should be checked by future investigations. Supposed it is true, the out-of plane admittance will dominate not only the mechanical string vibration, but will be directly related to the electric output signal. Since the out-of-plane direction is judged as more important than the direction in the fingerboard plane, all measurements which follow will be taken perpendicular to the fingerboard-body plane.

7.3. Lateral Dependence of the Neck Admittance

The vibration patterns obtained by Modal Analysis (Chapter 4) as well as the ODSs (Chapter 5) indicate that torsion may be superimposed on the bending of the neck. The influence of the torsional motion was checked by measuring the point admittance at different lateral positions on the fingerboard. Two examples for four-string basses are given in this paragraph. The measurements were taken along three lines between the

- bottom E₁ and A₁ strings,
- mid A₁ and D₂ strings and
- D₂ and top G₂ strings.

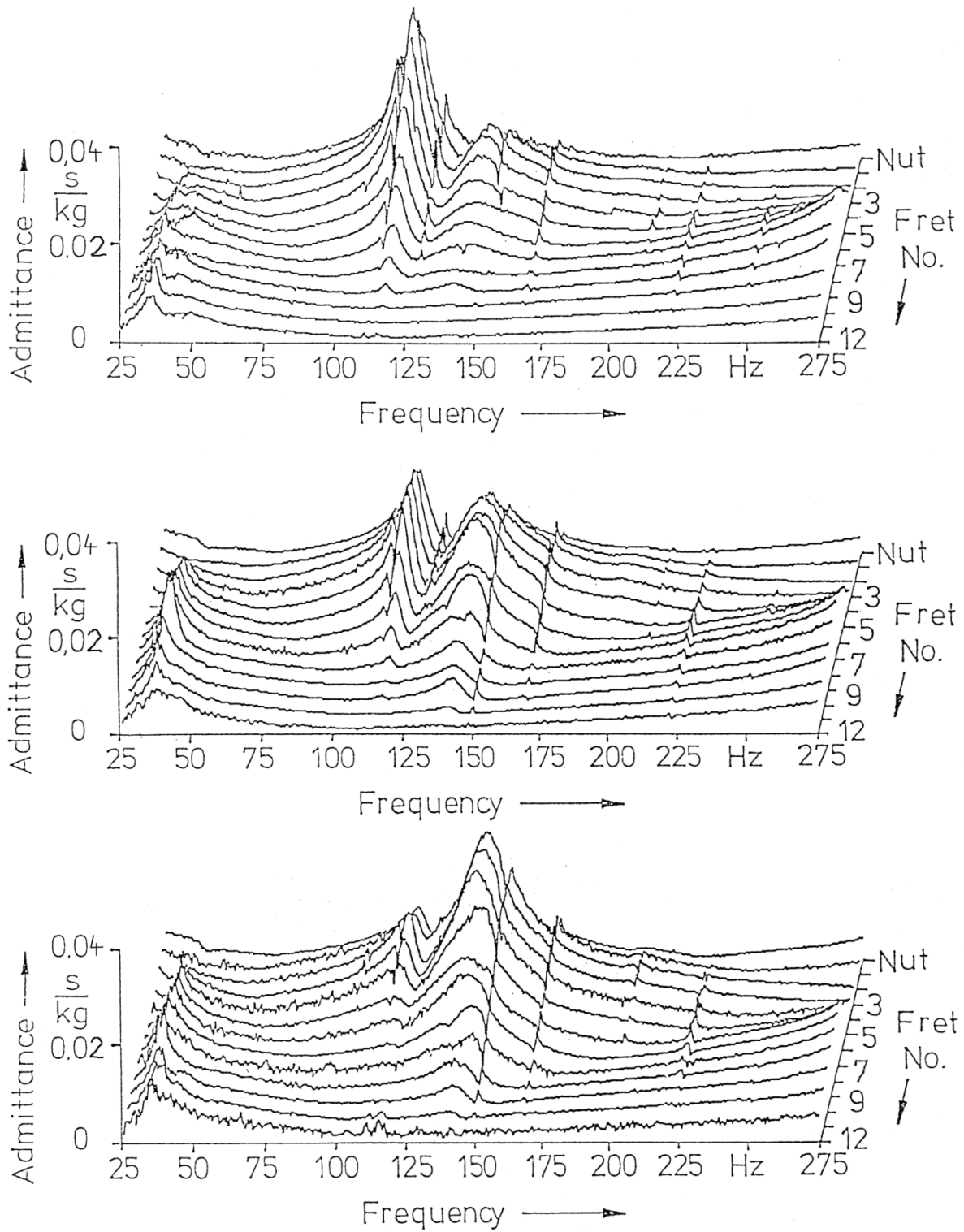


Fig. 39. Out-of-plane admittance on the neck of the Action Bass No. 1 as a function of frequency measured at thirteen locations from the nut to the 12th fret. Measuring positions are between the low E_1 and the A_1 strings (top), between the mid A_1 and D_2 strings (middle) and between the D_2 and the high G_2 strings (bottom).

The admittance is shown as a function of frequency for the Action Bass No. 1 in Fig. 39. Results for the nut and the first twelve frets are compiled to a 3 D-representation. The three diagrams refer to

measurements between the bottom strings, along the centre line of the fingerboard and between the top strings, respectively. The admittance landscapes show overall-similarities, but differences in detail. The discrepancies concentrate on the vibrations between about 100 Hz and 150 Hz. For their interpretation a comparison to the ODSs displayed in Fig. 18 is recommended. The frequencies of the maxima yielded by the vibration and the admittance measurements, respectively, are not exactly the same. This may be a consequence of the differing support by the left hand: While during the vibration measurements (Chapter 5) the hand grasped the neck at a constant position in the low-fret region, during the admittance measurements the hand wanders along with the measuring point in order to simulate the player fingering the string at the corresponding fret.

The multiple mountain chain in Fig. 39 is related to the ODSs at 115 Hz (Fig. 18c), 142 Hz (Fig. 18d) and 150 Hz (Fig. 18e). According to the nomenclature of Chapter 6 they are basically of the ODS 2 type. As can be taken from Fig. 31, they differ in a superimposed torsion which is most pronounced in the lower-fret and head region and adds in phase and out of phase, respectively, to the basic bending motion. The mountain chains are similar in shape; maxima always occur at the lower frets while minima are observed at about the 12th fret. Dependent on the lateral position the corresponding vibration patterns are excited to a different extent which results in maxima at different frequencies. An excitation close to the bottom strings (Fig. 39 top) evokes a pronounced response of the neck at about 115 Hz. Along the centre line of the fingerboard (Fig. 39 middle) two admittance mountains of approximately equal height appear at about 115 Hz and 140 Hz. An excitation close to the top strings (Fig. 39 bottom), however, results in a maximum admittance at about 140 Hz.

A further example, given in Fig. 40, refers to the Dyna Bass No. 3. The admittance mountains at about 40 Hz and 275 Hz are not dependent on the lateral measuring position. Discrepancies are observed in the frequency region between 120 Hz and 150 Hz. A multiple-peak structure is observed. The corresponding admittance mountains are related to the ODSs at 120 Hz (Fig. 24d), 140 Hz (Fig. 24e) and 150 Hz (Fig. 24f). According to Chapter 6 they are variants of the ODS 2 type. They differ in a torsional motion superimposed on the basic bending. The resulting patterns are similar, but - as can be taken from Fig. 24 - differ slightly in frequency. They all exhibit maxima at the lower frets and minima at about the 10th fret. Depending on the lateral position of the excitation, these closely related vibration patterns are maximally evoked at different frequencies. While an excitation at the bottom strings (Fig. 40 top) results in a pronounced response of the low-fret region of the neck at about 120 Hz, a lateral shift towards the top strings yields maximum admittance at about 140 Hz. For an excitation along the centre line of the fingerboard (Fig. 40 middle) as well as close to the top strings (Fig. 40 bottom) the maximum admittance is observed at the same frequency with only minor differences in height.

These results reveal that the admittance at one and the same fret may depend on the lateral position and, as a consequence, differ between strings. During experiments on electric guitars (Fleischer and Zwicker (1998)) an interaction between bending of the neck (ODS 2) and torsion of the neck-head system was observed which was most pronounced for instruments with asymmetric headstocks. In consequence, the admittance proved as highly dependent on the lateral measuring position for asymmetric instruments. As most basses are conventionally constructed with asymmetric heads, in the normal case the admittance will be different at the low-string side, the centre and the high-string side of the fingerboard. For the headless Riverhead Bass No. 5, however, no superposition of torsion and bending was observed in the region below 275 Hz (see Fig. 30; torsion was only found for 421 Hz). The admittance can be expected to depend only weakly on the lateral position and, for this particular instrument, the mid-string admittance can be regarded as representative for all strings. In the normal case, however, it has to be kept in mind that the measurements at the centre position barely represent some kind of a mean value of the admittance at the outer positions.

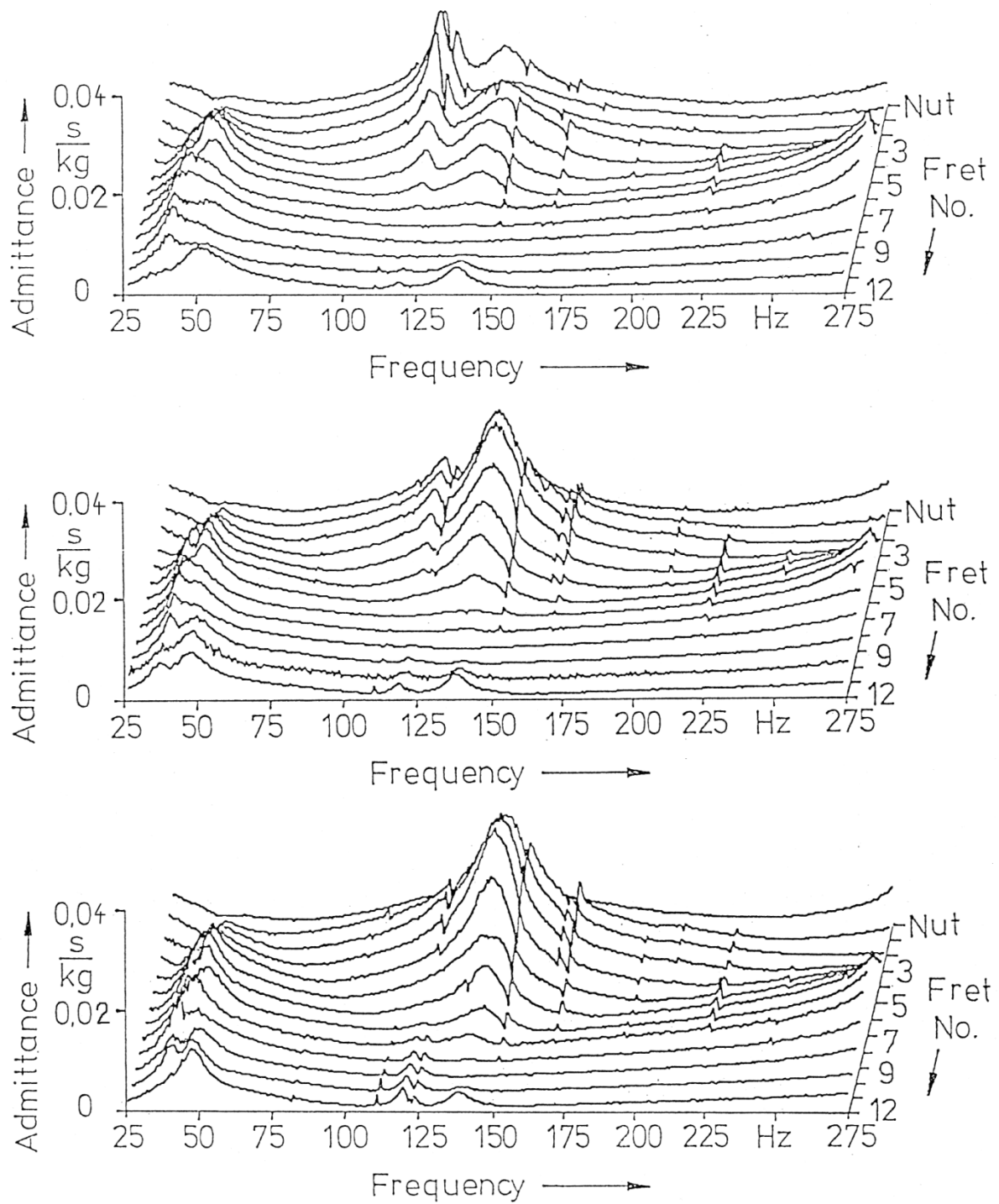


Fig. 40. Out-of-plane admittance on the neck of the Dyna Bass No. 3 as a function of frequency measured at thirteen locations from the nut to the 12th fret. Measuring positions are between the low E_1 and the A_1 strings (top), between the mid A_1 and D_2 strings (middle) and between the D_2 and the high G_2 strings (bottom).

7.4. Admittance, Conductance and Susceptance

A measurement at the nut-end termination of the A_1 string of the Music Man Bass is used to illustrate the relationship between the components of the complex admittance. The magnitude (admittance) is plotted versus frequency in the bottom part of Fig. 41. In the middle of the chosen frequency range the nut proves to be very mobile; several ODSs (see Fig. 21c - 21e) are reflected as a cluster of maxima between 137 Hz and 165 Hz. Beside the magnitude the imaginary and real part are given in the remaining diagrams of Fig. 41.

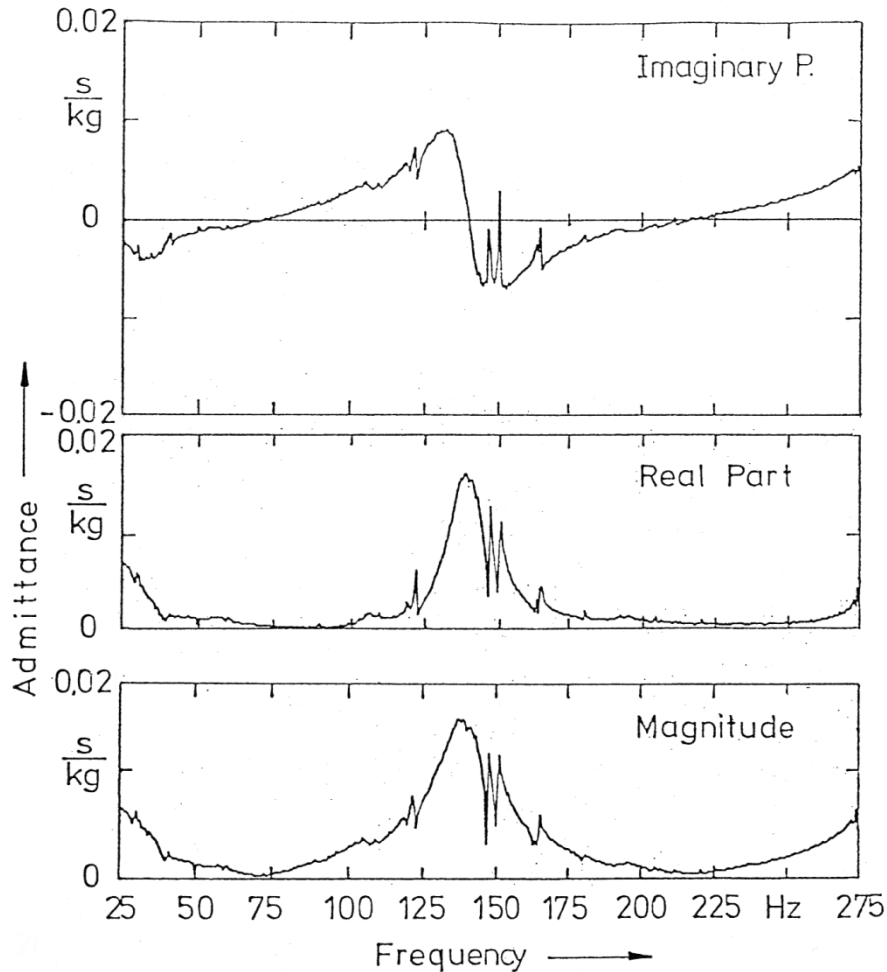


Fig. 41. Complex nut admittance of the Music Man Bass No. 2 as a function of frequency:
Admittance (magnitude; bottom),
conductance (real part; middle) and
susceptance (imaginary part; top).

The imaginary part, *i.e.* the susceptance, in the top diagram of Fig. 41 shows the well-known fact that, dependent on frequency, the nut-end termination of the string can behave like a mass (if the sign is negative) or like a spring (if the sign is positive). This is one of the causes of the inharmonicity of the partial tones of plucked stringed instruments.

The real part, *i.e.* the conductance, represents the ratio of the in-phase components of force and velocity. It is a measure for the transfer of active energy via the nut-end support of the string and therefore a direct indicator of the damping of the string motion due to the mobility of the end support. For the Music Man Bass an efficient energy transfer may take place at the low and the high

end of the displayed frequency range. In particular, energy can be effectively transferred to the nut at frequencies between about 120 Hz and 170 Hz. In this region, the conductance reaches 15 ms/kg.

The conductance at the termination of a string has to be compared to the characteristic admittance Y_{char} , *i.e.* the inverse of the characteristic impedance. The characteristic admittance of a string can be calculated from

$$Y_{\text{char}} = 1/(\mu c) \quad (19)$$

where

- μ linear density (mass per length unit) and
- c speed of transverse waves on the string.

The speed c can be derived from the fundamental frequency f_1 of the string signal and the length l of the speaking part of the string as

$$c = 2 l f_1 \quad (20)$$

Inserting Eq. (20) into Eq. (19) yields

$$Y_{\text{char}} = 1/(2 m f_1) \quad (21)$$

with

- f_1 fundamental frequency and
- m mass of the speaking part of the string.

These parameters are easily obtained. The fundamental frequency of *e.g.* the open A_1 string is $f_1 = 55$ Hz. The mass m of the string can be derived from the total mass, the total length and the length between the bridge and nut which is 0.87 m. For the example of the A_1 string this calculation results in a characteristic admittance of

$$Y_{\text{char}} = 0.55 \dots 0.6 \text{ s/kg} \quad (22)$$

That means that the maximum conductance at the nut termination of the A_1 string amounts to some percent of the characteristic admittance of the string.

While for an acoustic stringed instrument there is an intrinsic need to transfer energy from the string to the radiating part of the body, the contrary is true for an electric bass, in particular not for the solid-body type. Loss of energy is regarded as parasitic. This loss via the string terminations is determined by the conductance: That is why only this part of the complex admittance will be discussed in the following.

7.5. Neck and Bridge Conductance

In contrast to the landscapes displayed in the previous figures, Fig. 42 shows not the admittance, but its real part, the conductance. The conductance is plotted versus frequency and was measured in perpendicular direction along the centre line of the fingerboard at the nut (top curve), the first twelve frets and at the bridge (bottom curve). As can be expected from Fig. 41, the mountains have steeper edges and are more pronounced than in the comparable landscape of the admittance. Distinct mountain chains appear at low frequencies at about 50 Hz and in the frequency region around 250 Hz. They reflect the ODSs which are compiled in Figs. 27c - 27f. An additional mountain occurs at about 270 Hz (*cf.* Fig. 27g).

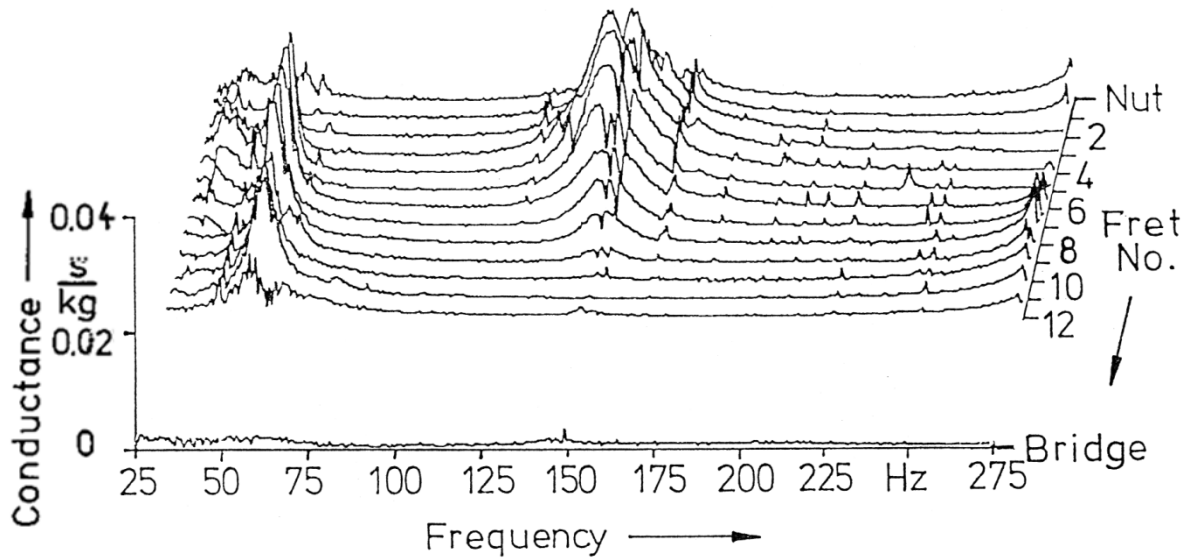


Fig. 42. Conductance at the nut, the first twelve frets and the bridge of the Carvin Bass No. 4 as a function of frequency measured along the centre line of the fingerboard between the A_1 and D_2 strings.

While the conductance exhibits pronounced maxima at the neck (upper curves in Fig. 42), it is, practically independent on frequency, very small at the bridge. The corresponding curve at the bottom of the diagram is flat with only minor deviations. Thus, the conductance turns out to be considerably smaller at the bridge of a well-made solid-body bass than it may be on the neck. This result holds also if the measuring position is laterally shifted. It implies that, as a rule, each string "sees" an approximately immobile support at the bridge end and, since the conductance proved as low, only minor energy losses via this termination are expected. With respect to energy losses, this means that the "weak" end is the upper termination of the string. That is why the neck conductance is a strong indicator for dead spots.

7.6. Concluding Remarks

The measurements described in this chapter reveal that the bridge of a well-balanced solid-body bass is much less mobile than the neck at the position of the nut and frets. The real part of the admittance, the conductance, measured perpendicular to the fingerboard, is a most relevant parameter to describe energy losses at the neck-end terminations of the strings. There may be a dependence of the conductance on the lateral measuring position indicating that at the same fret the different strings may "see" different conductances. In the normal case, however, the conductance determined along the centre line of the fingerboard is at least some kind of a mean value for one and the same fret, and therefore gives a good impression of the additional damping which will act upon the string vibration as a consequence of the mobility of its termination.

8. NECK CONDUCTANCE OF THE BASSES

In this chapter the conductances as measured on the necks of all basses under consideration are compiled. The 3D representation is used in order to give an impression of at which fret and at which frequency the neck tends to draw vibration energy from the string. This way, the frets and frequencies are indicated at which the prerequisites for dead spots are given.

8.1. Experimental Results for the Action Bass

The 3D landscape representation as introduced in the previous chapter is used in order to condense the results of thirteen measurements on the neck of each bass. The real part of the complex admittance, the conductance, is plotted as a function of the fret position and frequency within the range from 25 Hz to 275 Hz.

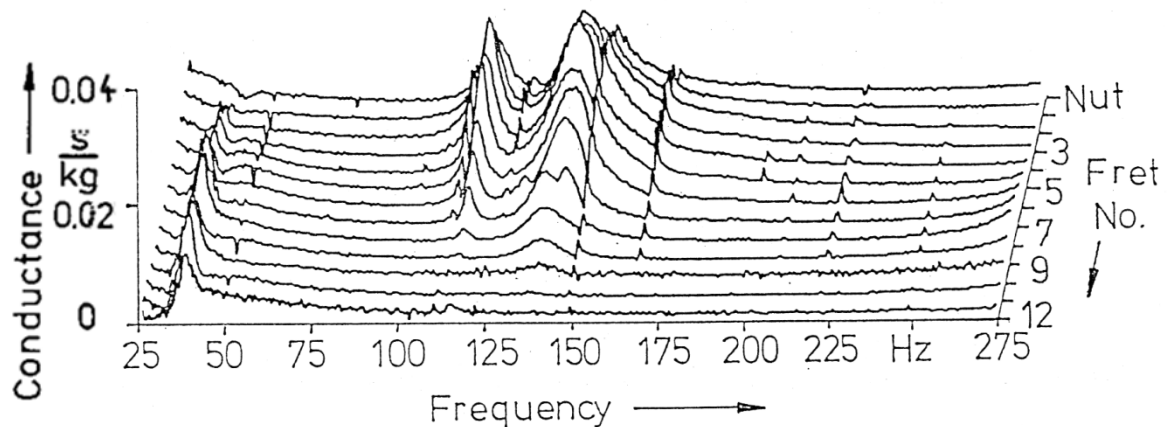


Fig. 43. Conductance at the nut and the first twelve frets of the Action Bass No. 1 as a function of frequency measured along the centre line of the fingerboard between the A_1 and D_2 strings.

Three sharply pronounced mountain chains appear in the conductance landscape at about 40 Hz and between 110 Hz and about 150 Hz. They correspond to the first and second bending motion, respectively, which can be distinguished by the number and location of the nodes, in which the conductance equals zero. The maximum conductance does not exceed 30 ms/kg.

8.2. Experimental Results for the Music Man Bass

Again, the first bending mode with a node close to the nut is reflected by the mountain chain at about 40 Hz. In contrast to the Action Bass (cf. Fig. 43), the Music Man Bass (Fig. 44) exhibits no pronounced splitting of the second bending mode. In the region around 140 Hz essentially only one mountain chain is found. For better comparability, the same scaling is used in all diagrams. The highest maxima are clipped in Fig. 44 indicating that they are higher than 30 ms/kg.

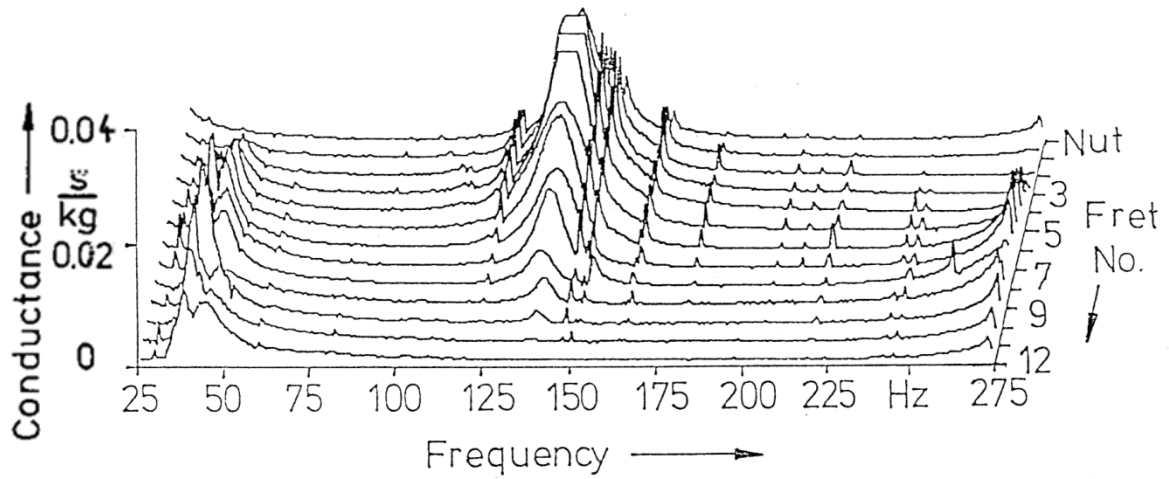


Fig. 44. Conductance at the nut and the first twelve frets of the Music Man Bass No. 2 as a function of frequency measured along the centre line of the fingerboard between the A_1 and D_2 strings.

8.3. Experimental Results for the Dyna Bass

The first bending mode is reflected by a mountain chain between 40 Hz and 50 Hz. Similar to the Music Man Bass (cf. Fig. 44) the Dyna Bass (Fig. 45) exhibits only one mountain chain in the vicinity of 140 Hz. This zone of high conductance is the consequence of the second bending mode. No clipping is observed in Fig. 44 indicating that no maximum reaches 30 ms/kg.

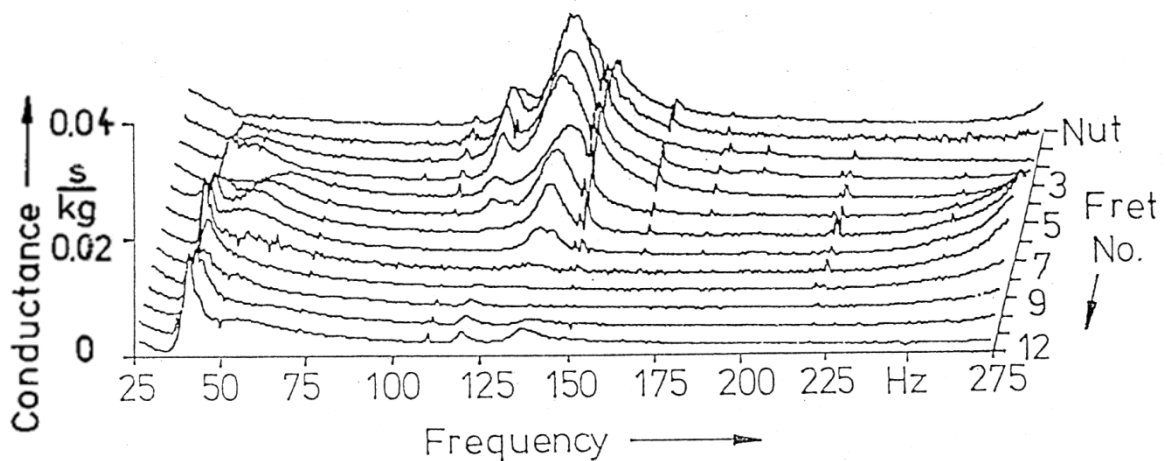


Fig. 45. Conductance at the nut and the first twelve frets of the Dyna Bass No. 3 as a function of frequency measured along the centre line of the fingerboard between the A_1 and D_2 strings.

8.4. Experimental Results for the Carvin Bass

The first bending mode becomes visible in the conductance landscape as a well-pronounced mountain chain at about 50 Hz. The low-frequency motion that was observed for 29 Hz in the vibration measurement plays no role in the conductance. Comparable to *e.g.* the Dyna Bass (cf. Fig. 45), the Carvin Bass (Fig. 46) shows not such a wide frequency separation of the cluster of the variants of the second bending mode as the Action Bass (cf. Fig. 43). Nevertheless, at least two crests are found in the mountain chain around 150 Hz. No maxima higher than 30 ms/kg occur.

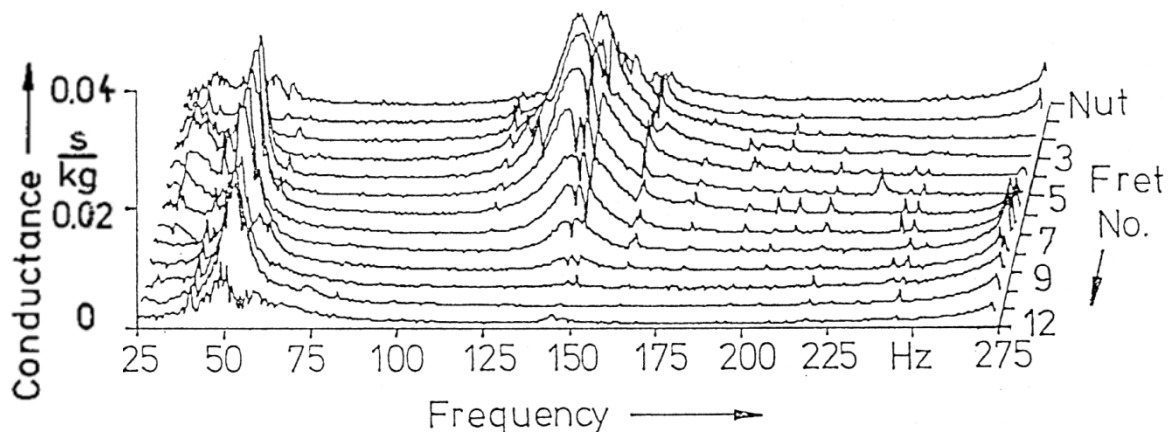


Fig. 46. Conductance at the nut and the first twelve frets of the Carvin Bass No. 4 as a function of frequency measured along the centre line of the fingerboard between the A_1 and D_2 strings.

8.5. Experimental Results for the Riverhead Bass

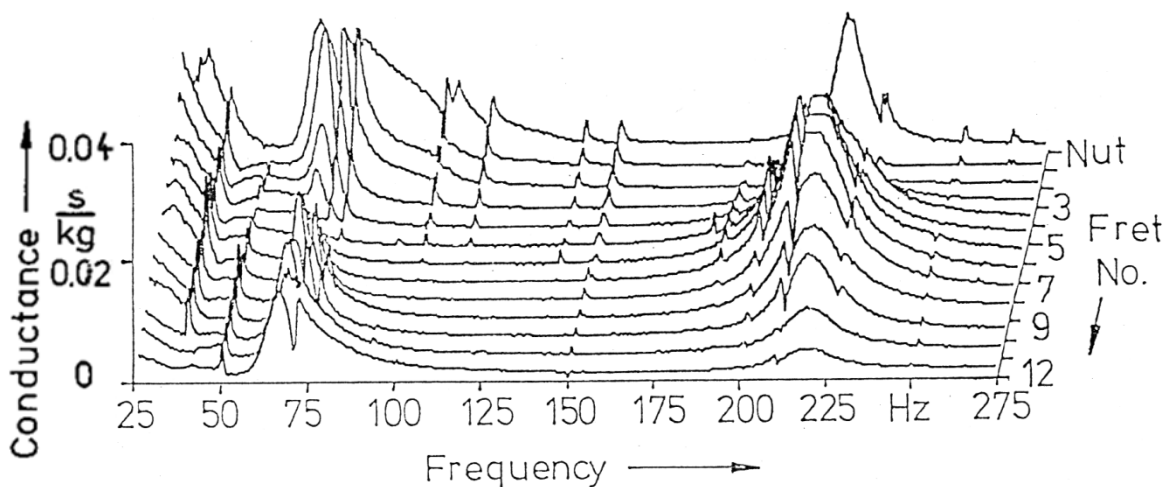


Fig. 47. Conductance at the nut and the first twelve frets of the Riverhead Bass No. 5 as a function of frequency measured along the centre line of the fingerboard between the A_1 and D_2 strings.

While the conductance landscapes of the first four basses are rather similar, the Riverhead Bass (Fig. 47) exhibits a basically different behaviour. The diagram shows a multitude of mountain chains which are closely related with the ODSs in Fig. 30. (The smaller peaks at 50 Hz and multiples are suspected to originate from the hum of power supplies.) The conductance reflects the following motional patterns: The rigid body motion with an antinode at the nut for 40 Hz, the first bending mode around 70 Hz and the second bending mode between 200 Hz and 220 Hz. Particularly in the vicinity of the first bending mode there are relatively wide regions of high conductance. Some maxima (at the 4th to 6th fret) are clipped at about 210 Hz which means that the conductance happens to exceed 30 ms/kg.

8.6. Concluding Remarks

There are two groups of basses in the ensemble of the instruments under consideration. The first one consists in only one item, the headless carbon fibre bass No. 5, which differs considerably from the other basses and does not fit into the common scheme. The second group comprises the remaining four instruments No. 1 through No. 4. The conductance diagrams of these conventionally manufactured instruments prove as relatively similar. They use to exhibit a mountain chain at low frequencies (between 40 Hz and 50 Hz) with very small values at the lower frets close to the nut. They all have in common a second (single-peaked or multiple-peaked) mountain chain which shows very high values in the region of the lower frets. On this part of the fingerboard, for frequencies in the vicinity of about 150 Hz values are measured that sometimes exceed 30 ms/kg. Thus, in the extreme case, the conductance at the neck termination of a bass string may be estimated to amount to about one twentieth of the characteristic admittance. As a consequence, a considerable flow of vibration energy to the instrument structure via the neck, resulting in a faster decay and therefore a dead spot, may be expected. Although the quantitative consequences are not yet known in detail, the effect is obvious. It will be subject to further investigations which are not covered by this report.

9. FINAL DISCUSSION

In the electric bass the musical signal, generated by the string, is picked up and amplified electrically. Thus, in contrast to an acoustic instrument, the generation and radiation of the signal are distinctly separated. In consequence, there is no need for the transfer of vibration energy from the string to the body of an electric bass. The experiments performed on solid-body basses show that the mechanical conductance at the bridge is relatively low and, consequently, only a small amount of energy is transferred to the body via the bridge end of the vibrating string. The result is a generally better "sustain" of an electric bass compared to an acoustic one, which most players appreciate as a quality attribute.

However, it is obvious that the bridge represents only one termination of a bass string. Energy can be transferred to the instrument structure via the neck-end, too. This means that knowledge of the energy loss at both string supports is required. The neck-end termination of the string is defined by the fret against which the player presses the string (fingered situation), or the nut (open situation). For a well-made solid-body bass the neck proves to be much more flexible than the bridge. That is why, concerning the sustain of the musical signal, the neck termination is suspected to be the "worse" of the two terminations of a bass string.

This idea is confirmed by practical observations. There are particular locations on the fingerboard which bass players call "dead spots". They are characterised by an extremely fast decay of the musical signal of a string. Investigations on electric guitars and basses have suggested that the non-rigid behaviour, *i.e.* the continuum vibrations, of the instrument itself is the cause of the dead spot phenomenon. Several experimental approaches have been described in this report which were used to ascertain the mechanical vibrations of bass structures. They all have in common fixed shaker excitation. The first series dealt with Modal Analysis using laser vibrometry to pick up the surface velocity. The fundamental shortcoming of this investigation was that the boundary conditions during the measurement differed from those during normal playing. When a bass is played it is in contact with the body of the player. For a physical investigation, as a rule, it is fixed in an experimental set-up. As it was shown by means of some examples of beam vibrations, the eigenpatterns and eigenfrequencies depend on the boundary conditions to a great extent. Therefore, the same object, vibrating under different boundary conditions, is expected to behave considerably different. Thus, in order to make results comparable, great care has to be taken to approximate the "natural" boundary conditions of the bass, as they are during the playing process, with the measuring conditions as far as possible.

The solution of this problem presented in this report is to perform experimental studies with the instrument held by the subject in sitting playing position ("*in situ*"). In a first step, the vibrations of the instruments were investigated. No complete Modal Analysis was performed, but a determination of Operating Deflection Shapes (ODSs) was considered as sufficient. A Laser Scanning Vibrometer was used to measure the surface velocity of five basses which were held by a person during the data acquisition. Because the procedure lasted only a few minutes, the person could keep his position during the measuring time. As a result of these *in-situ* vibration measurements, certain groups of vibrational patterns were found which are similar in frequency and shape for the conventional wooden basses. Solely the futuristic headless carbon fibre bass, which differs in design and material as compared to the other instruments, does not fit into this scheme. As a standard model, a simply supported-free beam proves as suited for describing essential features of the vibrations. Bending of the body-neck-head structure dominates; torsion may be superimposed.

In a second step, a more direct approach was used. Rather the behaviour of the string terminations than the mechanical vibration of the instrument structure is subject to the investigations. In order to characterise the "vibration willingness" of the string supports, the mechanical point admittance was

measured at the bridge and neck. The transfer of energy from the string to the instrument structure, which is the key for the understanding of dead spots, is determined by the real part, the conductance. It is a measure of the damping at the supports which terminate a string. Therefore, the conductance is directly related to irregularities in the decay times of the string vibration. Since the bridge end proves as relatively immobile, the most pronounced effect is expected from the opposite end. Thus, the neck conductance can be regarded as the fundamental parameter in studies of dead spots.

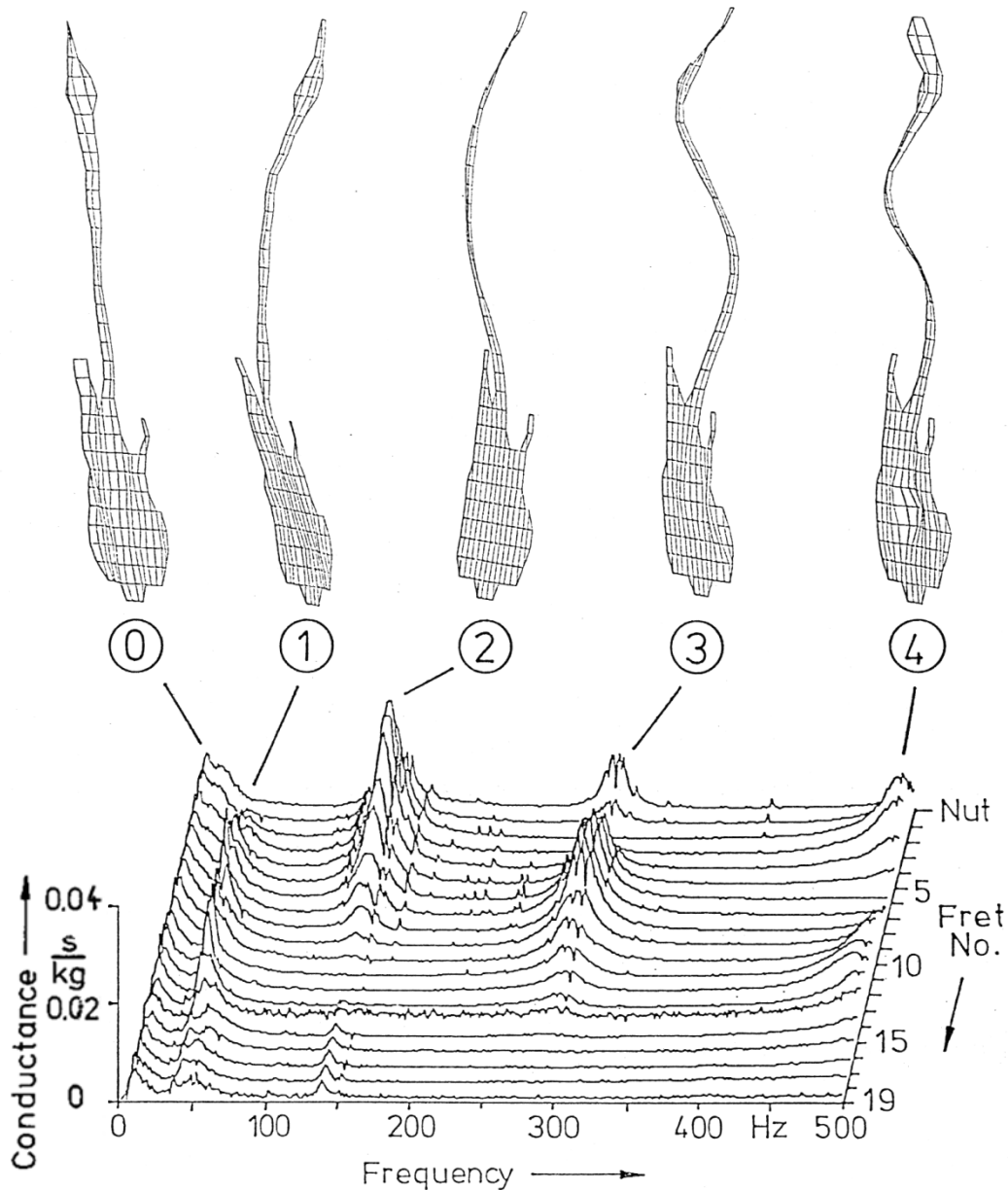


Fig. 48. Conductance at the nut and the first nineteen frets of the Music Man Bass No. 2 as a function of frequency measured along the centre line of the fingerboard between the A_1 and D_2 strings including the corresponding ODSs.

It was considered as favourable to compile the conductances measured at the nut and frets in one diagram. This way, a conductance "landscape" is created. As can be taken from Fig. 48, it exhibits characteristic "mountain chains" which are related to the vibration patterns of the structure which are given by the ODSs. A rigid body motion (0) appears at very low frequencies. At about 40 Hz the first continuum bending mode (1) is observed resulting in maximum conductance at about the

7th fret and a minimum close to the nut. The second bending mode (2) around 150 Hz is characterised by a conductance minimum in the vicinity of the 12th fret and a maximum in the region of the lower frets. At frequencies slightly smaller than 300 Hz the third bending mode (3) with an additional antinode occurs which shows up in the conductance as an extra minimum at the 2nd fret. If the frequency just exceeds 500 Hz, the fourth bending mode (4) causes conductance minima at the nut, the 6th fret and the 18th fret. It happens that the bending is superimposed by torsion of the neck-head system which may result in a lateral dependence of the conductance for one and the same fret position. Compared to the ODSs, the conductance is not only easier (and less expensive) to determine, but above all it is easier to interpret in terms of its influence on the damping of the string vibration.

As already mentioned above, coincidence of the boundary conditions is the necessary prerequisite for the comparability of results. Care was taken to ensure "natural" boundaries for the basses in the different measurements. During the ODS experiments as well as the conductance measurements normal sitting position was chosen with the experimenter holding the bass on his thigh and his left hand grasping the neck of the instrument. This *in-situ* approach has created realistic and similar boundary conditions when measuring parameters such as the surface velocity, the conductance and, as will be reported in a subsequent paper, the decay time of the string signal. In spite of the living boundary, the results proved to be reproducible.

In summary, above all the measurements of the neck conductance *in situ* have proved as a powerful tool for studying the power-consuming properties of the string terminations of electric basses: By moving the measuring device along the fingerboard, a relevant parameter (mechanical conductance) is measured by exciting at the actual locations (nut and frets) with the bass having realistic boundary conditions (held by a person in playing position). Future work will focus on the damping of string vibrations. The effect of non-ideal terminations on the decay rates of the string signals will be investigated and yield the basis for the diagnosis of dead spots.

Acknowledgements

The author wishes to thank Tobias Fleischer, the player and owner of most of the basses which were investigated in this study, and his willingness to leave them for (as he did not always believe) non-destructive experiments.

LITERATURE

- Carlson, M., *Application of Finite Element Analysis for an improved musical instrument design. Technical Report, Fender Corp., Corona 1998 (?)*.
- Chaigne, A., *Évaluation subjective des qualités sonores des cordes de guitare. Acustica* **62** (1986), 16 - 29.
- Chladni, E.F.F., *Entdeckungen über die Theorie des Klanges. Weidmanns Erben und Reich, Leipzig 1787*.
- deDayans, H.G., Behar, A., *The quality of strings for guitars: An experimental study. J. Sound and Vibr.* **64** (1979), Vol. 3, 421 - 431 with Comments by Hanson, R.J., *J. Sound and Vibr.* **64** (1983), Vol. 2, 283 - 285.
- DIN 1320. *Acoustics. Fundamental terms and definitions*.
- Eggers, F., *Mechanische Impedanzmessungen am Violoncello. In: Fortschritte der Akustik (DAGA '87), DPG-GmbH, Bad Honnef 1987, 697 - 700*.
- Eggers, F., *Mechanical impedance measurements around the violoncello. Acustica* **74** (1991), 264 - 270.
- Fleischer, H., *Glockenschwingungen. Beiträge zur Vibro- und Psychoakustik 1/97. Editors H. Fleischer and H. Fastl. University of the Federal Armed Forces Munich, Neubiberg 1997a*.
- Fleischer, H., *Admittanzmessungen an akustischen Gitarren. Forschungs- und Seminarberichte aus dem Gebiet Technische Mechanik und Flächentragwerke 01/97. Editors F.A. Emmerling and A.H. Heinen, University of the Federal Armed Forces Munich, Neubiberg 1997b*.
- Fleischer, H., *In-situ-Messung der Schwingungen von E-Gitarren. In: Fortschritte der Akustik (DAGA '98), DEGA, Oldenburg 1998a, 630 - 631*.
- Fleischer, H., *Schwingungen akustischer Gitarren. Beiträge zur Vibro- und Psychoakustik 1/98. Editors H. Fleischer and H. Fastl. University of the Federal Armed Forces Munich, Neubiberg 1998b*.
- Fleischer, H., *Messen und Berechnen von Glockenschwingungen. In: Glocken und Glockenspiele. 17th Symposium on Instrument Making in Michaelstein. Stiftung Kloster Michaelstein, Blankenburg 1998c, 240 - 264*.
- Fleischer, H., *Diagnosing dead spots of electric guitars and basses by measuring the mechanical conductance. Acustica - acta acustica* **85**, Suppl. 1, 404 and *Proceedings of the ASA/EAA/DAGA '99 Joint Meeting, Berlin 1999*.
- Fleischer, H., Zwicker, T., *Dead Spots. Zum Schwingungsverhalten elektrischer Gitarren und Baßgitarren. Beiträge zur Vibro- und Psychoakustik 1/96. Editors H. Fleischer and H. Fastl. University of the Federal Armed Forces Munich, Neubiberg 1996*.
- Fleischer, H., Zwicker, T., *Admittanzmessungen an Elektrobässen. In: Fortschritte der Akustik (DAGA '97) DEGA, Oldenburg 1997, 301 - 302*.
- Fleischer, H., Zwicker, T., *Mechanical vibrations of electric guitars. Acustica - acta acustica* **84** (1998), 758 - 765.
- Fleischer, H., Zwicker, T., *Investigating dead spots of electric guitars. Acustica - acta acustica* **85** (1999), 128 - 135.

- Fletcher, H., Normal vibration frequencies of a stiff piano string. *J. Acoust. Soc. Amer.* **36** (1964), 203 - 209.
- Fletcher, N.H., Design and performance of harpsichords. *Acustica* **37** (1977), 139- 147.
- Fletcher, N.H. and Rossing, T.D., *The physics of musical instruments*. 2nd ed. Springer, New York 1998.
- Garrelfs, M., Schneiders, C., *Schwingungsformen elektrischer Baßgitarren*. Studies report, Institute of Mechanics, Faculty of Aerospace Technology, University of the Federal Armed Forces Munich, Neubiberg 1995.
- Gough, C.E., The theory of string resonances on musical instruments. *Acustica* **49** (1981), 124 - 141.
- Heise, U., Untersuchungen zur Ursache von Dead Spots an Baßgitarren. *Das Musikinstrument* **42** (1993), Heft 6/7, 112 - 115.
- Jansson, E.V., Acoustics for the guitar player. In: *Function, construction and quality of the guitar*. Royal Swedish Academy of Music, Publication No. 38 (1983a), 7 - 26.
- Jansson, E.V., Acoustics for the guitar maker. In: *Function, construction and quality of the guitar*. Royal Swedish Academy of Music, Publication No. 38 (1983b), 27 - 50.
- Jansson, E.V., Experiments with the violin string and bridge. *Applied Acoustics* **30** (1990), 133 - 146.
- Jansson, E.V., Admittance measurements of 25 high quality violins. *Acustica - acta acustica* **83** (1997), 337 - 341.
- Jansson, E.V., Niewczyk, B.K., Admittance measurements of violins with high arching. *Acustica - acta acustica* **83** (1997), 571 - 574.
- Lemme, H., *Elektrogitarren*, 4. edition. Frech-Verlag, Stuttgart 1982.
- May, U., *Elektrische Saiteninstrumente in der populären Musik*. Doctoral dissertation, University Münster, Münster 1984.
- Meinel, E., *Elektrogitarren*. E. Bochinsky, Frankfurt a. M. 1987.
- Moral, J.A., Jansson, E.V., Eigenmodes, input admittance, and the function of the violin. *Acustica* **50** (1982), 329 - 337.
- Müller, H., Messung der Eigenfrequenzen biegesteifer Saiten. *Acustica* **19**, (1967/68), 89 - 97.
- Pfaffelhuber, K., *Das dynamische Verhalten der Geige an der Anstreichstelle und sein Einfluß auf das Klangsignal*. Doctoral dissertation, TU München, München 1993.
- Richardson, M.H., Is it a mode shape, or an operating deflection shape? *Sound and Vibration* **31** (1997), 54 - 61.
- Twork, Th., *Laser-Vibrometrie: Berührungsfreies Messen von Oberflächenschwingungen*. Master's thesis, Institute of Mechanics, Faculty of Aerospace Technology, University of the Federal Armed Forces Munich, Neubiberg 1997.
- Valenzuela, M. N., *Zur Rolle des Gehörs bei akustischen Untersuchungen an Musikinstrumenten*. Beiträge zur Vibro- und Psychoakustik 1/99. Editors H. Fleischer and H. Fastl. University of the Federal Armed Forces Munich, Neubiberg 1999.
- Wogram, K., *Schwingungsuntersuchungen an Musikinstrumenten*. In: *Fortschritte der Akustik (DAGA '94)*, DPG-GmbH, Bad Honnef 1994, 53 - 64.

- Wolf, D., Müller, H., Normal vibration modes of stiff strings. J. Acoust. Soc. Amer. 44 (1968), 1093 - 1097.*
- Ziegenhals, G., Zum mechanisch-akustischen Verhalten von Halbresonanz-Elektrogitarren. In: Fortschritte der Akustik (DAGA '97), DEGA, Oldenburg 1997, 309 - 310.*
- Zimmermann, P., Theoretische Untersuchungen zur Funktion des Steges bei Streichinstrumenten. Acustica 18 (1967), 287 - 299.*

In der Reihe

Beiträge zur Vibro- und Psychoakustik

sind bisher erschienen:

Heft 1/96: Fleischer, H. und Zwicker, T., DEAD SPOTS. Zum Schwingungsverhalten elektrischer Gitarren und Baßgitarren.

Heft 1/97: Fleischer, H., Glockenschwingungen.

Heft 1/98: Fleischer, H., Schwingungen akustischer Gitarren.

Heft 1/99: Valenzuela, M.N., Zur Rolle des Gehörs bei akustischen Untersuchungen an Musikinstrumenten.

ISSN 1430-936X

Beiträge zur Vibro- und Psychoakustik